UNIVERSITÀ DEGLI STUDI DI PADOVA

UNIVERSITÀ DEGLI STUDI DI PADOVA
Dipartimento di Ingegneria Industriale
Corso di Laurea Magistrale in Ingegneria Aerospaziale

Investigation of different strategies for access to space and positioning of small satellites

Indagine su diverse strategie di accesso allo spazio e posizionamento di piccoli satelliti

Relatore: Prof. Francesco Barato

Laureando: Matteo Fiorio
Matricola: 2005714

ANNO ACCADEMICO 2022-2023

Abstract

The Space Economy is expanding and has shown that space no longer belongs only to governments and its access is increasingly possible even to small private companies. Each will soon play an important role in the space race, leading to increased launches and the possibility of ever-faster industry development. Consequently, each company will manage all the parts concerning a space mission in complete autonomy, from the launch to the positioning of its satellite in the desired orbit.
However, a company must still consider the most efficient solution to achieve its goal and this thesis is at the heart of the matter.
Initially, an overview on space propulsion is provided, explaining the characteristics and operating principles of main types of engines and the major differences between them, which allows to figure out the best solution based on the mission.
It has been studied how access to LEO orbits can take place, through transporter missions or microlaunchers with a particular focus to the transportable payload mass in function of the desired final orbit as suggested from the various launchers manuals.
Then, an analysis of various orbital maneuvers is carried out for the correct positioning of one or more satellites in target orbit aiming to the maximum efficiency in terms of times and costs, considering both chemical and electric propulsion.
The maneuvers that have been investigated are: Hohmann Transfer, Phasing maneuver, where various ways to perform it are shown, Change inclination maneuver, Right ascension of the ascending node (RAAN) change maneuver.
All the cases have been studied considering different specific impulses, to simulate all the possible thrusters and find the optimal configuration according to the mission.
Finally, particular attention is paid to the effects of J_2 zonal perturbation in order to understand how different parameters vary during maneuvers and to save propellant in some of them.

Sommario

La Space Economy si sta espandendo e ha provato che lo spazio non appartiene più solamente ai governi ed il suo accesso è possibile sempre più anche a piccole aziende private. Ognuno presto giocherà un ruolo importante nella corsa allo spazio, portando ad un aumento di lanci e la possibilità di uno sviluppo del settore sempre più rapido. Conseguentemente, ogni azienda gestirà tutte le parti che concernono una missione spaziale in completa autonomia, dal lancio al posizionamento del proprio satellite nell'orbita desiderata.
Tuttavia, un'azienda deve comunque considerare la soluzione più efficiente per raggiungere il proprio obiettivo e questa tesi si pone al centro della questione.
Inizialmente, viene fornita una panoramica sulla propulsione spaziale, spiegando le caratteristiche ed i principi di funzionamento dei principali tipi di motori e le maggiori differenze tra di essi, il che permette di capire la soluzione migliore in base alla missione.
Viene studiato come può avvenire l'accesso in LEO, tramite missioni transporter o attraverso microlanciatori con particolare focus alla massa dei payload trasportabile in funzione dell'altitudine dell'orbita finale desiderata suggerita dai manuali dei lanciatori.
Dopodichè, viene effettuata un'analisi di varie manovre orbitali per il corretto posizionamento di uno o più satelliti in orbita target avendo come obiettivo la massima efficienza in termini di tempi e costi, considerando sia propulsione chimica sia elettrica.
Le manovre che sono state studiate sono: trasferimento di Hohmann, manovra di fasatura, dove vengono mostrati vari modi per eseguirla, manovra di cambio inclinazione e manovra di cambio ascensione retta del nodo ascendente (RAAN).
Tutti i casi sono stati studiati considerando diversi impulsi specifici, al fine di simulare tutti i possibili propulsori e trovare la configurazione ottimale in base alla missione.
Infine, particolare attenzione viene prestata agli effetti della perturbazione zonale J_2 al fine di comprendere come variano i diversi parametri durante le manovre e per risparmiare propellente in alcune esse.

to my family

Contents

1 Space Propulsion **1**
- 1.1 Generalities . . . 1
- 1.2 Chemical propulsion . . . 1
  - 1.2.1 Liquid propellant rocket engines . . . 2
  - 1.2.2 Solid propellant rocket engines . . . 3
  - 1.2.3 Hybrid propellant rocket engines . . . 3
- 1.3 Electric propulsion . . . 4
- 1.4 Chemical and electric propulsion comparison . . . 4

2 Mission analysis **9**
- 2.1 Overview . . . 9
- 2.2 Launch . . . 9
  - 2.2.1 Launchers . . . 9
  - 2.2.2 Micro-launchers . . . 15
- 2.3 Deployment . . . 20
  - 2.3.1 Deployers . . . 20
  - 2.3.2 Platforms . . . 21
- 2.4 In-space propulsion . . . 22

3 LEO Constellations **23**
- 3.1 Telesat System . . . 23
- 3.2 OneWeb System . . . 24
- 3.3 Starlink System . . . 25

4 Orbital Mechanics **27**
- 4.1 Orbital parameters . . . 27
- 4.2 Orbital perturbations . . . 28
  - 4.2.1 Atmospheric drag . . . 28
  - 4.2.2 J_2 perturbation . . . 29
- 4.3 Orbital maneuvers . . . 30
  - 4.3.1 Orbit raising . . . 30
  - 4.3.2 De-orbiting . . . 34
  - 4.3.3 Access to space . . . 37
  - 4.3.4 Phase change maneuver . . . 39
  - 4.3.5 Inclination change maneuver . . . 47
  - 4.3.6 RAAN change maneuver . . . 51
  - 4.3.7 Argument of Perigee change maneuver . . . 82

Conclusions **99**

Bibliography **102**

List of Figures

1.1 Three types of chemical rocket engines: (a) solid propellant, (b) liquid bi propellant, (c) hybrid propellant [1] . . . 2
1.2 Propellant mass % in function of the required ΔV . . . 5
1.3 Relative Error % in function of the required ΔV - focus on $\pm$ 10 % relative error 5
1.4 Relative Error % in function of the required ΔV - focus on $\pm$ 2 % and $\pm$ 5 % relative error . . . 6
1.5 Comparison between the overestimated and underestimated ΔV respect to the Tsiolkovsky one . . . 6

2.1 Capability of the Falcon 9 in function of the altitude for LEO orbits [2] . . . 10
2.2 Capability of the Falcon 9 in function of the altitude for a circular polar orbit [2] 10
2.3 Capability of the Falcon 9 in function of the altitude for a SSO orbit [2] . . . 11
2.4 Capability of the Vega launcher in function of the altitude [3] . . . 11
2.5 Capability of the Terran launcher in function of the altitude [4] . . . 12
2.6 Capability of the Epsilon launcher in function of the orbit apogee [5] . . . 13
2.7 Capability of the Epsilon launcher in function of the altitude for a SSO mission [5] 13
2.8 Capability of the Epsilon launcher in function of the altitude for an inclination equal to 30^o [5] . . . 14
2.9 Capability of the LM3A launcher in function of the altitude [6] . . . 14
2.10 Capability of the RS1 launcher in function of the altitude [7] . . . 15
2.11 Capability of the Launcher One launcher in function of the altitude [8] . . . 16
2.12 Capability of the Terran launcher in function of the altitude [9] . . . 16
2.13 Capability of the Electron launcher in function of the altitude [10] . . . 17
2.14 Capability of the ALPHA launcher in function of the altitude launching in east side [11] . . . 18
2.15 Capability of the ALPHA launcher in function of the altitude launching in west side [11] . . . 18
2.16 Capability of the Skyrora XL launcher in function of the altitude in SSO orbit [12] 19
2.17 Capability of the Skyrora XL launcher in function of the altitude in polar orbit [12] . . . 19

3.1 Telesat system representation [13] . . . 23
3.2 OneWeb system representation [13] . . . 24
3.3 Starlink system representation [13] . . . 25

4.1 3D orbit representation [14] . . . 28
4.2 RAAN regression velocity depending on the orbital inclination . . . 29
4.3 Argument of perigee advancement velocity depending on the orbital inclination . 29
4.4 Hohmann transfer [14] . . . 30
4.5 Required ΔV for an Hohmann transfer from low to high orbits . . . 32
4.6 Spiral transfer [14] . . . 32
4.7 Required ΔV for a spiral transfer from low to high orbits . . . 33
4.8 Difference in terms of ΔV between Hohmann and spiral transfer from low to high orbits . . . 33
4.9 Required ΔV for an Hohmann transfer from high to low orbits . . . 34

4.10 Required ΔV for a spiral transfer from high to low orbits . . . 34
4.11 Difference in terms of ΔV between Hohmann and spiral transfer from high to low orbits . . . 35
4.12 Required propellant mass % for an Hohmann transfer in range $200 - 1000\ km$ with $I_{sp} = 150\ s$ . . . 35
4.13 Required propellant mass % for an Hohmann transfer in range $200 - 1000\ km$ with $I_{sp} = 300\ s$ . . . 36
4.14 Required propellant mass % for an Hohmann transfer in range $200 - 1000\ km$ with $I_{sp} = 1000\ s$ . . . 36
4.15 Required propellant mass % for an Hohmann transfer in range $200 - 1000\ km$ with $I_{sp} = 3000\ s$ . . . 37
4.16 Final mass in function of the altitude considering Hohmann transfer and $I_{sp} = 150\ s$ 37
4.17 Final mass in function of the altitude considering Hohmann transfer and $I_{sp} = 300\ s$ 38
4.18 Final mass in function of the altitude considering Hohmann transfer and $I_{sp} = 1000\ s$ . . . 38
4.19 Final mass in function of the altitude considering Hohmann transfer and $I_{sp} = 3000\ s$ . . . 39
4.20 External and internal Phasing maneuver [14] . . . 39
4.21 Required ΔV for a internal phasing maneuver in range $200-1000\ km$ at different longitudes $\Delta\Lambda$ . . . 41
4.22 Required ΔV for a internal phasing maneuver in range $0-180^o$ at different altitudes 41
4.23 Required ΔV for a internal phasing maneuver in range $0 - 180^o$ considering different number of orbits . . . 42
4.24 Height of the transfer orbit perigee in function of the number of orbits . . . 42
4.25 Required propellant mass % for a phasing maneuver in range $200-1000\ km$ with $I_{sp} = 150\ s$ . . . 43
4.26 Required propellant mass % for a phasing maneuver in range $200-1000\ km$ with $I_{sp} = 300\ s$ . . . 43
4.27 Required propellant mass % for a phasing maneuver in range $0 - 180^o$ with $I_{sp} = 150\ s$ . . . 44
4.28 Required propellant mass % for a phasing maneuver in range $0 - 180^o$ with $I_{sp} = 300\ s$ . . . 44
4.29 Required propellant mass % for a phasing maneuver in range $200-1000\ km$ with $I_{sp} = 1000\ s$ . . . 45
4.30 Required propellant mass % for a phasing maneuver in range $200-1000\ km$ with $I_{sp} = 3000\ s$ . . . 45
4.31 Required propellant mass % for a phasing maneuver in range $0 - 180^o$ with $I_{sp} = 1000\ s$ . . . 46
4.32 Required propellant mass % for a phasing maneuver in range $0 - 180^o$ with $I_{sp} = 3000\ s$ . . . 46
4.33 Required ΔV for a inclination change maneuver in range $0 - 180^o$ at different altitudes . . . 47
4.34 Required ΔV for a inclination change maneuver in range $0 - 10^o$ at different altitudes . . . 47
4.35 Required ΔV for a inclination change maneuver in range $200 - 1000\ km$ at different inclinations . . . 48
4.36 Required ΔV for a inclination change maneuver in range $200 - 1000\ km$ at different inclinations . . . 48
4.37 Required propellant mass % for a inclination change maneuver in range $0 - 10^o$ at different inclinations and altitudes with $I_{sp} = 150\ s$ . . . 49
4.38 Required propellant mass % for a inclination change maneuver in range $0 - 10^o$ at different inclinations and altitudes with $I_{sp} = 300\ s$ . . . 49
4.39 Required propellant mass % for a inclination change maneuver in range $0 - 10^o$ at different inclinations and altitudes with $I_{sp} = 1000\ s$ . . . 50
4.40 Required propellant mass % for a inclination change maneuver in range $0 - 10^o$ at different inclinations and altitudes with $I_{sp} = 3000\ s$ . . . 50

4.41 RAAN change maneuver representation [14] 51
4.42 Required ΔV for a RAAN change maneuver at different altitudes and $i = 98^o$ . . 51
4.43 Required ΔV for a RAAN change maneuver at different altitudes and $i = 98^o$ . . 52
4.44 Required ΔV for a RAAN change maneuver at different altitudes and $i = 63.43^o$ 52
4.45 Required ΔV for a RAAN change maneuver at different altitudes and $i = 63.43^o$ 53
4.46 Required ΔV for a RAAN change maneuver at different altitudes and $i = 45^o$ . . 53
4.47 Required ΔV for a RAAN change maneuver at different altitudes and $i = 45^o$ . . 54
4.48 Required propellant mass % for a RAAN change maneuver in range $0 - 10^o$ with $I_{sp} = 150\ s$ 54
4.49 Required propellant mass % for a RAAN change maneuver in range $0 - 10^o$ with $I_{sp} = 300\ s$ 55
4.50 Required propellant mass % for a RAAN change maneuver in range $0 - 10^o$ with $I_{sp} = 150\ s$ 55
4.51 Required propellant mass % for a RAAN change maneuver in range $0 - 10^o$ with $I_{sp} = 300\ s$ 56
4.52 Required propellant mass % for a RAAN change maneuver in range $0 - 10^o$ with $I_{sp} = 150\ s$ 56
4.53 Required propellant mass % for a RAAN change maneuver in range $0 - 10^o$ with $I_{sp} = 300\ s$ 57
4.54 Required ΔV for a RAAN change maneuver at different altitudes and $i = 98^o$ . . 57
4.55 Required ΔV for a RAAN change maneuver at different altitudes and $i = 98^o$ . . 58
4.56 Required ΔV for a RAAN change maneuver at different altitudes and $i = 63.43^o$ 58
4.57 Required ΔV for a RAAN change maneuver at different altitudes and $i = 63.43^o$ 59
4.58 Required ΔV for a RAAN change maneuver at different altitudes and $i = 45^o$ . . 59
4.59 Required ΔV for a RAAN change maneuver at different altitudes and $i = 45^o$ . . 60
4.60 Required propellant mass % for a RAAN change maneuver in range $0 - 10^o$ with $I_{sp} = 1000\ s$ 60
4.61 Required propellant mass % for a RAAN change maneuver in range $0 - 10^o$ with $I_{sp} = 3000\ s$ 61
4.62 Required propellant mass % for a RAAN change maneuver in range $0 - 10^o$ with $I_{sp} = 1000\ s$ 61
4.63 Required propellant mass % for a RAAN change maneuver in range $0 - 10^o$ with $I_{sp} = 3000\ s$ 62
4.64 Required propellant mass % for a RAAN change maneuver in range $0 - 10^o$ with $I_{sp} = 1000\ s$ 62
4.65 Required propellant mass % for a RAAN change maneuver in range $0 - 10^o$ with $I_{sp} = 3000\ s$ 63
4.66 RAAN variation due to J_2 perturbation at different inclinations and fixed altitude 63
4.67 RAAN variation due to J_2 perturbation at different altitudes and $i = 98^o$ 64
4.68 RAAN variation due to J_2 perturbation at different altitudes and $i = 63.43^o$ . . . 64
4.69 RAAN variation due to J_2 perturbation at different altitudes and $i = 45^o$ 65
4.70 RAAN regression velocity due to J_2 perturbation at different inclinations 65
4.71 Required waiting time in order to have $\Delta\Lambda = 60^o$ for satellites positioning 66
4.72 $\Delta\Omega_{rel}$ variation during the waiting time at $i = 98^o$ 66
4.73 $\Delta\Omega_{rel}$ variation during the waiting time at $i = 63.43^o$ 67
4.74 $\Delta\Omega_{rel}$ variation during the waiting time at $i = 45^o$ 67
4.75 $\Delta\Omega_{rel}$ variation due to J_2 perturbation at $i = 98^o$ considering Hohmann transfer 68
4.76 $\Delta\Omega_{rel}$ variation due to J_2 perturbation at $i = 98^o$ considering phasing transfer . 68
4.77 $\Delta\Omega_{rel}$ variation due to J_2 perturbation at $i = 63.43^o$ considering Hohmann transfer 69
4.78 $\Delta\Omega_{rel}$ variation due to J_2 perturbation at $i = 63.43^o$ considering phasing transfer 69
4.79 $\Delta\Omega_{rel}$ variation due to J_2 perturbation at $i = 45^o$ considering Hohmann transfer 70
4.80 $\Delta\Omega_{rel}$ variation due to J_2 perturbation at $i = 45^o$ considering phasing transfer . 70
4.81 Hohmann and phasing transfer comparison for a period of 30 days 71
4.82 Hohmann and phasing transfer comparison for a period of 365 days 71
4.83 Hohmann and phasing transfer comparison 72

4.84 $\Delta\Omega_{rel}$ variation due to J_2 perturbation at $i = 98^o$ considering Hohmann transfer 72
4.85 $\Delta\Omega_{rel}$ variation due to J_2 perturbation at $i = 98^o$ considering phasing transfer . 73
4.86 $\Delta\Omega_{rel}$ variation due to J_2 perturbation at $i = 63.43^o$ considering Hohmann transfer 73
4.87 $\Delta\Omega_{rel}$ variation due to J_2 perturbation at $i = 63.43^o$ considering phasing transfer 74
4.88 $\Delta\Omega_{rel}$ variation due to J_2 perturbation at $i = 45^o$ considering Hohmann transfer 74
4.89 $\Delta\Omega_{rel}$ variation due to J_2 perturbation at $i = 45^o$ considering phasing transfer . 75
4.90 Hohmann and phasing transfer comparison for a period of 30 days 75
4.91 Hohmann and phasing transfer comparison for a period of 365 days 76
4.92 Hohmann and phasing transfer comparison 76
4.93 $\Delta\Omega_{rel}$ variation due to J_2 perturbation at $i = 98^o$ considering Hohmann transfer 77
4.94 $\Delta\Omega_{rel}$ variation due to J_2 perturbation at $i = 98^o$ considering phasing transfer . 77
4.95 $\Delta\Omega_{rel}$ variation due to J_2 perturbation at $i = 63.43^o$ considering Hohmann transfer 78
4.96 $\Delta\Omega_{rel}$ variation due to J_2 perturbation at $i = 63.43^o$ considering phasing transfer 78
4.97 $\Delta\Omega_{rel}$ variation due to J_2 perturbation at $i = 45^o$ considering Hohmann transfer 79
4.98 $\Delta\Omega_{rel}$ variation due to J_2 perturbation at $i = 45^o$ considering phasing transfer . 79
4.99 Hohmann and phasing transfer comparison for a period of 30 days 80
4.100Hohmann and phasing transfer comparison for a period of 365 days 80
4.101Hohmann and phasing transfer comparison 81
4.102Representation of the argument of perigee change maneuver (angle of line rotation $\Delta\omega$ in red) [15] 82
4.103Required ΔV for a 180° argument of perigee change maneuver considering different altitudes of perigee and apogee 82
4.104Required ΔV for a 90° argument of perigee change maneuver considering different altitudes of perigee and apogee 83
4.105Required ΔV for a 45° argument of perigee change maneuver considering different altitudes of perigee and apogee 83
4.106Required propellant mass % for a 180° argument of perigee change maneuver at different altitudes of apogee and perigee with Isp = 150 s 84
4.107Required propellant mass % for a 180° argument of perigee change maneuver at different altitudes of apogee and perigee with Isp = 300 s 84
4.108Required propellant mass % for a 90° argument of perigee change maneuver at different altitudes of apogee and perigee with Isp = 150 s 85
4.109Required propellant mass % for a 90° argument of perigee change maneuver at different altitudes of apogee and perigee with Isp = 300 s 85
4.110Required propellant mass % for a 45° argument of perigee change maneuver at different altitudes of apogee and perigee with Isp = 150 s 86
4.111Required propellant mass % for a 45° argument of perigee change maneuver at different altitudes of apogee and perigee with Isp = 300 s 86
4.112Required propellant mass % in function of the $\Delta\omega$, considering a fixed perigee and Isp = 150 s 87
4.113Required propellant mass % in function of the $\Delta\omega$, considering a fixed perigee and Isp = 300 s 87
4.114Required propellant mass % in function of the $\Delta\omega$, considering a fixed apogee and Isp = 150 s 88
4.115Required propellant mass % in function of the $\Delta\omega$, considering a fixed apogee and Isp = 300 s 88
4.116Required propellant mass % for a 180° argument of perigee change maneuver at different altitudes of apogee and perigee with Isp = 1000 s 89
4.117Required propellant mass % for a 180° argument of perigee change maneuver at different altitudes of apogee and perigee with Isp = 3000 s 89
4.118Required propellant mass % for a 90° argument of perigee change maneuver at different altitudes of apogee and perigee with Isp = 1000 s 90
4.119Required propellant mass % for a 90° argument of perigee change maneuver at different altitudes of apogee and perigee with Isp = 3000 s 90

4.120Required propellant mass % for a 45° argument of perigee change maneuver at different altitudes of apogee and perigee with Isp = 1000 s 91
4.121Required propellant mass % for a 45° argument of perigee change maneuver at different altitudes of apogee and perigee with Isp = 3000 s 91
4.122Required propellant mass % in function of the $\Delta\omega$, considering a fixed perigee and Isp = 1000 s 92
4.123Required propellant mass % in function of the $\Delta\omega$, considering a fixed perigee and Isp = 3000 s 92
4.124Required propellant mass % in function of the $\Delta\omega$, considering a fixed apogee and Isp = 1000 s 93
4.125Required propellant mass % in function of the $\Delta\omega$, considering a fixed apogee and Isp = 3000 s 93
4.126Argument of perigee variation in function of the time considering $i = 98^o$ and the apogee fixed at 1000 km 94
4.127Argument of perigee variation in function of the time considering $i = 63.435^o$ and the apogee fixed at 1000 km 94
4.128Argument of perigee variation in function of the time considering $i = 45^o$ and the apogee fixed at 1000 km 95
4.129Argument of perigee variation in function of the time considering $i = 98^o$ and the perigee fixed at 200 km 95
4.130Argument of perigee variation in function of the time considering $i = 63.435^o$ and the perigee fixed at 200 km 96
4.131Argument of perigee variation in function of the time considering $i = 45^o$ and the perigee fixed at 200 km 96
4.132Argument of perigee variation in function of the apogee considering $i = 98^o$ and a period of 30 days 97
4.133Argument of perigee variation in function of the apogee considering $i = 63.435^o$ and a period of 30 days 97
4.134Argument of perigee variation in function of the apogee considering $i = 45^o$ and a period of 30 days 98
4.135Orbit raising: deployer worst case representation 101

List of Tables

1.1 Specific impulses of various propulsion system technologies 7

2.1 Deployers specifics 20
2.2 Platforms specifics 21
2.3 In-space propulsion overview [16] 22

3.1 Specifics of the Telesat constellation 23
3.2 Specifics of the Starlink constellation 25

4.1 Maneuvers summary 99
4.2 Ratios considering $\Delta V = 500\ \frac{m}{s}$ 100
4.3 Ratios considering $\Delta V = 1000\ \frac{m}{s}$ 100
4.4 Ratios considering $\Delta V = 1500\ \frac{m}{s}$ 101

Chapter 1

Space Propulsion

1.1 Generalities

Space propulsion is the technology used to provide the necessary thrust for a spacecraft to travel through space. It is the engine that propels the spacecraft and allows it to change velocity and trajectory. The propulsion system plays a critical role in determining the capabilities of a spacecraft, as it affects its speed, range, and payload capacity.
There are various types of space propulsion systems available, each with its own advantages and limitations. The most commonly used systems are chemical rockets, electric propulsion, and nuclear propulsion. Advancements in space propulsion technology are essential for future space exploration missions, as they can reduce travel times, increase payload capacities, and expand our reach into the solar system and beyond.
There are many performance characteristics that can be used to describe space propulsion, including:

$$thrust \qquad T = \dot{m}v + (P_e - P_s)A_e \tag{1.1}$$

$$effective\ discharge\ velocity \qquad c = c^*\, c_F \tag{1.2}$$

$$characteristic\ velocity \qquad c^* = \frac{P_{cc}A_g}{\dot{m}} \tag{1.3}$$

$$thrust\ coefficient \qquad c_F = \frac{T}{P_{cc}A_g} \tag{1.4}$$

$$specific\ impulse \qquad I_{sp} = \frac{T}{\dot{m}g} \tag{1.5}$$

1.2 Chemical propulsion

Chemical propulsion is a type of space propulsion that uses the energy released by a chemical reaction to produce thrust and propel a spacecraft.
In chemical propulsion, the fuel and oxidizer are combined in a combustion chamber, where high-temperature reaction product gases heated using the energy from a high-pressure combustion reaction leads to high-velocity exhaust that generates thrust.
As a result, these gases are expanded and accelerated to high speeds in a CD nozzle. Considering the high temperatures, it is crucial to cool down or insulate all the surfaces that are exposed to the gas flows. [17]

Chemical rocket propulsion systems can be divided into numerous categories based on the physical state of the propellant: Cold Gas, Liquid, Solid, Hybrid.

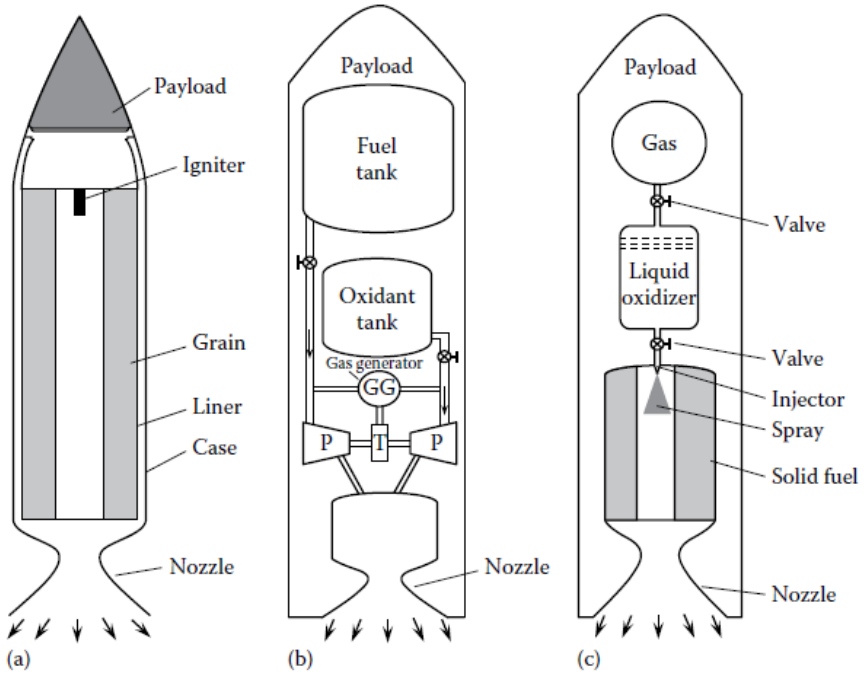

Figure 1.1: Three types of chemical rocket engines: (a) solid propellant, (b) liquid bi propellant, (c) hybrid propellant [1]

Chemical rockets are the most commonly used type of propulsion for launching spacecraft into orbit and beyond. They typically use liquid or solid propellants, and the choice of propellant depends on the specific mission requirements.

1.2.1 Liquid propellant rocket engines

In a liquid rocket engine, the fuel and oxidizer are stored separately in tanks on the spacecraft and are fed into the combustion chamber where they are mixed and burned to produce a high-velocity exhaust that generates thrust.
There are two types of liquids that can be used in the combustion chamber: mono- and bi-propellants. A liquid fuel plus a liquid oxidizer constitute the liquid bipropellant. When correctly catalysed, a monopropellant is a single liquid that includes both fuel and oxidising species and decomposes into hot gas.
The liquid propellants used in liquid rocket propulsion systems are typically highly reactive chemicals such as liquid hydrogen, kerosene, or hydrazine, which are used as fuel, and liquid oxygen, nitrogen tetroxide, or hydrogen peroxide, which are used as oxidizers.
Most low thrust, low total energy propulsion systems, such as those used to regulate the attitude of orbiting vehicles, frequently with more than one thrust chamber per engine, utilise gas pressure feed systems. Pump-fed liquid rocket systems are often utilised in applications requiring stronger thrusts and bigger fuel loads, such space launch systems.
One of the primary advantages of liquid rocket propulsion is that it provides a high specific impulse, which is a measure of the amount of thrust generated per unit of propellant consumed. Liquid rocket engines can be highly efficient, allowing spacecraft to reach higher speeds with less fuel than other propulsion systems.
Another advantage of liquid rocket propulsion is that it provides a high degree of control over the thrust and can be easily throttled up or down as needed. This allows for more precise maneuvers and greater flexibility during space missions.
However, liquid rocket propulsion also has some disadvantages. This type of engines are complex and require significant infrastructure and support systems, making them more expensive

to develop and operate. They are also prone to certain types of failures, such as leaks or combustion instability.
There are several approaches to cool the combustion chamber, including film cooling, regenerative cooling, ablative cooling, radiative cooling, and others.

1.2.2 Solid propellant rocket engines

A combination of fuel and oxidizer is cast into a solid form and moulded into the necessary geometry to make up solid rocket engines. In solid rocket engines, the propellant is generally composed of a fuel and oxidizer mixture that is intended to burn quickly and produce a high-velocity exhaust that produces thrust.
Some common types of fuel used in solid rocket propulsion include ammonium perchlorate, aluminum powder, and polybutadiene acrylonitrile.
The combustion chamber or case of solid propellant rocket engines houses the solid propellant. Different geometries of the grain form (circular, star, cross, etc.) result in various pressure profiles (progressive, regressive, neutral).
Solid rocket propulsion's simplicity and dependability are two of its main advantages. These engines are less complicated and have fewer moving parts than liquid rocket engines, making them less likely to malfunction. Also, because solid rocket engines do not need elaborate support systems or infrastructure, they are less expensive to manufacture and use.
Yet there are also some drawbacks to solid rocket propulsion. The same way that liquid rocket engines may be throttled, solid rocket engines cannot be stopped or controlled once they are fired. This may reduce the spacecraft's flexibility and ability to move while in flight.
The fact that solid rocket propulsion is less effective than liquid rocket propulsion is another drawback. As solid rocket engines often have lower specific impulses than liquid rocket engines, they require more fuel to produce the same amount of thrust.
Despite these constraints, solid rocket propulsion is nevertheless an essential tool for space exploration. It is frequently used to put spacecraft into orbit and for missions that need a lot of power, as those for ballistic missiles or boosters for big spacecraft.

1.2.3 Hybrid propellant rocket engines

In a hybrid rocket engine, a solid fuel is combined with a liquid oxidizer, such as liquid oxygen, to produce combustion and generate thrust.
In opposition to solid rocket engines, hybrid rocket engines may be throttled or even turned off as required. They become more adaptable and manageable during flight as a result. In addition, issues like leaks and combustion instability that can happen with liquid rocket engines are less likely to happen with hybrid rocket engines.
In comparison to conventional solid and liquid rocket propulsion systems, hybrid rocket propulsion systems provide a number of benefits. For example, they are more efficient than solid rocket engines, as the liquid oxidizer produces a larger specific impulse than the solid fuel. As a result, for a given amount of fuel, range and payload capacity may be increased.
Due to its simplicity of shutoff in an emergency, hybrid rocket propulsion systems are safer than conventional solid rocket engines. This qualifies them as being especially suitable for manned space missions.
These engines, despite their benefits, are still a more recent development than standard solid and liquid rocket engines. Yet, as hybrid rocket propulsion continues to be researched and developed, new uses and greater utilisation may result.

1.3 Electric propulsion

Electric propulsion is a type of space propulsion system that uses electrical energy to accelerate a propellant and generate thrust. Unlike traditional chemical propulsion systems that rely on the combustion of propellants, electric propulsion uses electrical energy to ionize a propellant, which is then accelerated using an electric field.
Electric propulsion technologies are far more effective than conventional chemical propulsion systems, enabling spacecraft to reach greater velocities while consuming less fuel. However because electric propulsion normally produces less thrust than chemical propulsion, it is unsuitable for applications that need for high thrust or quick acceleration, such as launch vehicles or spacecraft moving close to planets or moons.
These systems come in a variety of forms, such as ion thrusters, Hall effect thrusters, and pulsed plasma thrusters. All of these systems use electrical energy to accelerate a propellant and produce thrust, however each one does so in a somewhat different way.
High specific impulse, a measure of how well a propulsion system can utilise its fuel to create thrust, is one of the most crucial properties of electric propulsion.
In comparison to conventional chemical propulsion systems, electric propulsion systems are capable of generating particular impulses that are several times greater. For instance, some ion thrusters have specific impulses of over 10,000 seconds, as opposed to liquid rocket engines, which have specific impulses of about 450 seconds.
As electric propulsion systems have a high specific impulse compared to conventional chemical propulsion systems, they use a lot less fuel to reach a given velocity. Reduced spacecraft mass is a crucial factor in long-duration space missions, therefore this can be very relevant. Yet, compared to chemical propulsion systems, electric propulsion systems usually produce significantly less thrust. This implies that applications requiring high thrust or quick acceleration, like as launch vehicles or spacecraft moving close to planets or moons, are not well suited for electric propulsion. The applications where efficiency and long-term operation are more crucial than instantaneous acceleration are best suited for electric propulsion systems.
Electric propulsion also has the benefit of being able to operate for extended periods of time with little maintenance required. Electric propulsion systems don't have any moving components, and the ionisation and acceleration mechanisms are often relatively straightforward and dependable. Due to this, electric propulsion is a suitable option for far space missions and other scenarios involving difficult or impossible maintenance and repair.

1.4 Chemical and electric propulsion comparison

Considering a chemical propulsion system, the thrust is assumed instantaneous, hence, all the thrust is applied in an infinitesimal instant; conversely, if an electric propulsion system is considered, the thrust, which has a wide lower value than the chemical one, is assumed to be constantly applied.
The ΔV intensity is deeply linked to the Δm, which represent the propellant mass consumed, calculated from the Tsiolkovsky's formula:

$$\Delta V = I_{sp}\ g_0\ ln\left(\frac{m_i}{m_f}\right) \tag{1.6}$$

where:

- I_{sp}: specific impulse $[s]$
- g_0: sea level gravity acceleration $\left[\frac{m}{s^2}\right]$
- m_i: rocket initial mass $[kg]$
- m_f: rocket final mass $[kg]$

From this equation is possible to obtain the required propellant mass knowing the required ΔV in order to perform the desired maneuver.

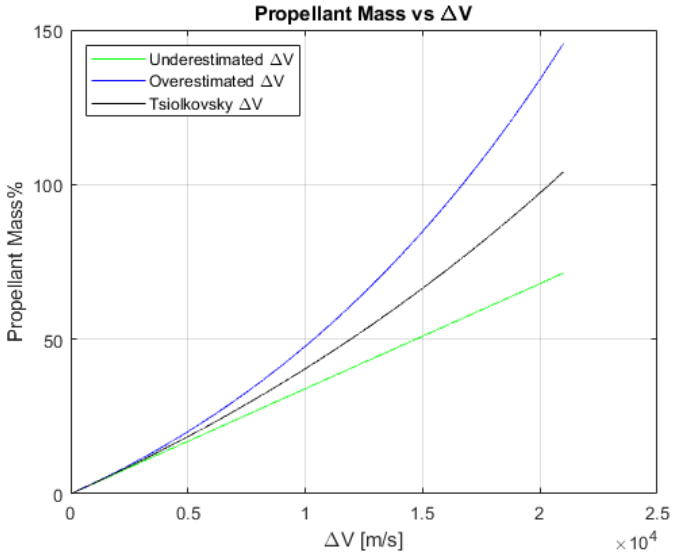

Figure 1.2: Propellant mass % in function of the required ΔV

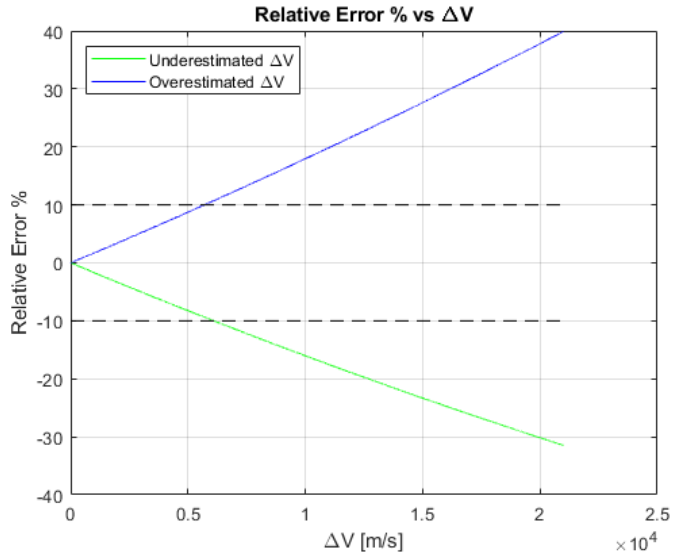

Figure 1.3: Relative Error % in function of the required ΔV - focus on $\pm$ 10 % relative error

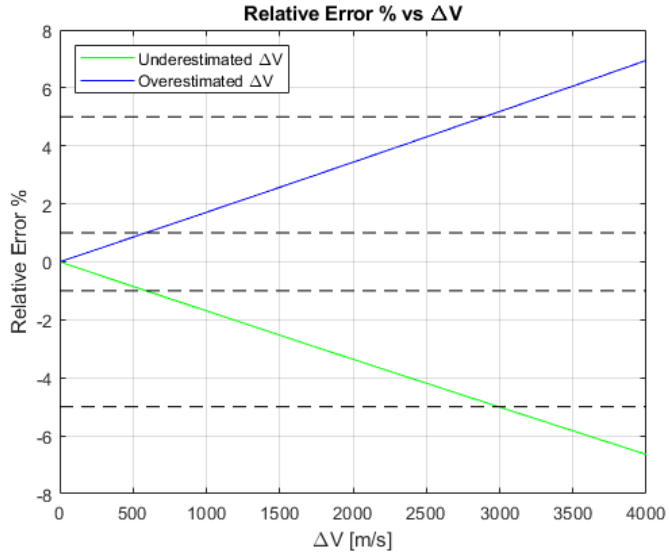

Figure 1.4: Relative Error % in function of the required ΔV - focus on $\pm$ 2 % and $\pm$ 5 % relative error

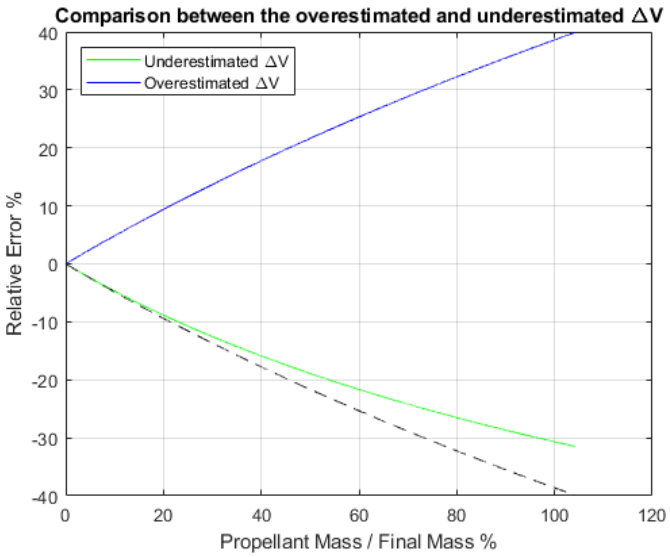

Figure 1.5: Comparison between the overestimated and underestimated ΔV respect to the Tsiolkovsky one

Another difference between this two propulsion systems lays in the specific impulse I_{sp} value, which results to be higher for the electric propulsion system, as it can be noticed from Table 1.1.

Technology	I_{sp} $[s]$
Cold Gas	$30 - 100$
Mono propellant	$150 - 250$
Bi propellant	$160 - 400$
Solid	$200 - 300$
Hybrid	$250 - 350$
Hall Effect	$800 - 1900$
Plasma	$500 - 3000$

Table 1.1: Specific impulses of various propulsion system technologies

Chemical thrusters have specific impulse values that are much lower than electric ones. However, the thrust values are significantly higher and this translates into missions of shorter duration compared to the duration which an electric thruster implies.
The required time to perform the maneuver induces variations in the orbital trajectories accessible using the two propulsion systems. Taking into account an *Hohmann transfer* and considering chemical propulsion to perform the maneuver, two impulses and two directions of the velocity vector results to be required. On the other side, considering electric propulsion it would be necessary to perform a spiral trajectory with various corrections of the velocity vector.

Since the two propulsion technologies imply different trajectories, the duration of the mission changes.
The way the trajectories change is implemented in the Edelbaum model, which approximates the planetary equations of Gauss concerning the variation in time of the orbital parameters.

$$\frac{da}{dt} \quad \frac{de}{dt} \quad \frac{di}{dt} \quad \frac{d\Omega}{dt} \quad \frac{d\omega}{dt} \quad \frac{d\nu}{dt} \tag{1.7}$$

Chapter 2

Mission analysis

2.1 Overview

Space mission analysis is a critical component in the planning and execution of any space mission. It implies the detailed examination and evaluation of all aspects of a space mission, including its objectives, requirements, design, operations, and safety considerations.
The goal of space mission analysis is to ensure that a mission is feasible, safe, and meets its scientific, technical, and operational objectives. It involves a range of disciplines, including aerospace engineering, systems engineering, mission operations, and safety analysis.
The analysis process typically begins with the definition of the mission objectives, followed by the development of a mission concept, and the evaluation of various mission options. This includes the selection of the launch vehicle, spacecraft design, trajectory, propulsion system, communication system, and ground support infrastructure.
Likewise, the choice regarding the propulsion system is a determinant part of the space mission.
Space mission analysis also includes risk assessment and contingency planning to ensure that the mission can be carried out safely and effectively. This involves identifying potential hazards, assessing their likelihood and consequences, and developing strategies to mitigate or manage risks.
Overall, space mission analysis plays a crucial role in ensuring the success of any space mission. It helps to identify and address potential issues before they become major problems, and ensures that the mission is executed safely, efficiently, and effectively.
A space mission is mainly divided in three steps: launch, deployment and satellites positioning. At the very beginning, a large number of launch solutions are explored in order to have a general overview. Then, a focus on how deploying and in-space transportation is performed by platforms will be faced.
Finally, everything concerning the positioning of the satellites in the final orbit will be addressed in the next chapters.

2.2 Launch

The launch can be faced either by transportation mission launcher or micro-launcher. The main difference lies in the fact that launchers missions are set usually about twice per year and deploy satellites at high LEO orbits, conversely, micro-launchers are a greater number and allow deployment in many more orbits.

2.2.1 Launchers

SpaceX - Falcon 9

The Falcon 9 is a two-stage rocket developed and manufactured by SpaceX and is used for a wide range of missions, including the launch of satellites into orbit, cargo resupply missions to the International Space Station (ISS), and even crewed missions to space.

The Falcon 9 rocket stands approximately 70 meters tall and has a diameter of 3.7 meters. The rocket is powered by nine Merlin engines on its first stage, which burns a mixture of liquid oxygen and rocket-grade kerosene (RP-1). The second stage is powered by a single Merlin engine that uses a similar propellant mixture.
One of the key features of the Falcon 9 is its reusability. Both the first and second stages of the rocket are designed to be recovered and reused for subsequent launches. This allows SpaceX to significantly reduce the cost of launch services, as well as increase the frequency of launches. The first stage of the rocket is recovered by landing it back on Earth, either on a landing pad or a drone ship in the ocean. The second stage is not currently recovered.

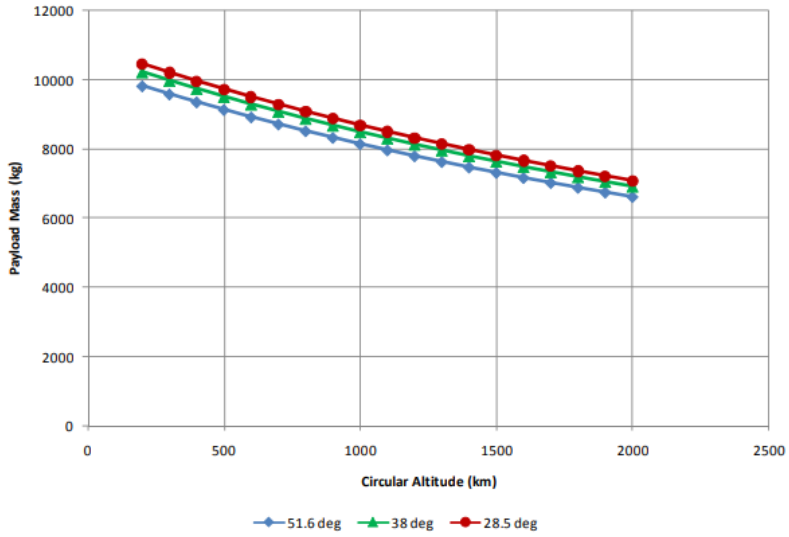

Figure 2.1: Capability of the Falcon 9 in function of the altitude for LEO orbits [2]

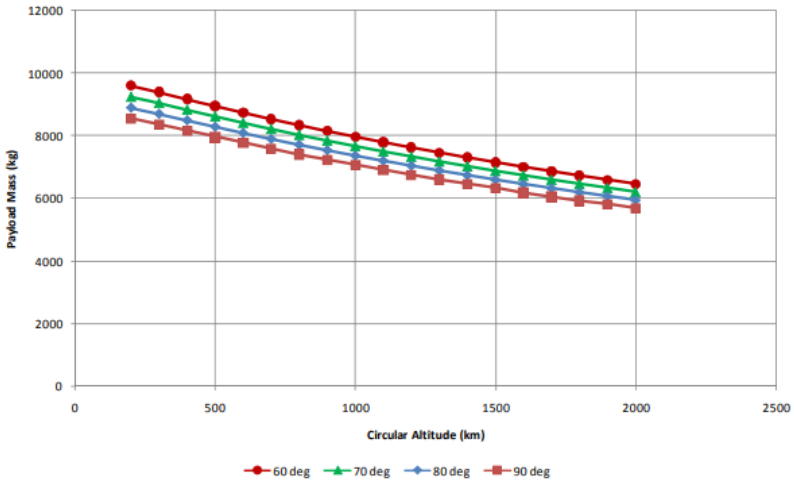

Figure 2.2: Capability of the Falcon 9 in function of the altitude for a circular polar orbit [2]

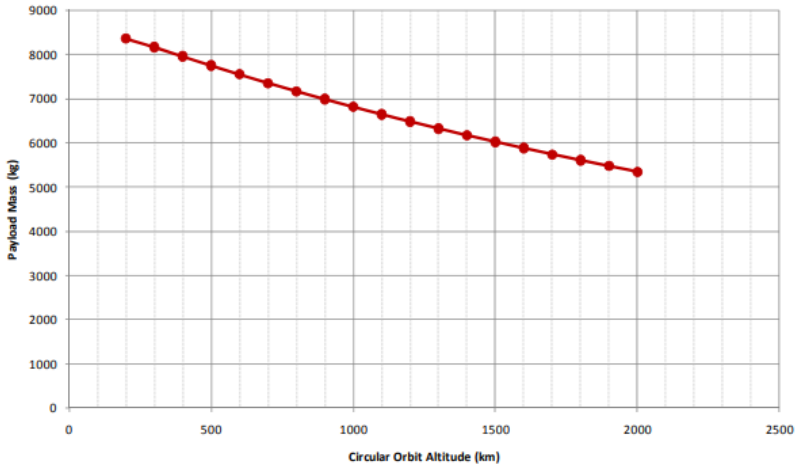

Figure 2.3: Capability of the Falcon 9 in function of the altitude for a SSO orbit [2]

Avio - Vega

Vega rocket is a small-to-medium-sized launch vehicle developed by the Italian aerospace company Avio. It is designed to provide launch services for small and medium-sized payloads, including satellites and scientific instruments.
The Vega rocket stands approximately 30 meters tall and has a diameter of 2.7 meters. It is a four-stage rocket, with three solid-fueled rocket motors for the first three stages and a liquid-fueled engine for the fourth stage.
The first stage of the Vega rocket is powered by a solid-fueled P80 rocket motor, which provides approximately 317500 kg of thrust at liftoff. The second stage is powered by a solid-fueled Zefiro 23 rocket motor, while the third stage is powered by a solid-fueled Zefiro 9 rocket motor. The fourth stage uses a liquid-fueled RD-843 engine, which is capable of multiple restarts and can provide up to 4750 kg of thrust.
One of the key advantages of the Vega rocket is its flexibility in terms of launch site and mission requirements. The Vega can be launched from a variety of locations, including the Guiana Space Centre in French Guiana and the European Spaceport in Kourou, as well as a mobile launch platform.

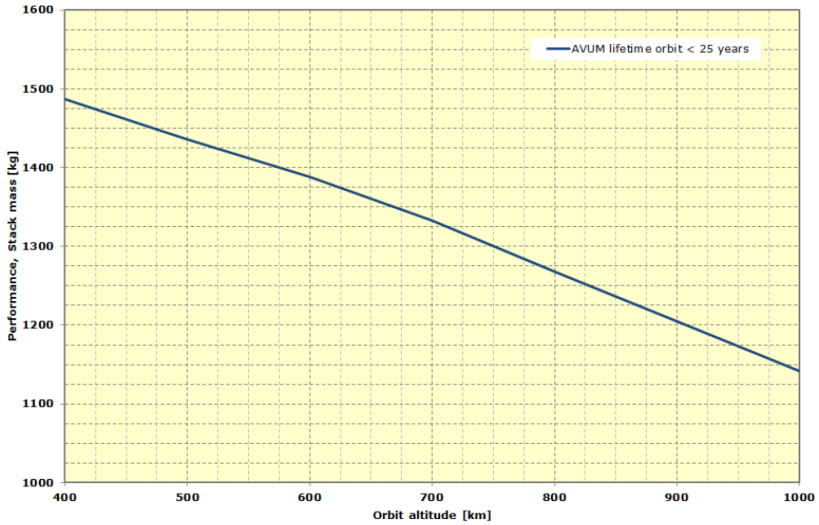

Figure 2.4: Capability of the Vega launcher in function of the altitude [3]

Relativity Space - Terran

The Terran 1 launcher is a small satellite launch vehicle developed by the American space company Relativity Space. It is designed to provide launch services for small and medium-sized payloads, including satellites and other space-based instruments.
The Terran 1 launcher is a two-stage rocket, with both stages powered by 3D-printed engines developed by Relativity Space. The rocket stands approximately 31.7 meters tall and has a diameter of 2.13 meters.
The first stage of the Terran 1 launcher is powered by seven Aeon 1 rocket engines, which are fueled by liquid methane and liquid oxygen. The second stage is powered by a single Aeon 1 engine.
The rocket's engines are designed to be reusable, and Relativity Space has stated that it aims to recover and reuse the first stage of the rocket in future missions.

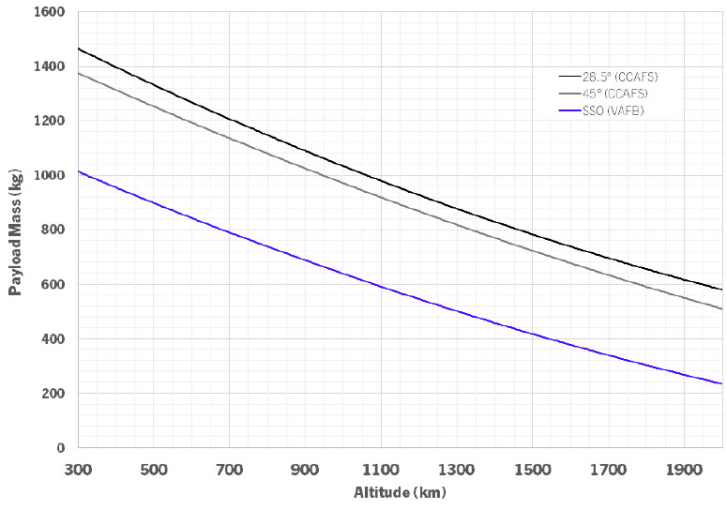

Figure 2.5: Capability of the Terran launcher in function of the altitude [4]

JAXA - Epsilon

The JAXA Epsilon launcher is a small solid-fueled rocket developed by the Japan Aerospace Exploration Agency (JAXA). It is designed to provide launch services for small scientific and observation satellites, with a payload capacity of up to 1200 kilograms to low Earth orbit.
The Epsilon launcher stands approximately 24 meters tall and has a diameter of 2.6 meters. It is a three-stage rocket, with the first two stages powered by solid-fueled rocket motors and the third stage powered by a liquid-fueled engine.
One of the key features of the Epsilon launcher is its autonomous launch capability, which allows it to be launched with a minimal ground crew. The rocket's onboard computer system handles many of the pre-launch checks and procedures, which helps to reduce launch costs and improve launch efficiency.

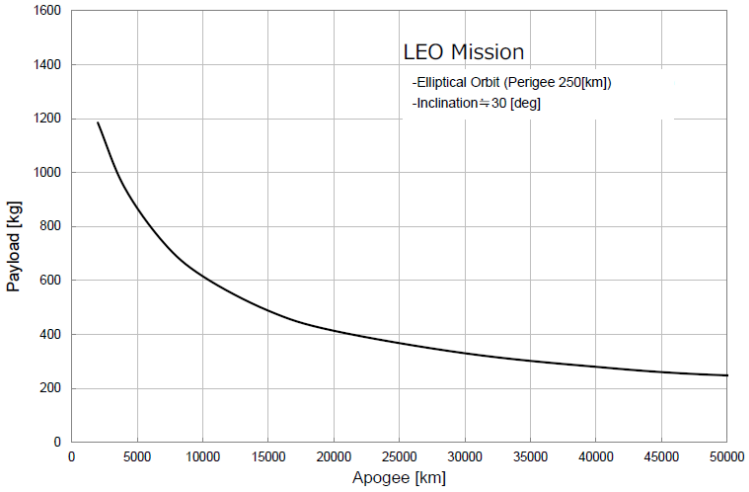

Figure 2.6: Capability of the Epsilon launcher in function of the orbit apogee [5]

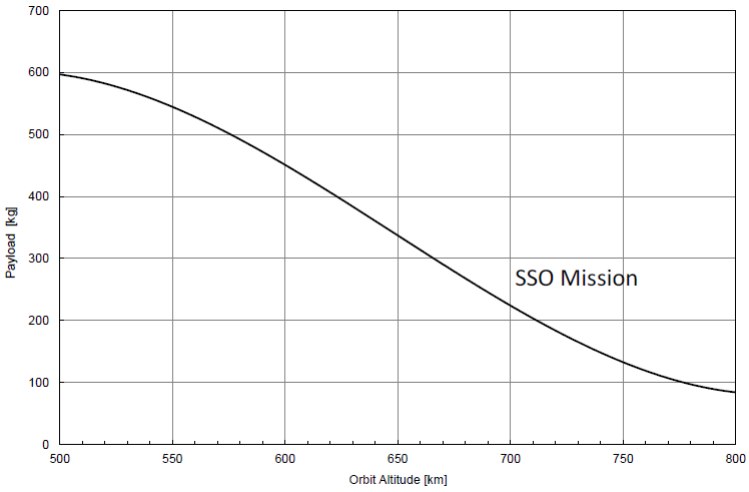

Figure 2.7: Capability of the Epsilon launcher in function of the altitude for a SSO mission [5]

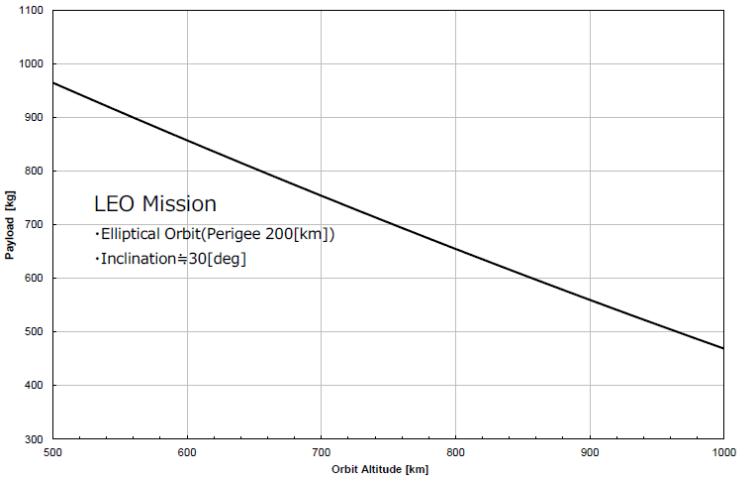

Figure 2.8: Capability of the Epsilon launcher in function of the altitude for an inclination equal to 30^o [5]

CALT - Long March 3A

The CALT Long March 3A (also known as Chang Zheng 3A) is a medium-size expendable launch vehicle developed by the China Academy of Launch Vehicle Technology (CALT), a subsidiary of the China Aerospace Science and Technology Corporation (CASC).
The Long March 3A rocket is approximately 52 meters tall and has a diameter of 3.35 meters. It uses a three-stage design, with the first stage powered by four YF-21C liquid-fueled engines, the second stage powered by one YF-24E liquid-fueled engine, and the third stage powered by a single YF-75 liquid-fueled engine. The rocket can carry payloads of up to 9000 kg to low Earth orbit, or up to 3500 kg to geostationary transfer orbit.

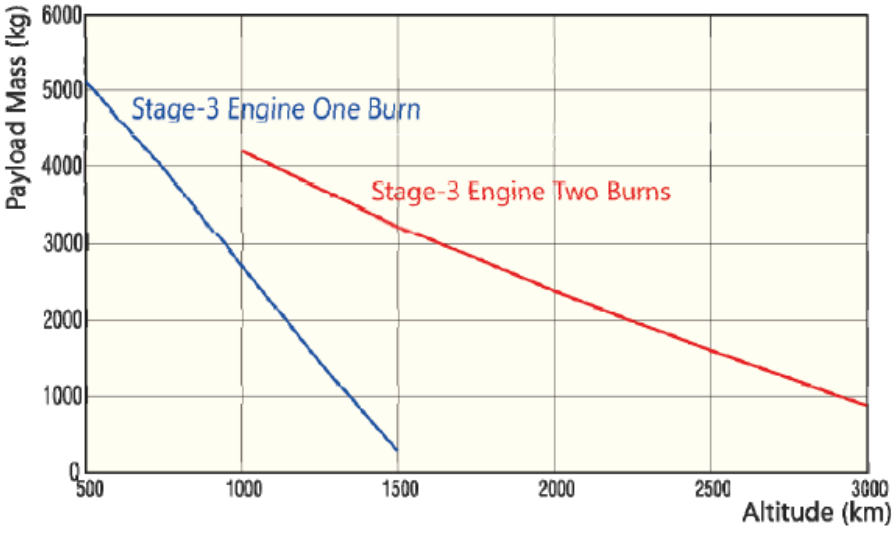

Figure 2.9: Capability of the LM3A launcher in function of the altitude [6]

2.2.2 Micro-launchers

ABL - RS1

The RS1 is designed to provide low-cost, high-performance launch services for a range of payloads, including small and medium-sized satellites.
The RS1 rocket is approximately 27 meters tall and 2 meters in diameter. It is powered by a single-stage engine that uses liquid oxygen and kerosene propellants to generate over 180000 kg of thrust at liftoff. The RS1 is designed to be a reusable rocket, with the first stage returning to the launch site for recovery and reuse.
One of the unique features of the RS1 is its mobile launch platform, which allows it to be transported and launched from a variety of locations. This gives the RS1 greater flexibility in terms of launch sites and enables it to respond quickly to changing customer needs.

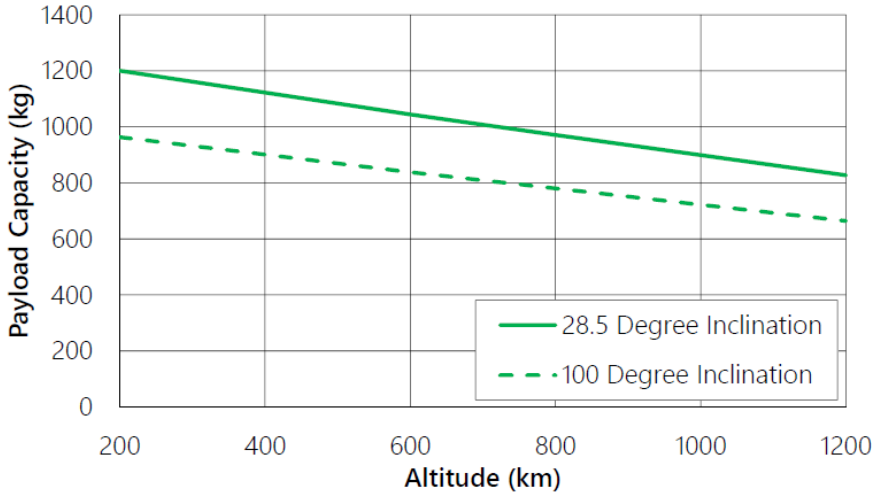

Figure 2.10: Capability of the RS1 launcher in function of the altitude [7]

Virgin Orbits - Launcher One

Virgin Orbit LauncherOne is an air-launched, two-stage rocket developed by the American space company Virgin Orbit. It is designed to provide launch services for small satellites weighing up to 300 kg, which can be deployed into low Earth orbit from a modified Boeing 747-400 aircraft called "Cosmic Girl".
LauncherOne uses a unique launch system that allows it to be carried to high altitude by the Cosmic Girl aircraft before being released and ignited in mid-air. This air-launch approach allows the rocket to avoid many of the constraints and limitations of traditional ground-based launch systems, such as range availability, launch scheduling, and weather constraints.
The rocket is approximately 21 meters long and has a diameter of 1.6 meters. The first stage is powered by a single NewtonThree engine, which is fueled by RP-1 kerosene and liquid oxygen. The second stage is powered by a single NewtonFour engine, which is also fueled by RP-1 kerosene and liquid oxygen.

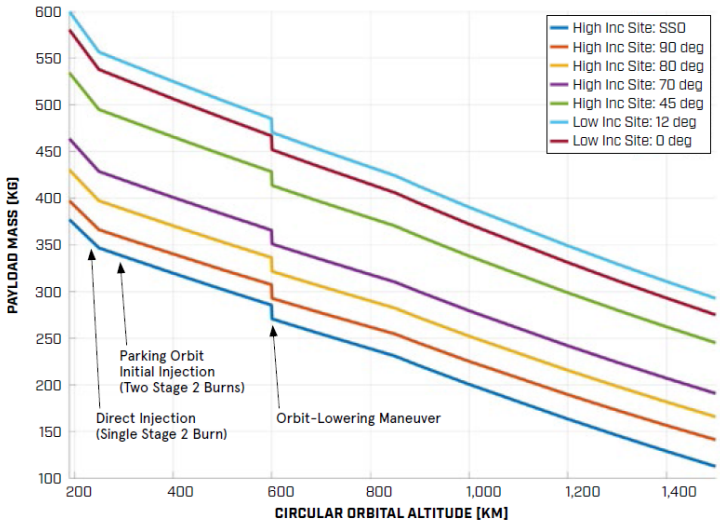

Figure 2.11: Capability of the Launcher One launcher in function of the altitude [8]

HyImpulse - SL1

Small Launcher One (SL1) is a small launch vehicle currently under development by the German aerospace startup HyImpulse Technologies. The rocket is designed to provide launch services for small satellites and payloads up to 500 kg to low Earth orbit.
The rocket is expected to use a combination of solid and liquid rocket motors, with a novel hybrid rocket engine being developed by HyImpulse for the first stage of the vehicle. The second stage is expected to use a liquid rocket engine. The rocket is also designed to be reusable, with plans to recover and refurbish both the first and second stages for multiple flights.

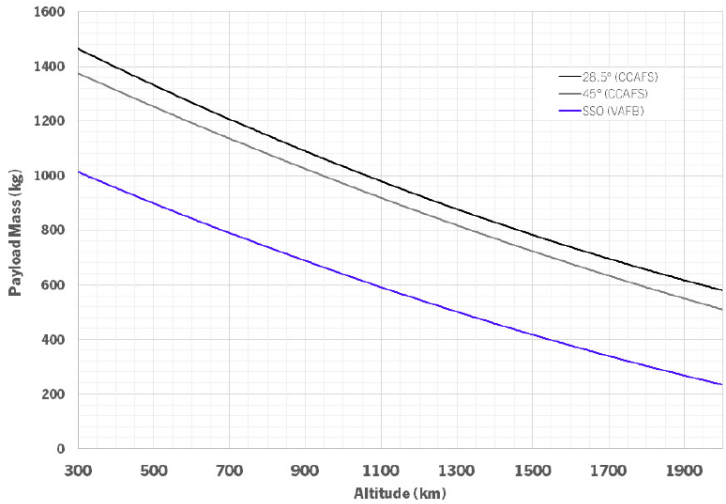

Figure 2.12: Capability of the Terran launcher in function of the altitude [9]

Rocket Lab - Electron

Rocket Lab Electron is a small, two-stage rocket developed by the American aerospace company Rocket Lab. It is designed to provide launch services for small satellites weighing up to 300 kg to a range of low Earth orbit (LEO) altitudes.
The Electron rocket is approximately 18 meters tall and 1.2 meters in diameter. The first stage is powered by nine Rutherford engines, which use electric motors instead of traditional combustion engines to pump propellants. The engines burn a mixture of liquid oxygen and kerosene to generate a thrust of 162 kN. The second stage is powered by a single vacuum-optimized Rutherford engine, which is also electrically-pumped and uses the same propellant mixture.
One of the unique features of the Electron rocket is its use of 3D printing technology to manufacture many of its components, which allows for rapid and cost-effective production of the rocket. The rocket is also designed to be fully reusable, with plans to recover and refurbish both the first and second stages for multiple flights.

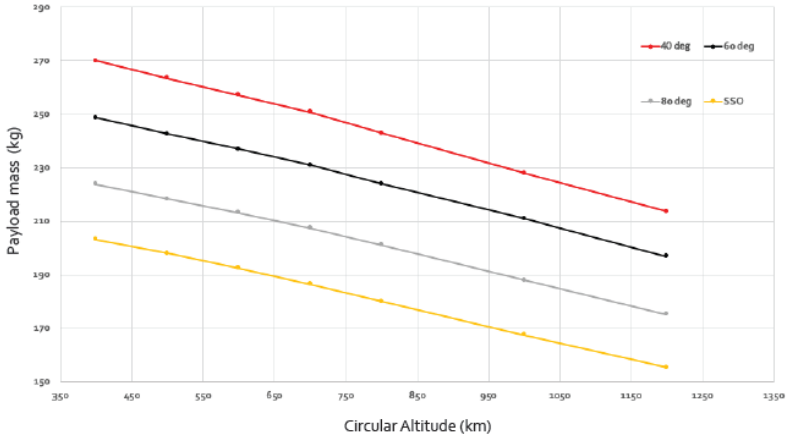

Figure 2.13: Capability of the Electron launcher in function of the altitude [10]

Firefly - Alpha

Firefly Alpha is a small, two-stage rocket developed by the American aerospace company Firefly Aerospace. It is designed to provide launch services for small satellites weighing up to 1,000 kg to a range of low Earth orbit (LEO) altitudes.
The Alpha rocket is approximately 29 meters tall and 1.82 meters in diameter. The first stage is powered by four Reaver engines, which use a mixture of liquid oxygen and kerosene to generate a thrust of approximately 1150 kN. The second stage is powered by a single Lightning engine, which also uses a mixture of liquid oxygen and kerosene to generate a thrust of approximately 29 kN.
One of the unique features of the Firefly Alpha rocket is its use of advanced composite materials in its construction, which makes the rocket lighter and more cost-effective to manufacture. The rocket is also designed to be fully reusable, with plans to recover and refurbish both the first and second stages for multiple flights.

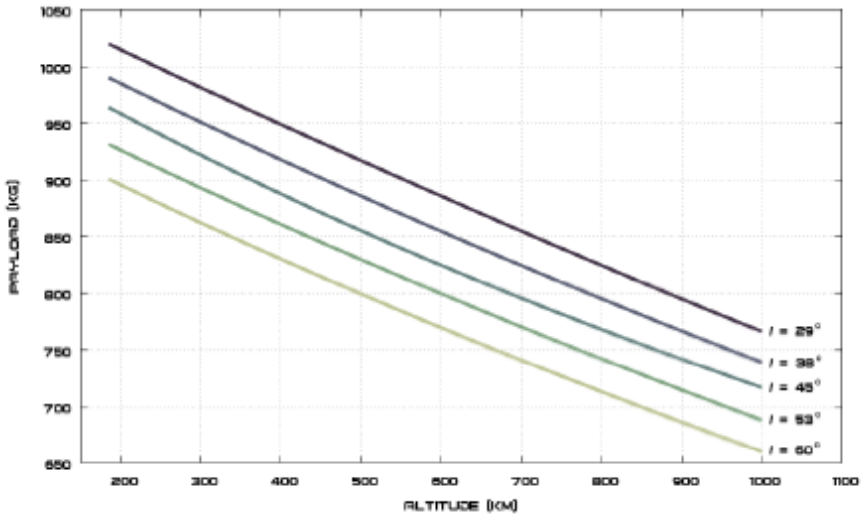

Figure 2.14: Capability of the ALPHA launcher in function of the altitude launching in east side [11]

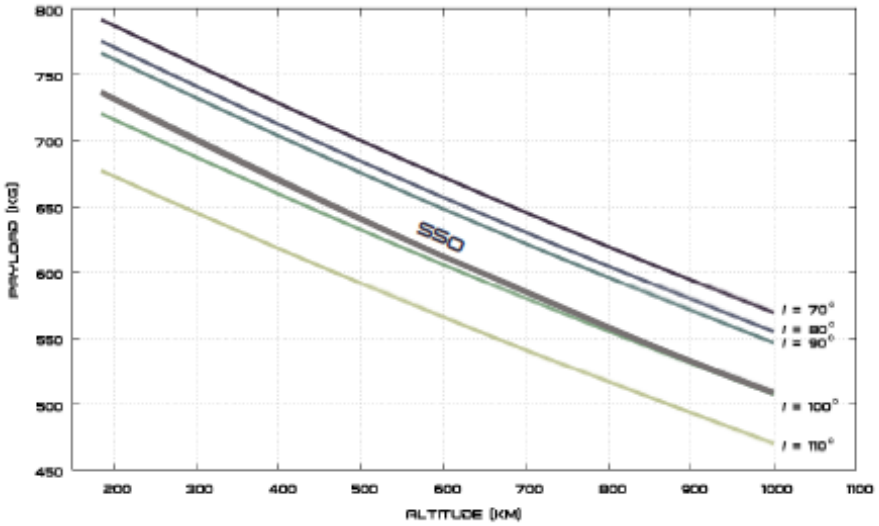

Figure 2.15: Capability of the ALPHA launcher in function of the altitude launching in west side [11]

Skyrora - Skyrora XL

Skyrora XL is a launch vehicle developed by Skyrora, a UK-based space technology company. The Skyrora XL is designed to be a versatile and reusable rocket capable of delivering payloads to a range of orbits. The Skyrora XL is a three-stage rocket that stands at 23 meters tall and has a diameter of 2.4 meters. The first stage is powered by four 3D printed engines, called LEO, and uses kerosene and hydrogen peroxide as propellants. The second stage is powered by a single LEO engine, while the third stage is equipped with a smaller LENA engine.
The Skyrora XL is capable of launching payloads of up to 315 kg to low Earth orbit (LEO) and up to 225 kg to Sun-synchronous orbit (SSO). The rocket can be launched from a range of locations, including vertical launch sites, horizontal launch sites, and even from ships.
One of the unique features of the Skyrora XL is its reusability. The first and second stages of the rocket are designed to be recovered and reused, which can significantly reduce the cost

of space launches. The rocket's advanced avionics and guidance systems also enable precision landings, making it possible to recover the stages with minimal damage.

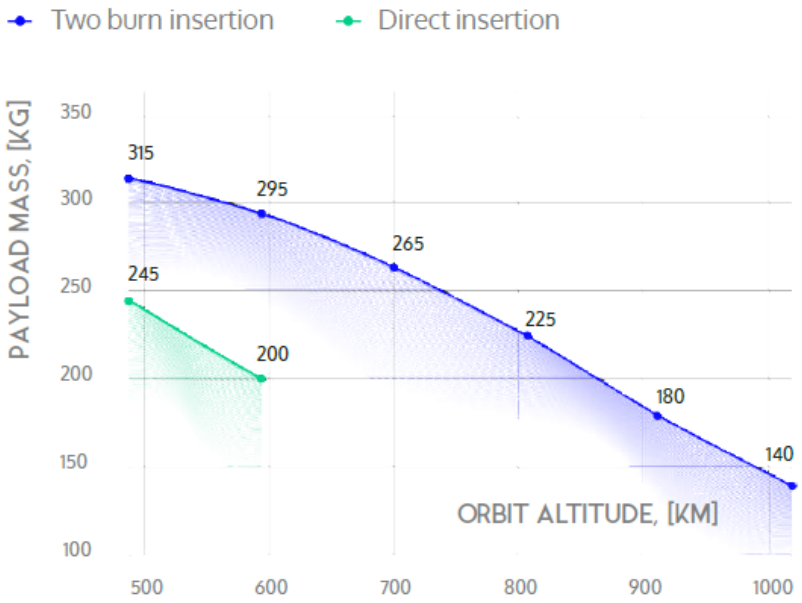

Figure 2.16: Capability of the Skyrora XL launcher in function of the altitude in SSO orbit [12]

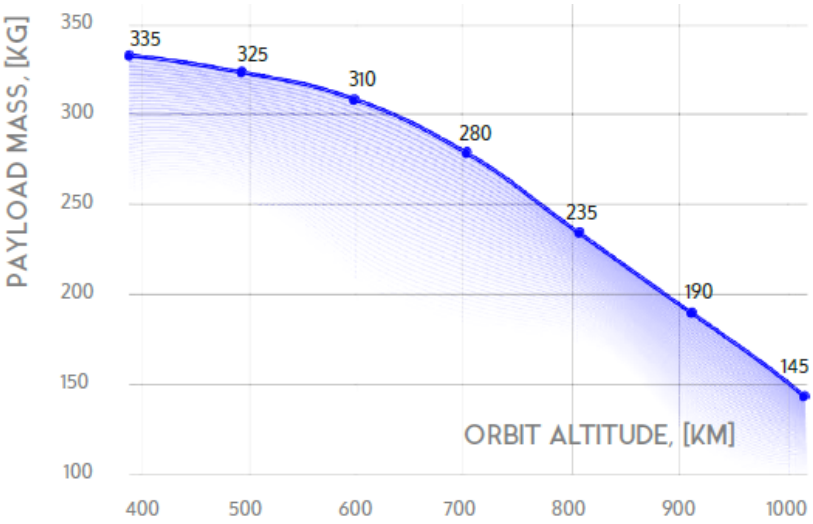

Figure 2.17: Capability of the Skyrora XL launcher in function of the altitude in polar orbit [12]

2.3 Deployment

2.3.1 Deployers

Satellite deployers, also known as satellite dispensers or deployer systems, are mechanisms used to release satellites from their launch vehicles into their intended orbit. These deployers are essential components of any space mission that involves launching one or more satellites.
There are several types of satellite deployers, each designed for different types of missions and spacecraft. Here are some of the most common types of satellite deployers:

- Spring-Loaded Deployers: These deployers use a spring-loaded mechanism to release the satellite from the launch vehicle. This type of deployer is simple and reliable and is often used for small and lightweight satellites
- Pneumatic Deployers: These deployers use compressed air or gas to release the satellite. They are commonly used for CubeSats and other small spacecraft
- Frangible Nut Deployers: These deployers use a frangible nut, which is a specially designed bolt that breaks when a specific force is applied. Once the nut is broken, the satellite is released from the launch vehicle.
- Separation Bolts: These deployers use explosive bolts to separate the satellite from the launch vehicle. The bolts are designed to break when a signal is sent from the ground, releasing the satellite.
- Rail-guided Deployers: These deployers use rails or tracks to guide the satellite into its intended orbit. They are commonly used for larger satellites that require precise positioning.

Satellite deployers are crucial components of any space mission that involves launching satellites. They ensure that the satellite is released into the correct orbit, allowing it to carry out its intended mission. The following agencies provides different solutions to launch and manage operations for in-orbit delivery.
For each company, various delivery system are shown, considering that the deployers have a own weight which has to be considered to launch a small satellite.

Company	Deployer	Mass $[Kg]$	PL mass $[Kg]$
Exolaunch [18]	EXOPOD 12U S1 — 1x12U	8	22
Exolaunch	EXOPOD 12U S2 — 2x6U	9.5	24
Exolaunch	EXOPOD 12U S3 — 2x3U, 1x6U	10	24
Exolaunch	EXOPOD 12U S4 — 4x3U	11	24
Exolaunch	EXOPOD 16U S1 – 1x16U	9	24
Exolaunch	EXOPOD 16U S2 – 2x8U	11	30
Gauss [19]	GPOD	1.9	5.2
ISISpace [20]	Deep Space	5	12
ISISpace	ISIPOD CubeSat	2	6
ISISpace	DuoPack CubeSat	5	12
ISISpace	QuadPack CubeSat	7.5	24

Table 2.1: Deployers specifics

2.3.2 Platforms

Satellite platforms are the basic structures or frameworks on which satellites are built. They provide the necessary structural support, power, and thermal control systems, as well as the communication and navigation subsystems required for a satellite to function in space. There are several types of satellite platforms [21], each designed to meet specific mission requirements:

- Geostationary Satellite Platform: These platforms are designed to orbit the Earth at an altitude of approximately 36000 kilometers, above the equator. They are often used for communication and weather observation applications, as they remain in a fixed position relative to the Earth's surface
- Low Earth Orbit (LEO) Satellite Platform: These platforms orbit the Earth at an altitude of approximately 2000 kilometers or less. They are used for a wide range of applications, including Earth observation, remote sensing, and scientific research
- Polar Orbiting Satellite Platform: These platforms orbit the Earth from pole to pole, passing over the Earth's surface at a fixed time each day. They are used for Earth observation and climate monitoring applications
- Medium Earth Orbit (MEO) Satellite Platform: These platforms orbit the Earth at an altitude of approximately 10000 to 20000 kilometers. They are used for navigation and global positioning applications, such as the GPS system
- Highly Elliptical Orbit (HEO) Satellite Platform: These platforms orbit the Earth in an elliptical path, ranging from a low altitude to a high altitude. They are used for communication and weather observation applications
- Lunar Orbiting Satellite Platform: These platforms are designed to orbit the Moon and are used for scientific research and exploration

The listed agencies provides platforms for payloads services.
In the table 2.2, all the products specifications are shown, considering the own mass of the system, the required propellant and, when available, details about the propulsion.

Company	Platform	Dry Mass $[Kg]$	Wet Mass $[Kg]$	PL mass $[Kg]$	T $[N]$	I_{tot} $[KNs]$
Avio [22]	SSMS	-	1100	400	-	-
D-Orbit [23]	Ion	-	-	150	-	-
Firefly [24]	ALPHA SUV	130	-	1000	4x0.07	-
MOOG [25]	COMET	348	501	1500	4x22	349
MOOG [26]	SL-OMV	48	65	155	6x1	38.3
Orbital ATK [27]	ESPAStar	430	740	1086	-	-
SAB Aerospace [28]	SSMS	-	-	450	-	-
Sidus Space [29]	LizzieSat	-	-	15	-	-
SNC [30]	SN-30L	50	-	20	-	-
SNC	SN-50L	80	-	50	-	-
SNC	SN-100L	115	-	100	-	-
SNC	SN-200L	200	-	150	-	-
Spaceflight [31]	Sherpa	-	-	700	-	-

Table 2.2: Platforms specifics

2.4 In-space propulsion

In-space propulsion refers to the propulsion systems that are used to move spacecraft once they are already in space. Unlike launch propulsion systems, which are designed to provide a high amount of thrust to get a spacecraft off the ground and into orbit, in-space propulsion systems are optimized for efficiency, allowing spacecraft to travel long distances and reach high speeds. In the following table is possible to see how in-space propulsion is performed by different companies.

Company	Propulsion	Technology	Propellant	I_{sp} $[s]$	T $[N]$
Aerojet Rocketdyne	Electric	Arcjet, Hall effect	various	2000	-
Astra	Electric	Hall effect	Krypton, Xenon	3500	0.06
Dawn Aerospace	Chemical	Liquid biprop	Nitrous + Propene	285	20
ExoTerra	Electric	Hall effect	Krypton, Xenon	1500	0.03
Exotrail	Electric	Hall effect	Xenon	1000	0.01
Moog	Chemical	Liquid mono/bi prop	Hydrazine	234	445
NanoAvionics	Chemical	Liquid monoprop	ADN	213	1
Orbion	Electric	Hall effect	Xenon	1370	0.02
QinetiQ	Electric	Gridded ion	Xenon	4000	0.25
Reach Space	Chemical	Liquid biprop	LOX + LH2	460	-
Safran	Electric	Hall effect	Xenon	1660	0.09
Stellar Exploration	Chemical	Liquid biprop	Hydrazine + LTO	300	5
Tethers Unlimited	Chemical	Liquid biprop	Hydrazine + NTO	300	1.2
T4i	Electric	Plasma	Iodine	650	-

Table 2.3: In-space propulsion overview [16]

Chapter 3

LEO Constellations

3.1 Telesat System

The Telesat constellation, which operates Ka band, includes 117 satellites distributed in two groups of orbits: the first group (polar orbits) consists of 6 circular orbital planes at an altitude equal to 1000 km, an inclination of 99.5 with at least 12 satellites in each plane; the second group (inclined orbits) has at least 5 circular orbital planes at an altitude of 1200 km with an inclination of 37.4^o, with a minimum of 10 satellites for each plane.

Shell	Inclination [^{o}]	Altitude [km]	Orbital planes	Sats in each plane
1	99.5	1000	6	12
2	37.4	1200	5	10

Table 3.1: Specifics of the Telesat constellation

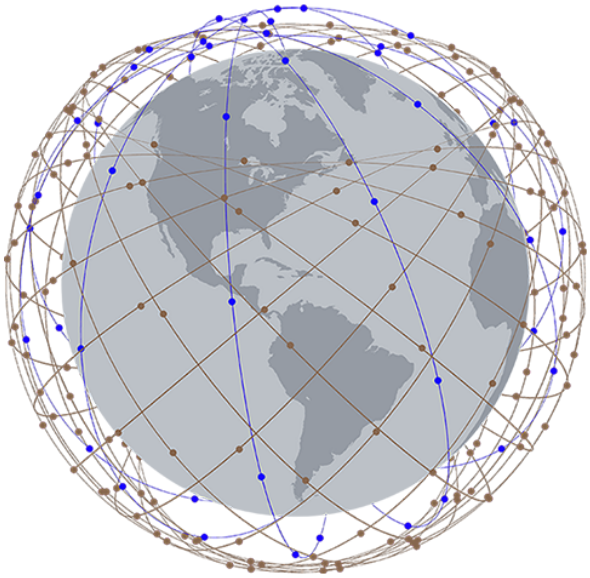

Figure 3.1: Telesat system representation [13]

Adjacent satellites, both within the same plane and within adjacent planes in the same set

of orbits and within the two orbital sets, communicate via inter-satellite optical links.
Crosslinks use allows any user to connect to the system from anywhere in the world, even when the user and gateway are not within line-of-sight of a satellite at the same time.
Each satellite will be a node of an IP network and carries on board an advanced digital communication payload with a directed radiating array (DRA).
This constellation features several gateways distributed evenly around the planet, each with multiple 3.5 $antennas; m$.
The ground station is located in Ottawa and monitors, coordinates and controls the processes of allocation, planning, scheduling and maintenance of radio communication.
Telesat operates on the 1.8 GHz frequency in the lower Ka-band spectrum ($17.8 - 20.2\ GHz$) for downlinks and on the 2.1 GHz frequency in the upper Ka-band spectrum ($27.5 - 30.0\ GHz$) for uplinks.

3.2 OneWeb System

The Oneweb constellation operates in the Ka-Ku band and includes 720 satellites distributed in 18 circular orbital planes at an altitude of 1200 km. Each orbital plane is inclined by 87^o.

Figure 3.2: OneWeb system representation [13]

Each satellite has a bent-pipe payload with 16 identical, non-steering and highly elliptical beams.
The footprint of these beams ensures users are within the line of sight of at least one satellite with an elevation angle greater than 55^o.
For each satellite there are two adjustable antennas, one of them is active and the second is a back-up one.
Each ray has a single Ka-band ray, which maps to the Ku-band. Channels in the return direction are at a frequency of 125 MHz while those in the forward direction are at a frequency of 250 MHz.
The OneWeb constellation uses the Ku band for user communications while the Ka is reserved for communication between gateways.
In particular, the $10.7 - 12.7\ GHz$ and $12.75 - 14.5\ Ghz$ bands are used for user downlink and uplink communication, while the $17.8 - 20.2\, Ghz$ and $27.5 - 30.0\ GHz$ bands are reserved for gateways.

The ground segment consists of 50 or more gateway stations with 2.4 m antennas.
This constellation has no inter-satellite links and services can only be offered in regions where users and ground stations are within line-of-sight of a satellite.

3.3 Starlink System

Starlink operates in the Ka and Ku bands and consists of 4408 satellites distributed in several orbit groups as described in the following table.

Shell	Inclination [^{o}]	Altitude [km]	Number of satellites
1	53.0	550	1584
2	70.0	570	720
3	97.6	560	348
4	53.2	540	1584
5	97.6	560	172

Table 3.2: Specifics of the Starlink constellation

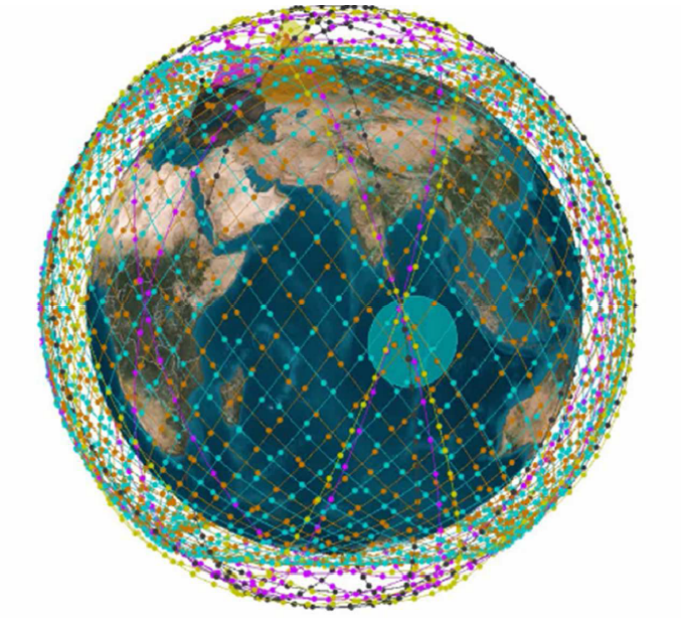

Figure 3.3: Starlink system representation [13]

Chapter 4

Orbital Mechanics

Orbital mechanics is the study of the motion of objects in space, such as planets, moons, and artificial satellites. It involves understanding the forces that affect the movement of these objects, including gravity, atmospheric drag, and other external forces, and how they interact with each other to determine the trajectory and orbit of an object.
One of the fundamental principles of orbital mechanics is Kepler's laws of planetary motion, which describe the elliptical paths that objects follow around a central body, such as a planet or star. These laws state that the orbit of an object around a central body is determined by its speed and distance from the central body, and that the object's speed and distance change as it moves through its orbit.
Another important concept in orbital mechanics is the idea of orbital transfers, which involve changing the trajectory of an object in space in order to reach a desired destination or orbit. This can be done using various techniques, such as a Hohmann transfer, which involves using the gravitational pull of a planet or other celestial body to change the trajectory of an object.
Orbital mechanics is essential for understanding and predicting the movements of objects in space, from the motion of planets and moons in our solar system to the complex trajectories of artificial satellites and spacecraft. It plays a critical role in space exploration and satellite operations, as well as in the design and control of space vehicles and missions

4.1 Orbital parameters

Eccentricity and *angular momentum* are the two factors that must be established in order to determine an orbit. These two are used to derive further parameters, including the *semimayor axis*, *specific energy*, and *period*. [14]
A third component, known as the *true anomaly*, which specifies the interval between the passage and the perigee, is necessary to spot a point on the orbit.
Then, it is determined where the equatorial plane and the orbital plane cross.
The *ascending node* is the point on the node line when the orbit crosses the equatorial plane from below.
The ascending node is the starting point of the node line vector (N), which radiates outward from there. The falling node is collocated at the other end of the node line, when the orbit descends beneath the equatorial plane. The initial Euler angle *right ascension of the ascending node* (Ω), is the angle between the positive X axis and the node line. It is a positive value that ranges from 0 to 360.
The *inclination* (i) measured anticlockwise around the node line vector from the equator to the orbit, is the angle between the orbital plane and the equatorial plane. The angle formed by the positive Z axis and the plane of the orbit's normal is known as the inclination. This parameter value lays in the range 0° - 180°.

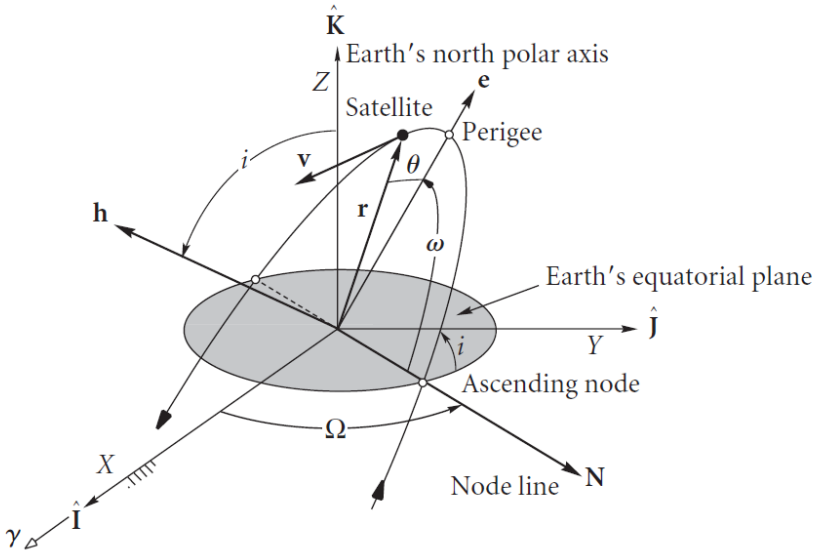

Figure 4.1: 3D orbit representation [14]

Finally, a summary of the the parameters that define a three dimensional orbit follows:

- h: specific angular momentum
- i: inclination
- e: eccentricity
- Ω: right ascension of the ascending node
- ω: argument of perigee
- θ: true anomaly

4.2 Orbital perturbations

Orbital perturbations are small deviations from the idealized motion of an object in orbit around another object, caused by various factors such as gravitational interactions with other objects, atmospheric drag, solar radiation pressure, and others. These perturbations can have a significant impact on the trajectory and stability of an object in orbit, and are therefore important to understand and account for in orbital calculations and space mission planning.
Understanding and modeling these perturbations is essential for predicting and controlling the motion of objects in orbit, and is important for a wide range of applications, including satellite operations, space mission planning, and astronomy.

4.2.1 Atmospheric drag

This perturbation is caused by the frictional forces exerted on an object in orbit by the thin upper atmosphere. Atmospheric drag causes the orbit to decay over time, leading to a gradual decrease in altitude and eventually causing the object to re-enter the atmosphere.
This type of orbital perturbation affects orbiting bodies up to 800 km, beyond this value it can be considered negligible.
During some missions, the atmospheric drag is exploited to lower the apses and circularize the orbit through a maneuver that does not involve the use of propellant.
Since this topic has already been extensively explored, it will not be dealt with in this thesis.

4.2.2 J_2 perturbation

These perturbations are caused by the oblateness, or flattening, of the central body around which an object is orbiting. The J_2 perturbation is the most significant perturbation due to oblateness and causes changes in the inclination and eccentricity of the orbit and also affects orbital parameters such as RAAN (Ω) and the perigee argument (ω) as it can be seen in the following expressions:

$$\frac{d\Omega}{dt} = -\frac{3}{2}\, n\, J_2 \left(\frac{R_E}{a(1-e^2)} \right)^2 cos(i) \tag{4.1}$$

$$\frac{d\omega}{dt} = \frac{3}{2}\, n\, J_2 \left(\frac{R_E}{a(1-e^2)} \right)^2 (4 - 5sen^2(i)) \tag{4.2}$$

where $n = \sqrt{\frac{\mu}{r^3}}$ is the *mean motion*.

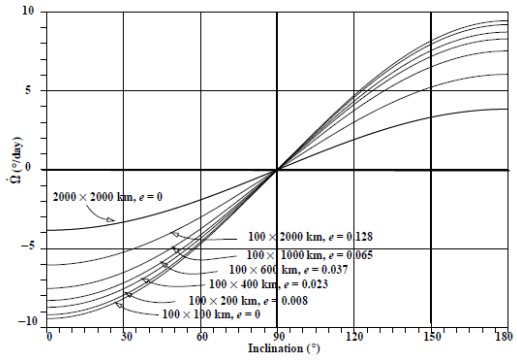

Figure 4.2: RAAN regression velocity depending on the orbital inclination

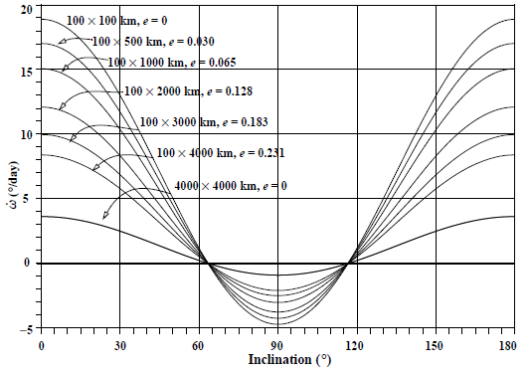

Figure 4.3: Argument of perigee advancement velocity depending on the orbital inclination

4.3 Orbital maneuvers

Orbital maneuvers transfer a spacecraft from one orbit to another. Orbital changes can results in high complexity maneuvers, such as the transfer from a low-earth parking orbit to an interplanetary trajectory. They can also be quite small, as in the final stages of the rendezvous of one spacecraft with another one.
The orbital transfer can be executed by using chemical or electric propulsion.
For each maneuver, a ΔV is required in order to attain the desired orbit and this critical parameter is quantified in $\frac{m}{s}$.

4.3.1 Orbit raising

Hohmann transfer

The Hohmann transfer is an impulsive maneuver. Hence, these maneuvers involve brief ignitions of the thrusters present on board the spacecraft in order to instantly vary the intensity and direction of the velocity vector.
Consequently, during the impulse, a fixed spacecraft position is assumed and only the velocity changes.
The impulsive maneuver is an idealization by means of which we can avoid having to solve the equations of motion with the rocket thrust included. The idealization is satisfactory for those cases in which the position of the spacecraft changes only slightly during the time that the maneuvering rockets act. This is true for high-thrust rockets with burn times short compared with the coasting time of the vehicle. Thus, each impulsive maneuver leads a change of velocity of the spacecraft, ΔV. This parameter means a change in the magnitude (pumping maneuver) or the direction (cranking maneuver) of the velocity vector, or both.

The Hohmann transfer is the most efficient two impulse maneuver in order to perform a transfer between two co-planar orbits sharing a common focus.
This maneuver consists of an elliptic orbit tangent to both circular orbits at is apse line as shown in Figure 4.4.
The periapsis and apoapsis of the transfer ellipse are the inner and outer circles radii, respectively. Obviously, only one-half of the ellipse is covered during the maneuver, which can take place in either direction, from the inner to the outer circular orbit, as well as from the outer to the inner one.

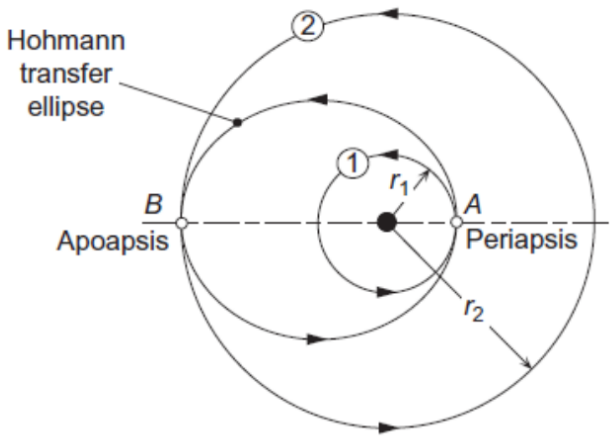

Figure 4.4: Hohmann transfer [14]

Known:

- Initial circular orbit radius, r_i
- Final circular orbit radius, r_f
- Earth radius, $R_E = 6371.14\ km$
- Earth's gravitational constant, $\mu = 398600\ \frac{km^3}{s^2}$

First of all, the initial circular velocity in calculated as:

$$v_i = \sqrt{\frac{\mu}{r_i}} \tag{4.3}$$

then, the final circular velocity is obtained by using:

$$v_f = \sqrt{\frac{\mu}{r_f}} \tag{4.4}$$

considering the transfer orbit, the eccentricity comes from:

$$e_{Hoh} = \frac{r_f - r_i}{r_f + r_i} \tag{4.5}$$

and consequently all the other parameters, such as the angular momentum:

$$h_{Hoh} = \sqrt{2\mu}\sqrt{\frac{r_i\, r_f}{r_i + r_f}} \tag{4.6}$$

the velocity at the transfer orbit perigee:

$$v_p = \frac{h_{Hoh}}{r_i} \tag{4.7}$$

the velocity at the transfer orbit apogee:

$$v_a = \frac{h_{Hoh}}{r_f} \tag{4.8}$$

the first ΔV applied is equal to:

$$\Delta V_1 = v_p - v_i \tag{4.9}$$

and the second ΔV, applied at the transfer orbit apogee, results to be:

$$\Delta V_2 = v_f - v_a \tag{4.10}$$

finally, the total ΔV required to perform the maneuver is:

$$\Delta V_{tot} = \Delta V_2 + \Delta V_1 \tag{4.11}$$

Results of the Hohmann transfer from low to high orbits are shown as follows:

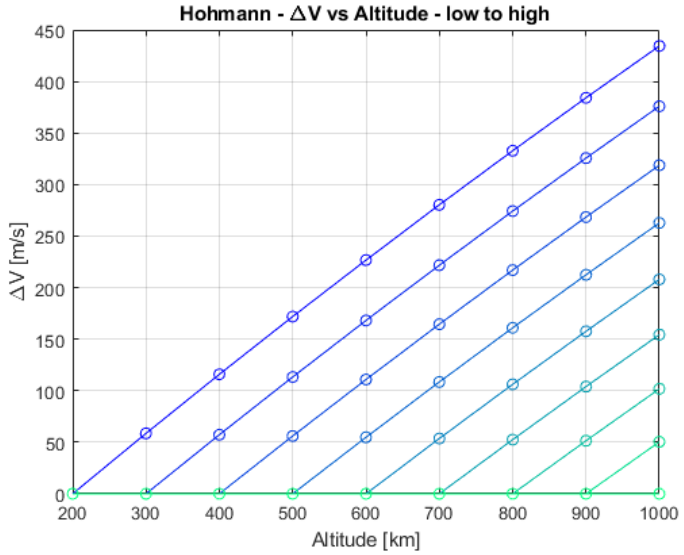

Figure 4.5: Required ΔV for an Hohmann transfer from low to high orbits

Spiral transfer

The thrust values obtained with electric propulsion are considerably lower than those obtainable with chemical engines. Furthermore, the thrust of an electric thruster is delivered in a continuous and not impulsive way as happens for chemicals.

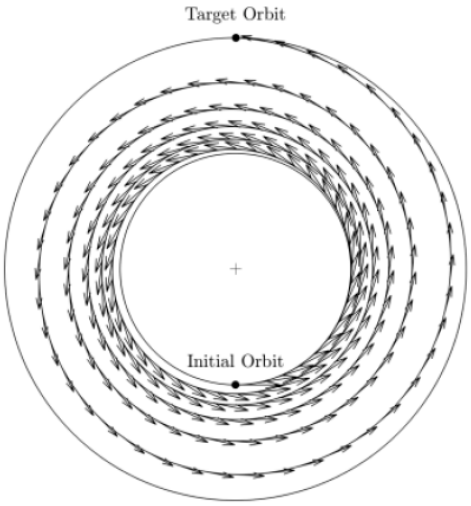

Figure 4.6: Spiral transfer [14]

The required ΔV, taken as the difference between final and initial velocity, in function of the orbits altitude is shown in the following plot.

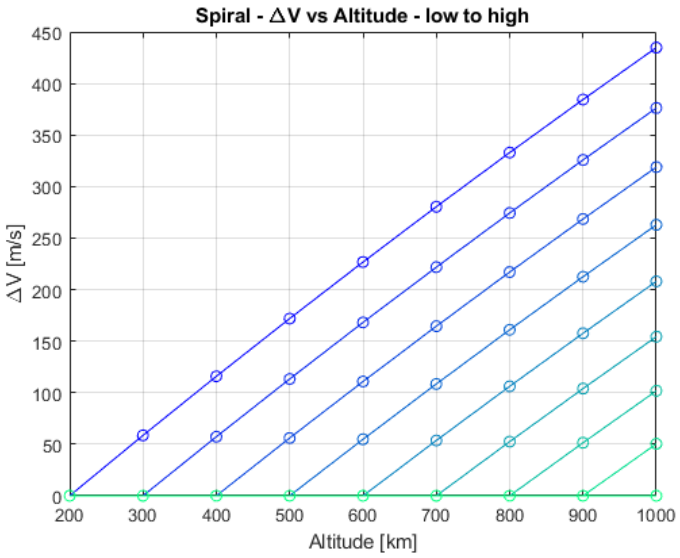

Figure 4.7: Required ΔV for a spiral transfer from low to high orbits

Hohmann and Spiral transfer comparison

Since the Hohmann transfer is the most efficient orbit transfer, a comparison with the Spiral maneuver is studied, with a focus on the difference in required ΔV varying the orbit altitude.

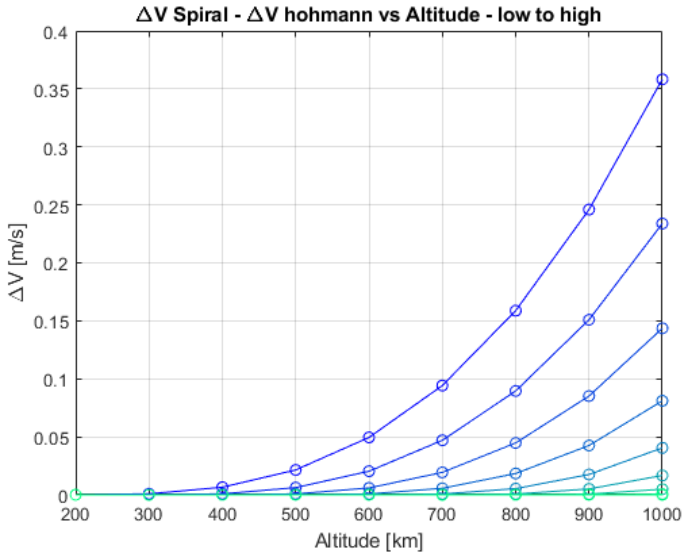

Figure 4.8: Difference in terms of ΔV between Hohmann and spiral transfer from low to high orbits

4.3.2 De-orbiting

In this paragraph, the previous maneuvers are faced considering high to low orbit transfer cases. Theoretical study has already been covered. Hence, results of this second part follow.

Hohmann transfer

The Hohmann transfer from high to low orbit has been studied too. Results show how the difference between this case and the *low to high orbit* one are numerically the same with small negligible variations.

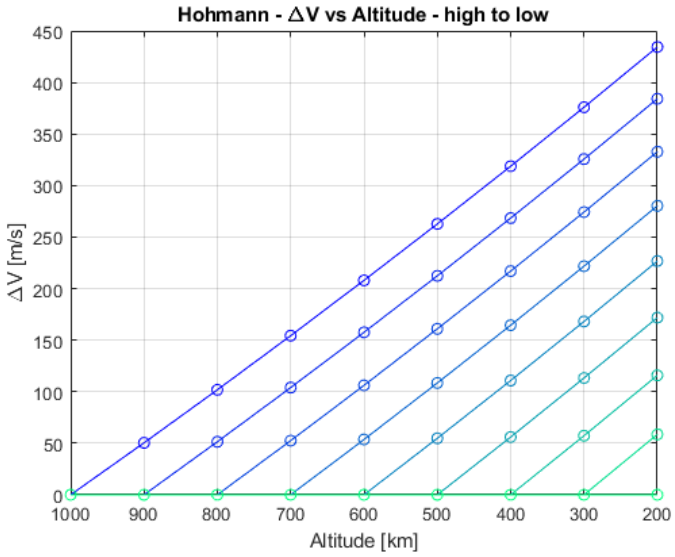

Figure 4.9: Required ΔV for an Hohmann transfer from high to low orbits

Spiral transfer

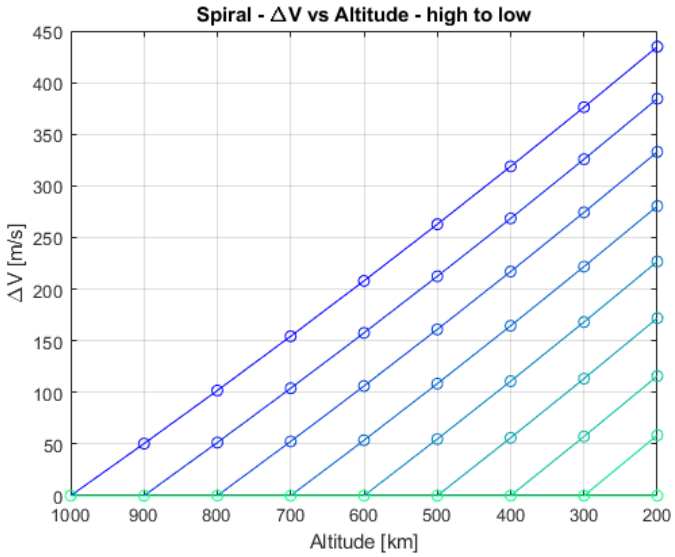

Figure 4.10: Required ΔV for a spiral transfer from high to low orbits

Hohmann and Spiral transfer comparison

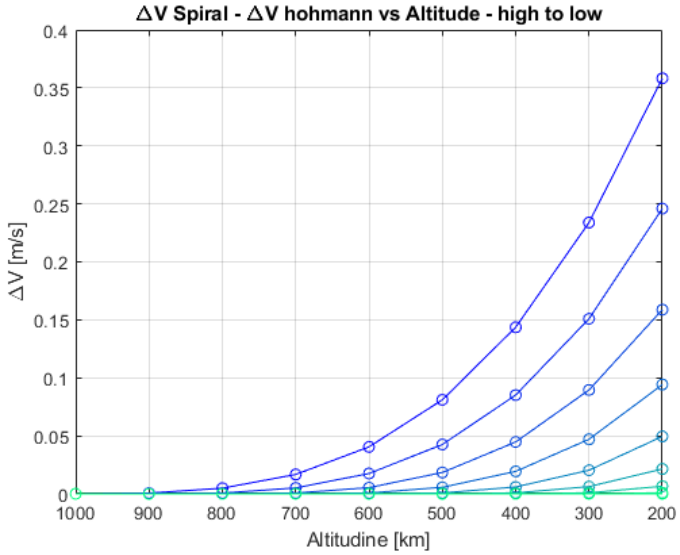

Figure 4.11: Difference in terms of ΔV between Hohmann and spiral transfer from high to low orbits

Chemical thruster - required propellant mass

Finally, considering the fact that the two cases, *orbit raising* and *de-orbiting*, do not show significant differences, the required propellant masses in order to perform the first case maneuvers are plotted, varying the I_{sp} considered.

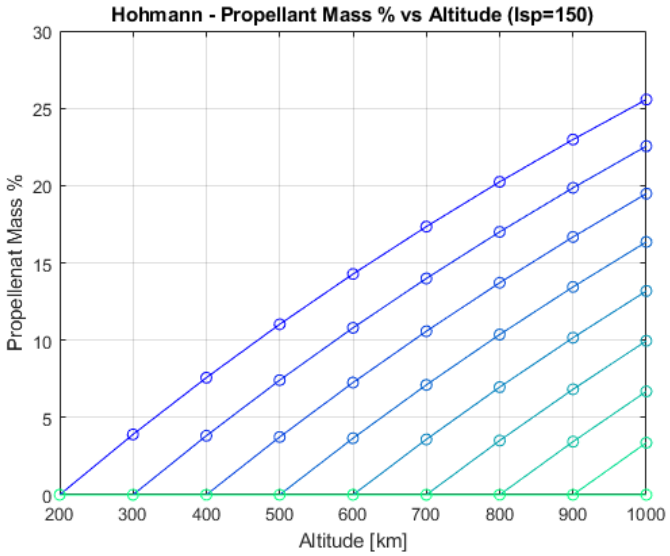

Figure 4.12: Required propellant mass % for an Hohmann transfer in range $200 - 1000\ km$ with $I_{sp} = 150\ s$

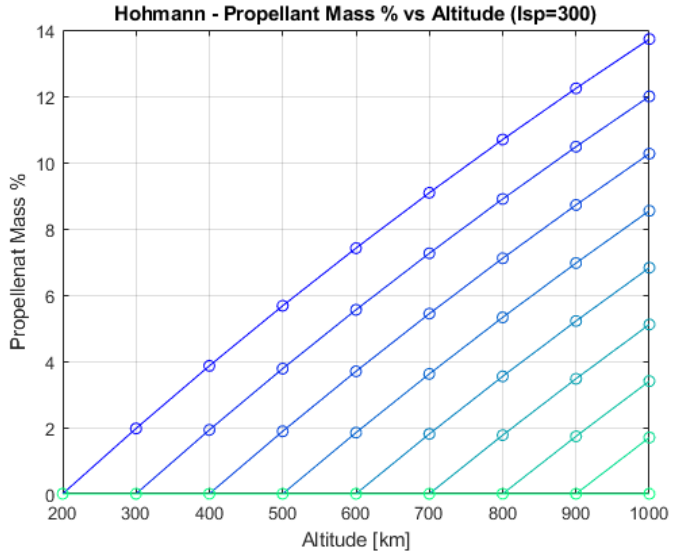

Figure 4.13: Required propellant mass % for an Hohmann transfer in range $200 - 1000\ km$ with $I_{sp} = 300\ s$

Electric thruster - required propellant mass

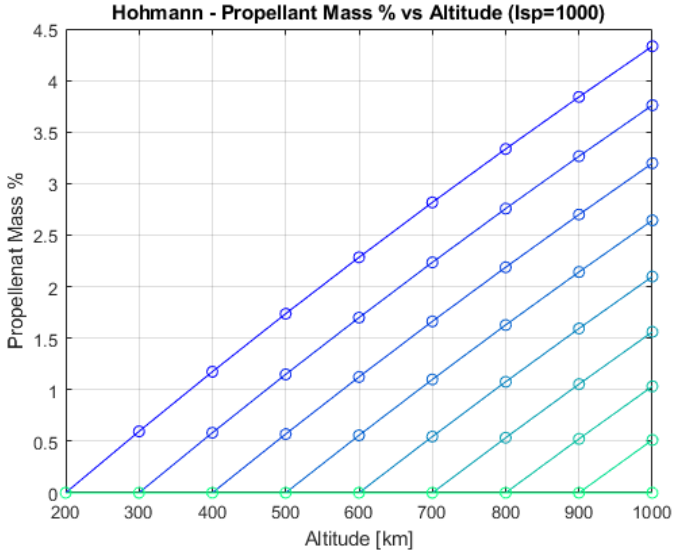

Figure 4.14: Required propellant mass % for an Hohmann transfer in range $200 - 1000\ km$ with $I_{sp} = 1000\ s$

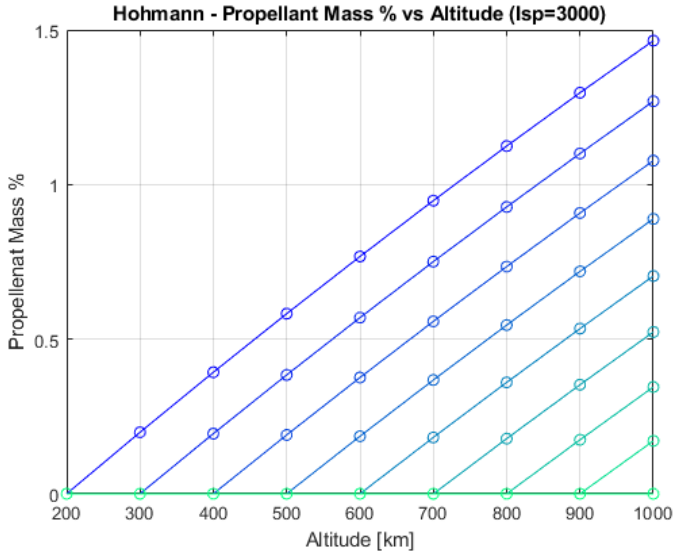

Figure 4.15: Required propellant mass % for an Hohmann transfer in range $200 - 1000\ km$ with $I_{sp} = 3000\ s$

4.3.3 Access to space

In order to introduce how the space is accessed, the ABL RS1 launcher has been considered. The following graphs shows the initial mass (dark line) carriable by the RS1 launcher at different altitudes and all the curves refer to the final mass after an Hohmann maneuver considering different specific impulses.

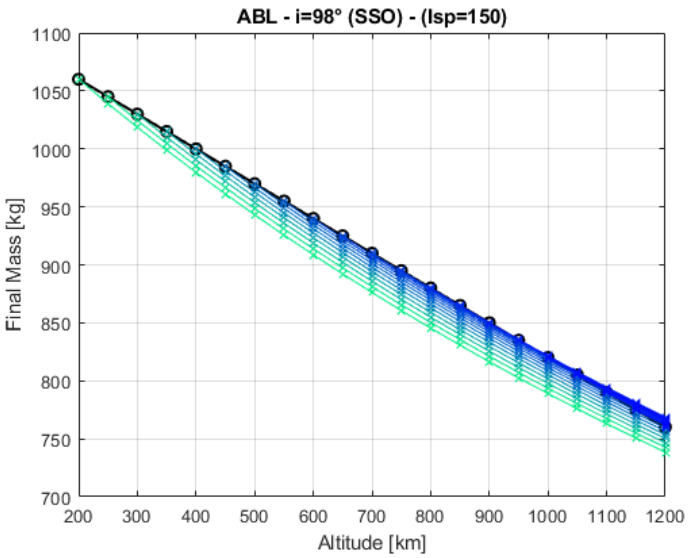

Figure 4.16: Final mass in function of the altitude considering Hohmann transfer and $I_{sp} = 150\ s$

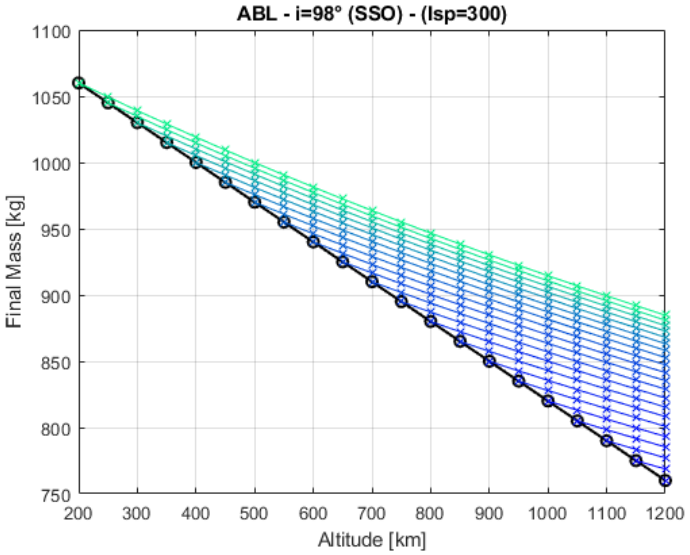

Figure 4.17: Final mass in function of the altitude considering Hohmann transfer and $I_{sp} = 300\ s$

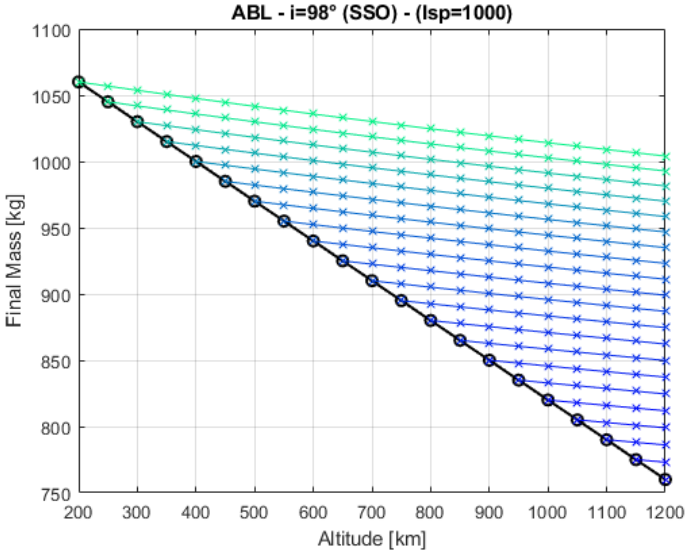

Figure 4.18: Final mass in function of the altitude considering Hohmann transfer and $I_{sp} = 1000\ s$

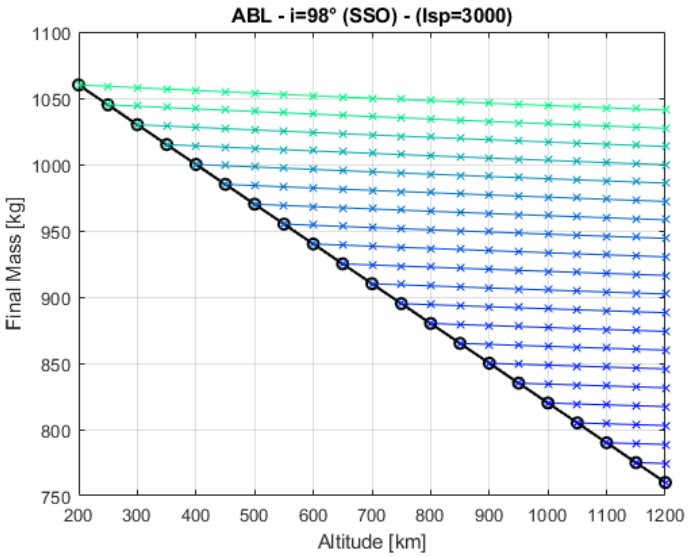

Figure 4.19: Final mass in function of the altitude considering Hohmann transfer and $I_{sp} = 3000\ s$

4.3.4 Phase change maneuver

A Phasing maneuver consists of a two-impulse Hohmann transfer from and back the same orbit, as it can be seen in Figure 4.20.

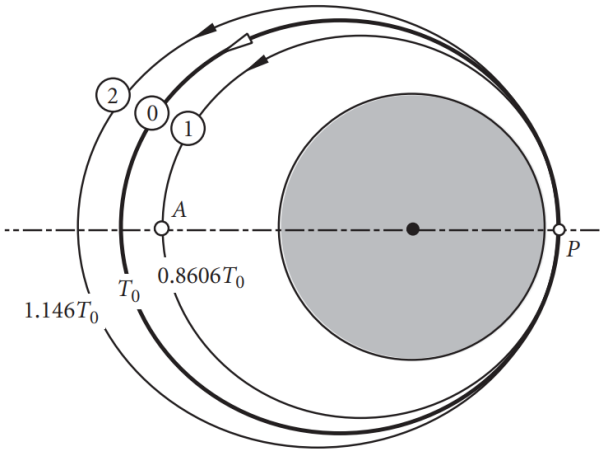

Figure 4.20: External and internal Phasing maneuver [14]

The transfer ellipse is the phasing orbit with a period selected to return the spacecraft to the initial orbit within a specified time. Phasing maneuvers are used to change the position of a spacecraft in its orbit. If two spacecraft, destined to rendezvous, are at different locations in the same orbit, then one of them may perform a phasing maneuver in order to catch the other one.
In the same way, a phasing maneuver could be executed in order to displace different satellites deployed in a common point of an orbit.
To recover the phase difference between the two orbits, it is possible to perform internal or external phasing according to the convenience in ΔV dictated by the phase difference of the two spacecaft.

In terms of fuel, there is no difference between the two maneuvers; the distinction takes place on the basis of the direction in which the ΔV is performed.
In the internal phase change maneuver it has to be verified that the perigee altitude is greater than 200 km in order to avoid the collision with Earth as shown in the Figure 4.24.

As mentioned before, it is possible to analyze the opposite situation of a ordinary phasing maneuver and this is the aim of this thesis: the deployment of the satellites takes place in the same orbital position and the objective is to distribute them along the orbit by means of a phasing maneuver, in positions of interest.

Taking into account two satellites released in the same orbital position, the following calculations are necessary for positioning them at a desired longitude difference ($\Delta\Lambda$).
Initially, the orbital velocity is found at the altitude of interest:

$$v = \sqrt{\frac{\mu}{r}} \tag{4.12}$$

It is possible to establish a number of orbits (n) for the phasing in order to decrease the required ΔV to complete the maneuver.
However, this leads to an increase in the mission time and a time and cost analysis must be performed to establish the optimal maneuver configuration.

After that, it is possible to calculate the the orbital transfer period:

$$T_{ph} = \frac{1}{n}\frac{2n\pi - \Delta\Lambda}{w} \tag{4.13}$$

where $w = \frac{v}{r}\ [\frac{rad}{s}]$, con $r = R_E + altitude = 6378.14 + altitude\ [km]$.

From the phasing period, it is now possible to determine the semimajor axis of the transfer orbit as:

$$a_{ph} = \left(\frac{T_{ph}\sqrt{\mu}}{2\pi}\right)^{2/3} \tag{4.14}$$

from which the apogee radius is calculated:

$$r_{a_{ph}} = 2\ a_{ph} - r \tag{4.15}$$

the angular momentum:

$$h_{ph} = \sqrt{2\mu}\sqrt{\frac{r\ r_{a_{ph}}}{r + r_{a_{ph}}}} \tag{4.16}$$

the velocity at the orbit apoapse:

$$v_{p_{ph}} = \frac{h_{ph}}{r} \tag{4.17}$$

finally, the values of the ΔV are determined as:

$$\Delta V_1 = v_{p_{ph}} - v \tag{4.18}$$

$$\Delta V_2 = \Delta V_1 \tag{4.19}$$

$$\Delta V_{tot} = \Delta V_1 + \Delta V_2 \tag{4.20}$$

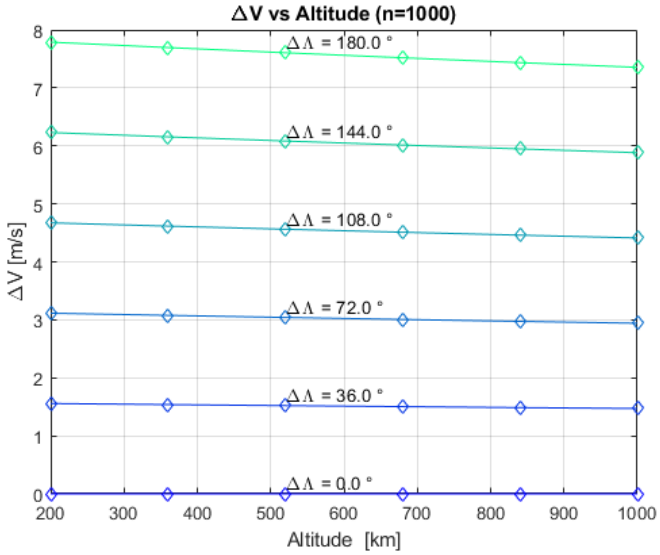

Figure 4.21: Required ΔV for a internal phasing maneuver in range $200 - 1000\ km$ at different longitudes $\Delta\Lambda$

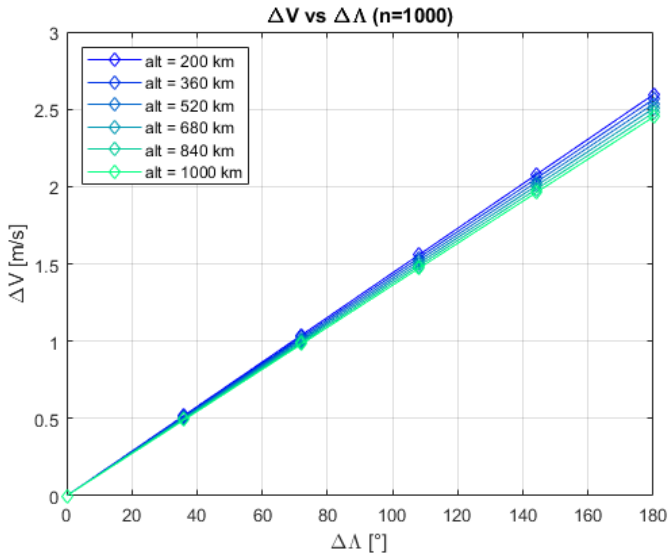

Figure 4.22: Required ΔV for a internal phasing maneuver in range $0 - 180^o$ at different altitudes

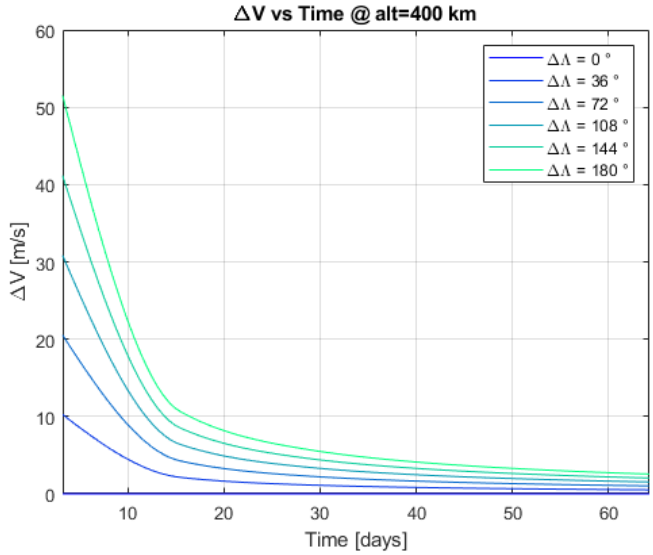

Figure 4.23: Required ΔV for a internal phasing maneuver in range $0-180^o$ considering different number of orbits

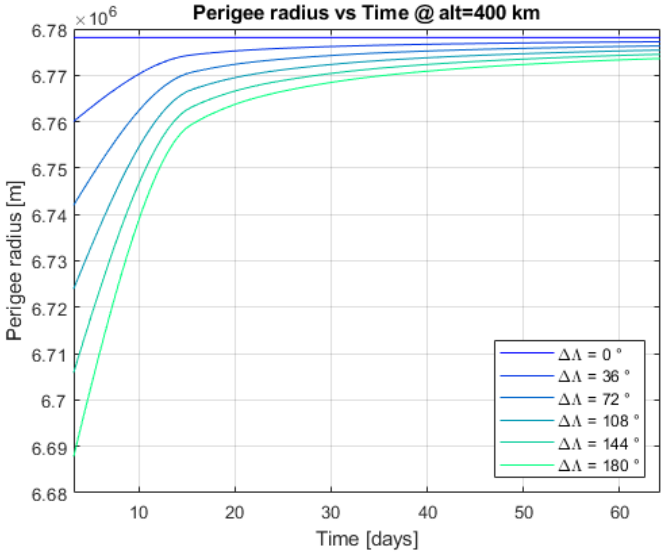

Figure 4.24: Height of the transfer orbit perigee in function of the number of orbits

Chemical thruster - required propellant mass

The % propellant mass required to perform this maneuver is shown in the following graphs, considering again the cases with $I_{sp} = 150,\ 300,\ 1000,\ 3000\ s$.
First, plots with propellant mass % in function of altitude considering different longitudes are presented.

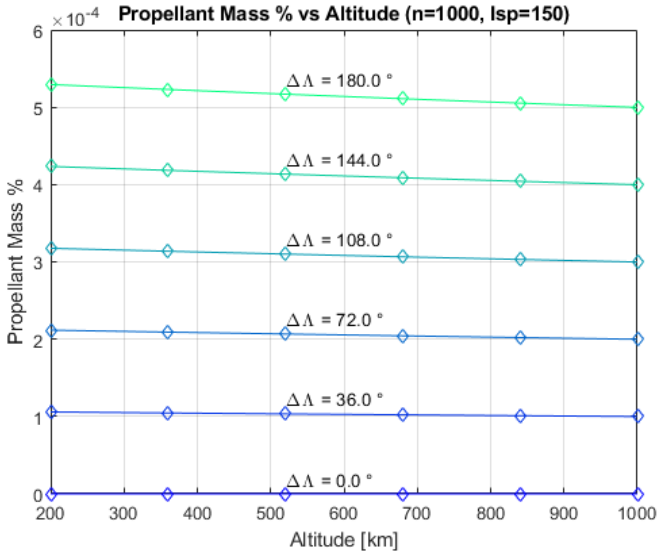

Figure 4.25: Required propellant mass % for a phasing maneuver in range $200 - 1000\ km$ with $I_{sp} = 150\ s$

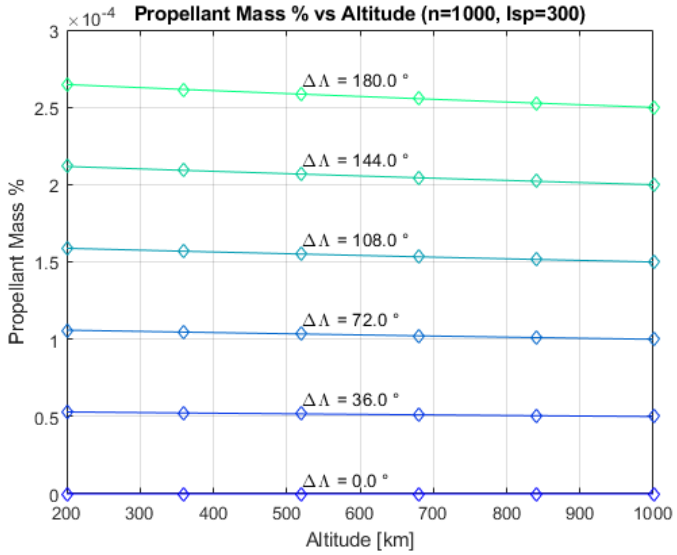

Figure 4.26: Required propellant mass % for a phasing maneuver in range $200 - 1000\ km$ with $I_{sp} = 300\ s$

Then, plots with propellant mass % in function of $\Delta\Lambda$ considering different altitudes are shown.

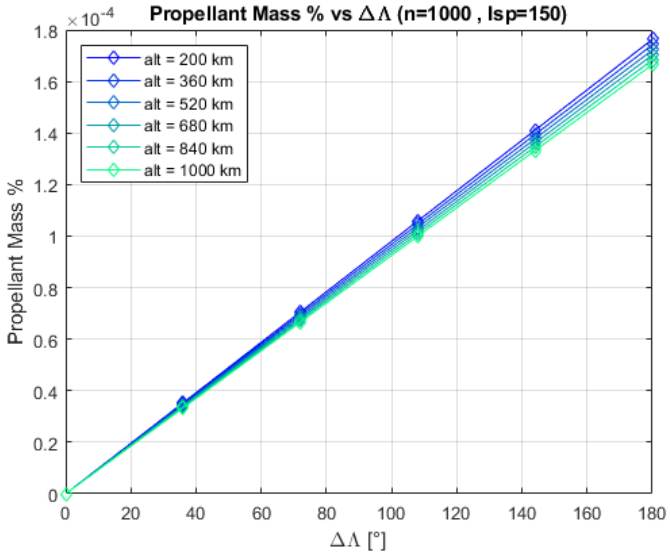

Figure 4.27: Required propellant mass % for a phasing maneuver in range $0 - 180^o$ with $I_{sp} = 150\ s$

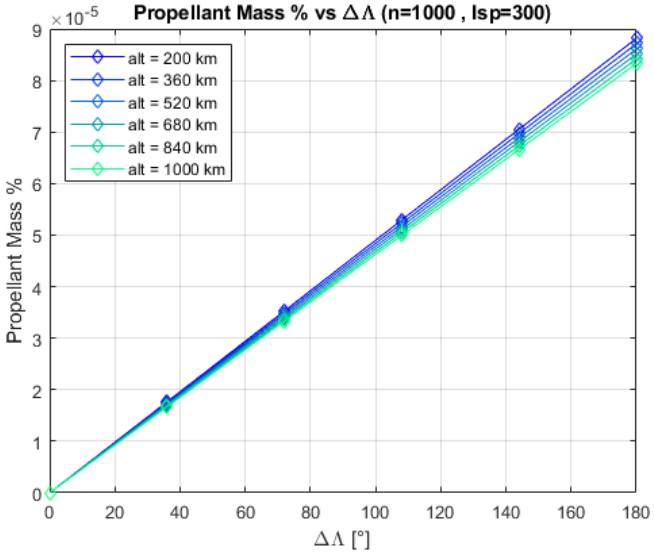

Figure 4.28: Required propellant mass % for a phasing maneuver in range $0 - 180^o$ with $I_{sp} = 300\ s$

Electric thruster - required propellant mass

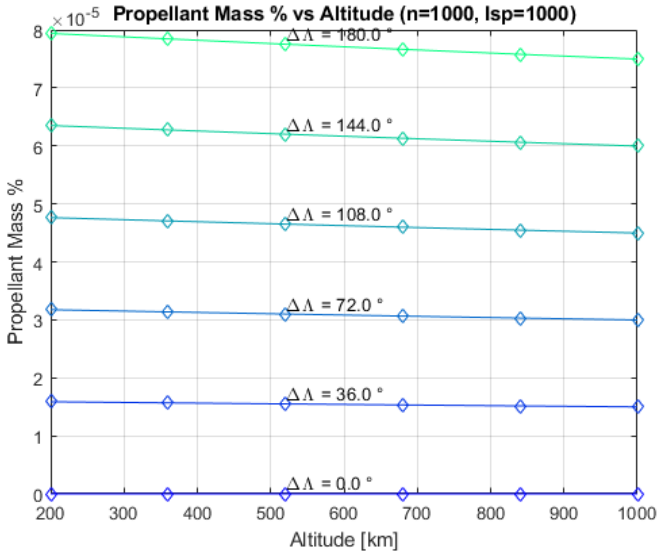

Figure 4.29: Required propellant mass % for a phasing maneuver in range $200 - 1000\ km$ with $I_{sp} = 1000\ s$

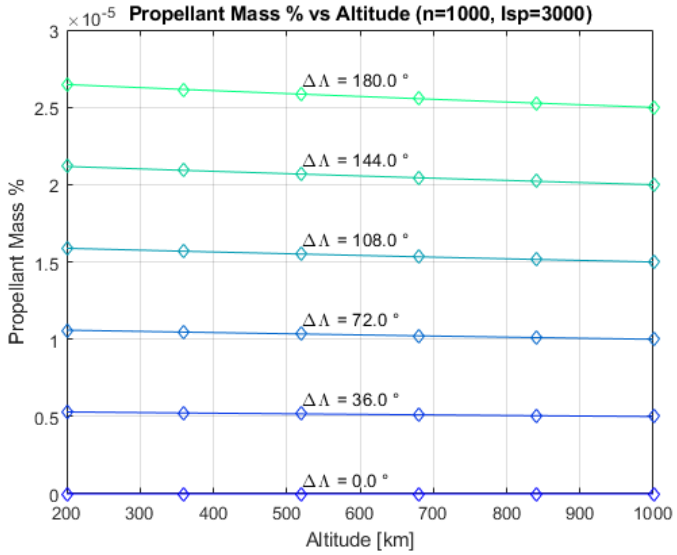

Figure 4.30: Required propellant mass % for a phasing maneuver in range $200 - 1000\ km$ with $I_{sp} = 3000\ s$

As the precious section,the following plots show propellant mass % in function of $\Delta\Lambda$ considering different altitudes are shown.

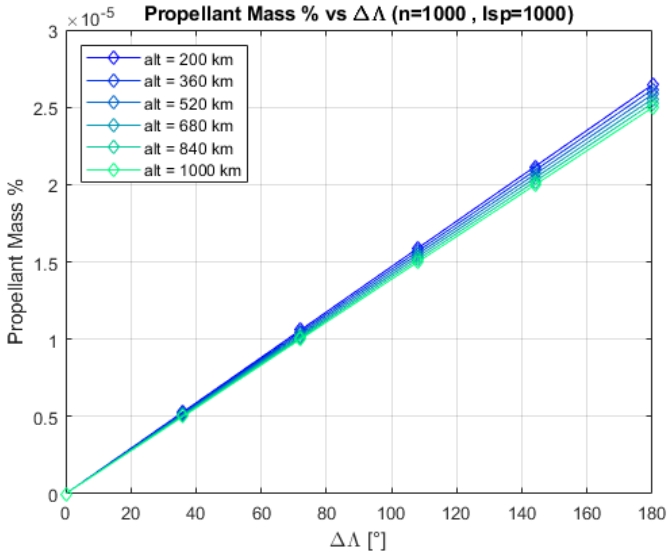

Figure 4.31: Required propellant mass % for a phasing maneuver in range $0 - 180^o$ with $I_{sp} = 1000\ s$

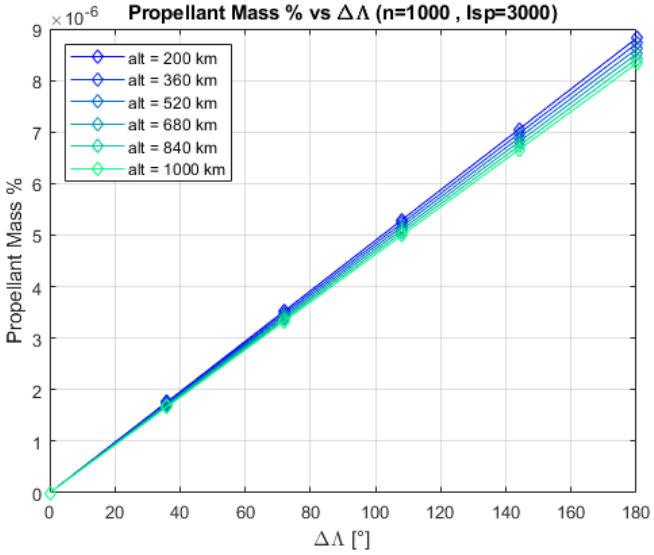

Figure 4.32: Required propellant mass % for a phasing maneuver in range $0 - 180^o$ with $I_{sp} = 3000\ s$

4.3.5 Inclination change maneuver

The maneuver for the change of orbital inclination takes place at the point of intersection between the nodal line and the ecliptic plane.
This maneuver is known as *pure plan change* and the required ΔV is equal to:

$$\Delta V = 2\ v\ sin\left(\frac{\Delta i}{2}\right) \tag{4.21}$$

where Δi is the difference between the inclination of the initial orbit and the inclination of the target one.

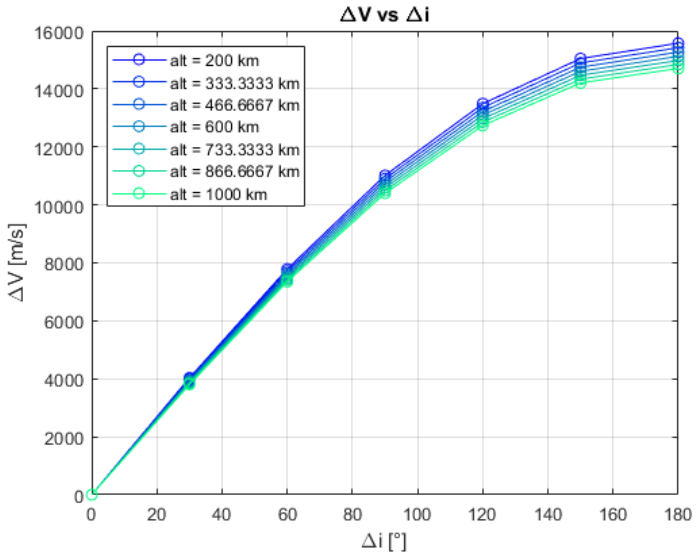

Figure 4.33: Required ΔV for a inclination change maneuver in range $0 - 180^o$ at different altitudes

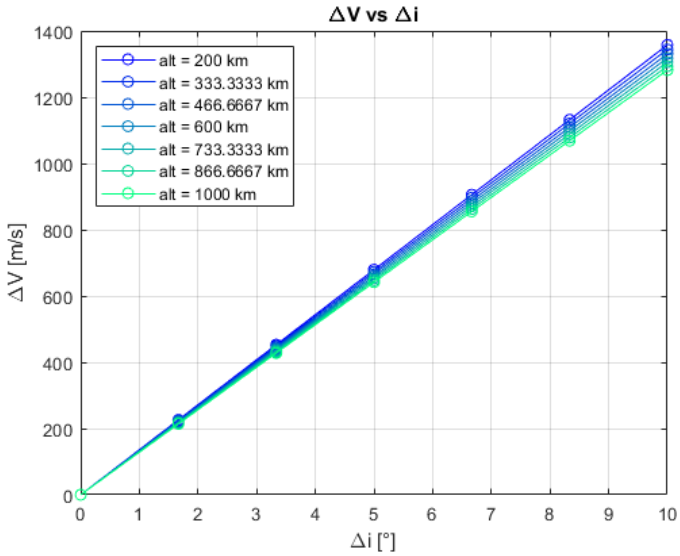

Figure 4.34: Required ΔV for a inclination change maneuver in range $0 - 10^o$ at different altitudes

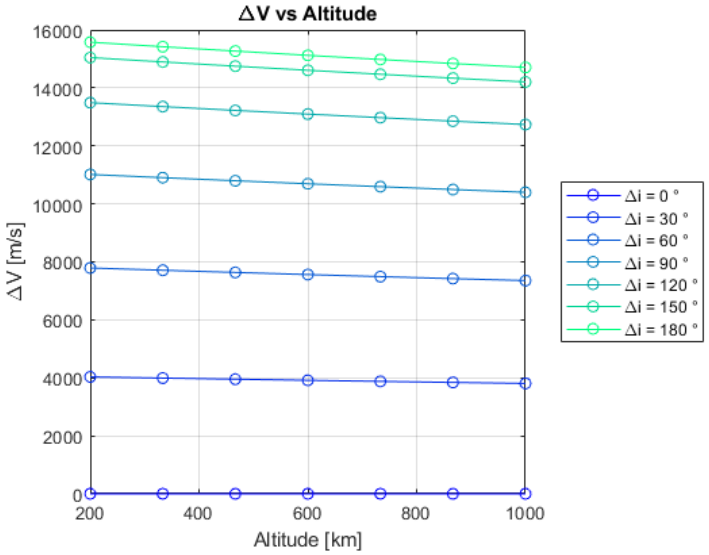

Figure 4.35: Required ΔV for a inclination change maneuver in range $200-1000$ km at different inclinations

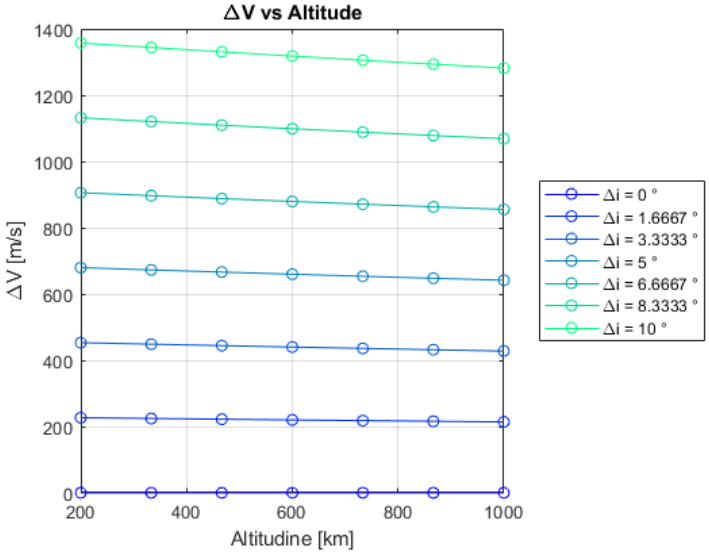

Figure 4.36: Required ΔV for a inclination change maneuver in range $200-1000$ km at different inclinations

Chemical thruster - required propellant mass

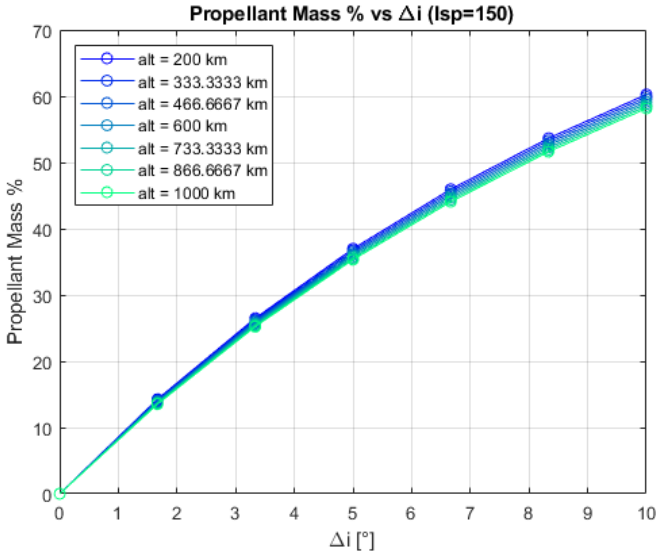

Figure 4.37: Required propellant mass % for a inclination change maneuver in range $0 - 10^o$ at different inclinations and altitudes with $I_{sp} = 150\ s$

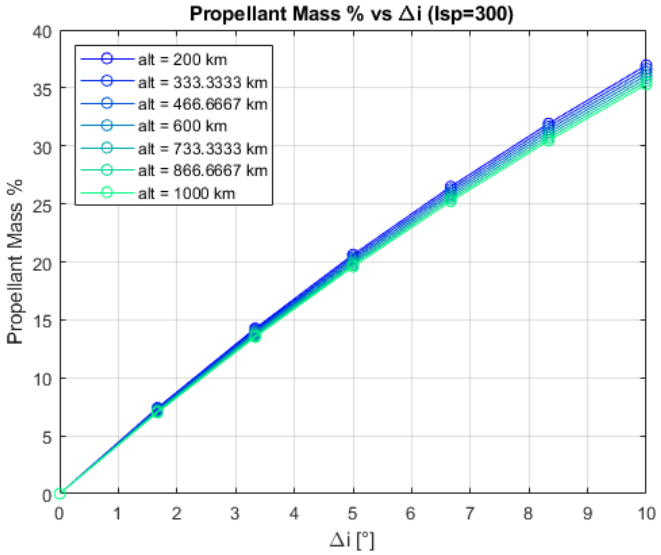

Figure 4.38: Required propellant mass % for a inclination change maneuver in range $0 - 10^o$ at different inclinations and altitudes with $I_{sp} = 300\ s$

Electric thruster - required propellant mass

The following graphs relating to electric thrusters serve to give a comparison with the chemical ones but are not real as this maneuver requires an impulsive ΔV at the node and this is not expected with electric motors.

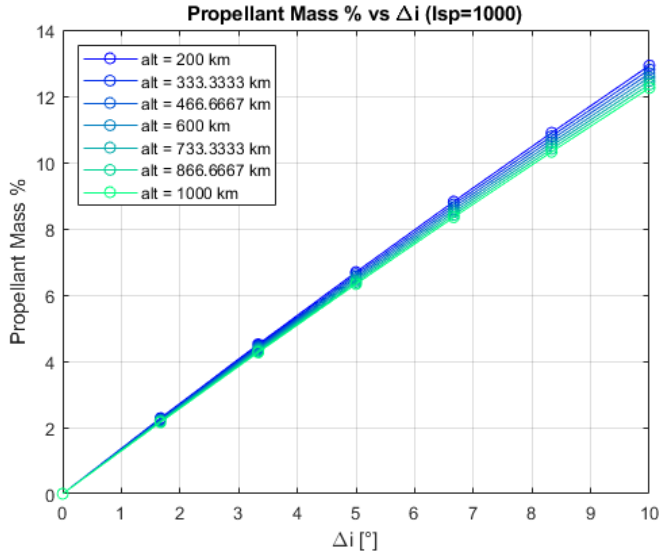

Figure 4.39: Required propellant mass % for a inclination change maneuver in range $0 - 10^o$ at different inclinations and altitudes with $I_{sp} = 1000\ s$

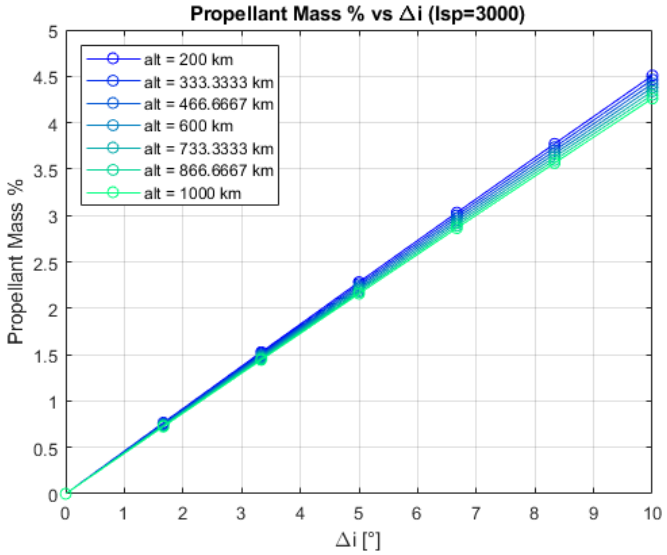

Figure 4.40: Required propellant mass % for a inclination change maneuver in range $0 - 10^o$ at different inclinations and altitudes with $I_{sp} = 3000\ s$

It is possible to see from the graphs above how an inclination change maneuver requires large amounts of ΔV and how this type of maneuver can be convenient only for small variations of inclination.

4.3.6 RAAN change maneuver

Chemical thruster

The maneuver to change the right ascension of the ascending node can be performed directly by the spacecraft at the intersection point between the starting orbit and the target one, considering a chemical thruster, in reference to [32], and the necessary ΔV is determined as it follows:

$$cos(\theta) = cos^2(i) + sin^2(i)\ cos(\Delta\Omega) \tag{4.22}$$

$$\Delta V = 2\, v\, sin\left(\frac{\theta}{2}\right) \tag{4.23}$$

where $\Delta\Omega$ is the desired target orbit RAAN (right ascension of the ascending node) difference and i is the inclination of the considered orbit.

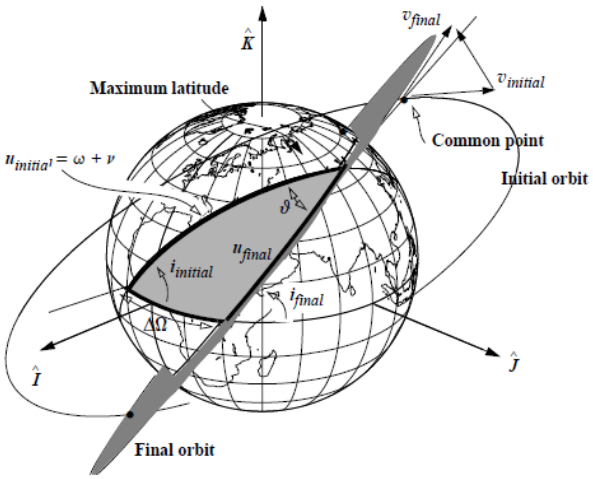

Figure 4.41: RAAN change maneuver representation [14]

In the following plots, it is notable how much ΔV is necessary in order to perform this type of maneuver, at different inclinations.

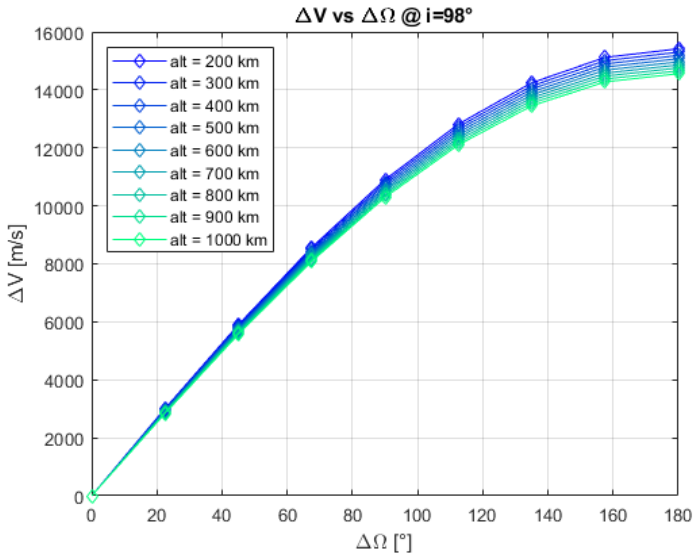

Figure 4.42: Required ΔV for a RAAN change maneuver at different altitudes and $i = 98^o$

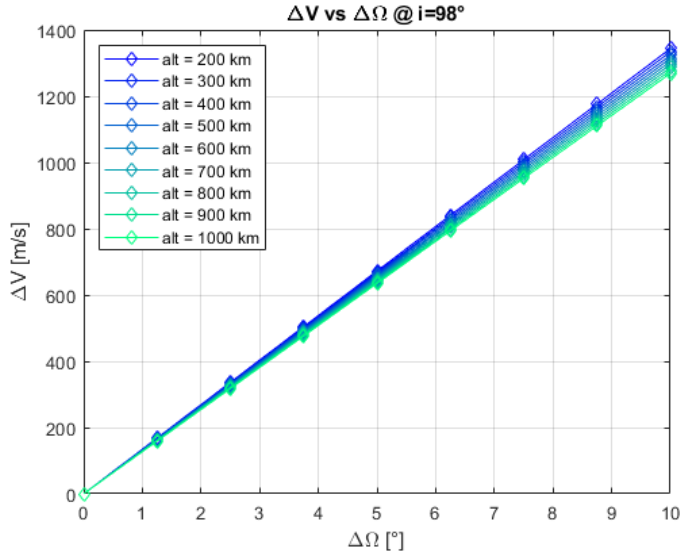

Figure 4.43: Required ΔV for a RAAN change maneuver at different altitudes and $i = 98^o$

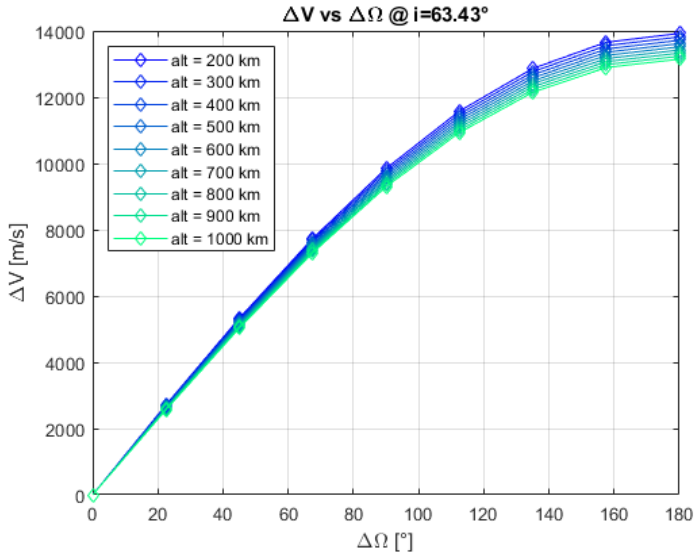

Figure 4.44: Required ΔV for a RAAN change maneuver at different altitudes and $i = 63.43^o$

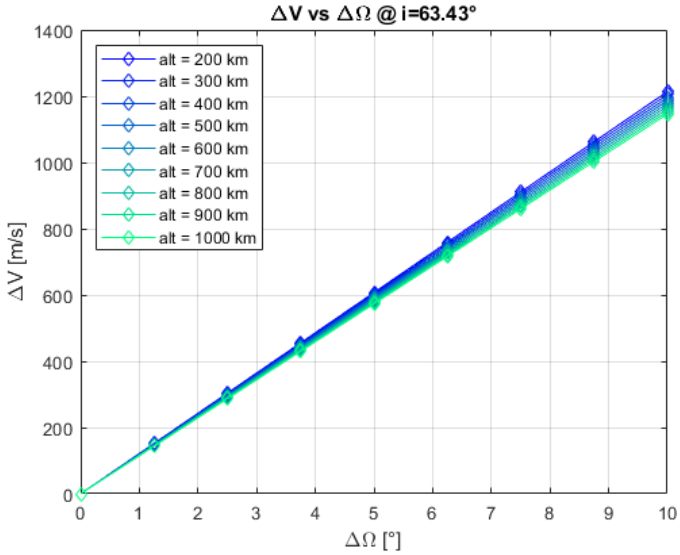

Figure 4.45: Required ΔV for a RAAN change maneuver at different altitudes and $i = 63.43^o$

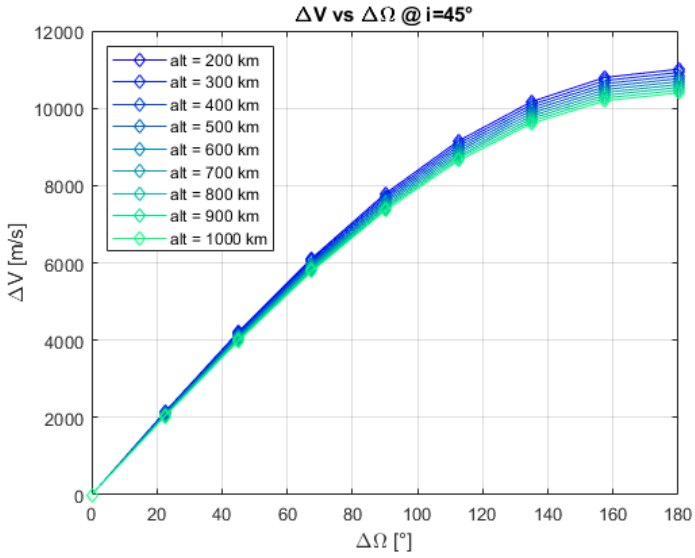

Figure 4.46: Required ΔV for a RAAN change maneuver at different altitudes and $i = 45^o$

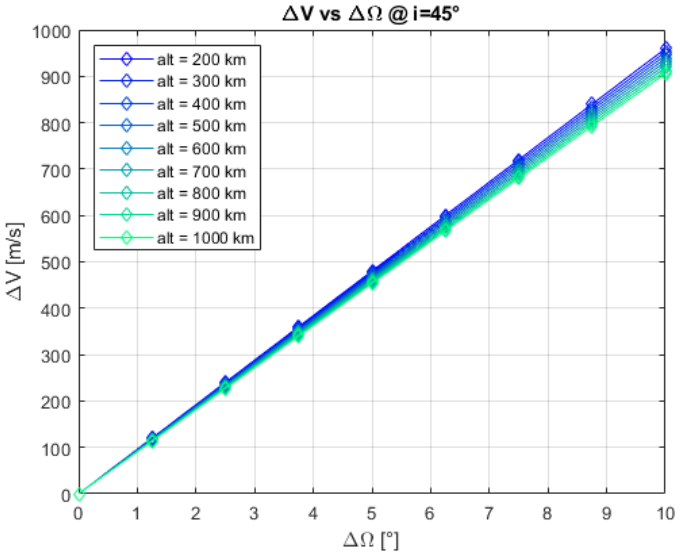

Figure 4.47: Required ΔV for a RAAN change maneuver at different altitudes and $i = 45^o$

Chemical thruster - required propellant mass

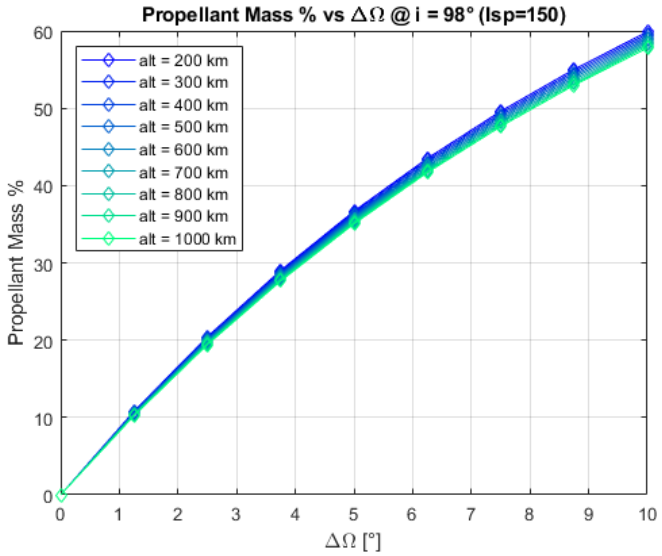

Figure 4.48: Required propellant mass % for a RAAN change maneuver in range $0 - 10^o$ with $I_{sp} = 150\ s$

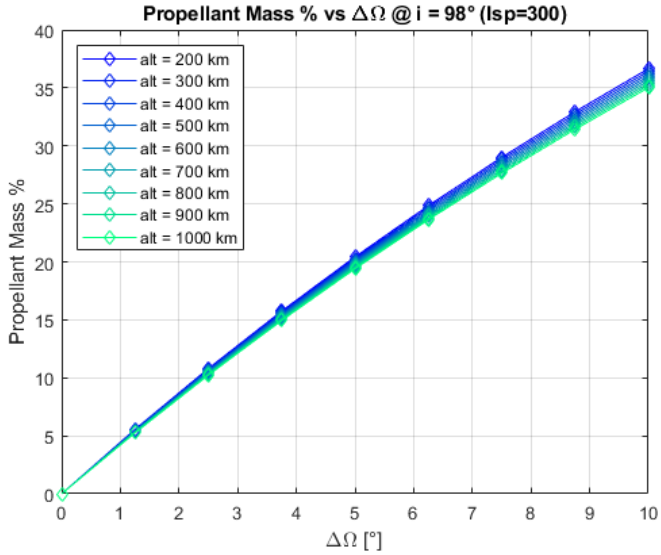

Figure 4.49: Required propellant mass % for a RAAN change maneuver in range $0 - 10^o$ with $I_{sp} = 300\ s$

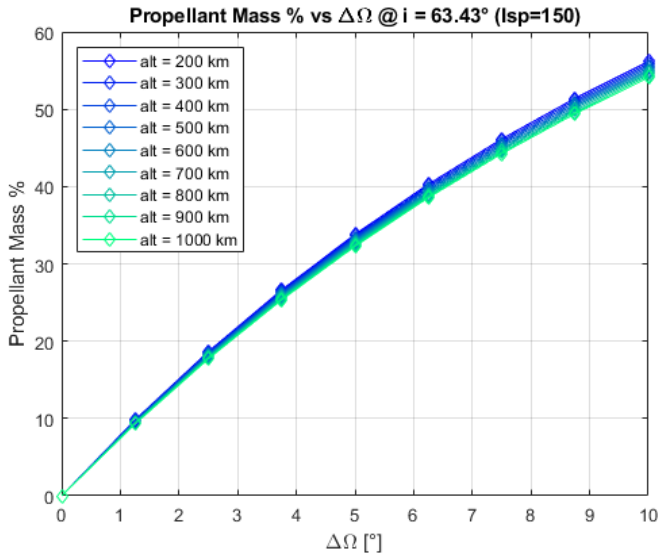

Figure 4.50: Required propellant mass % for a RAAN change maneuver in range $0 - 10^o$ with $I_{sp} = 150\ s$

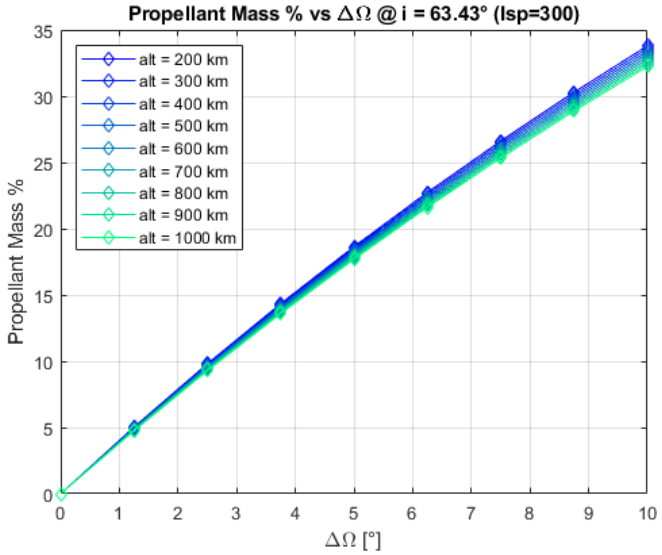

Figure 4.51: Required propellant mass % for a RAAN change maneuver in range $0 - 10^o$ with $I_{sp} = 300\ s$

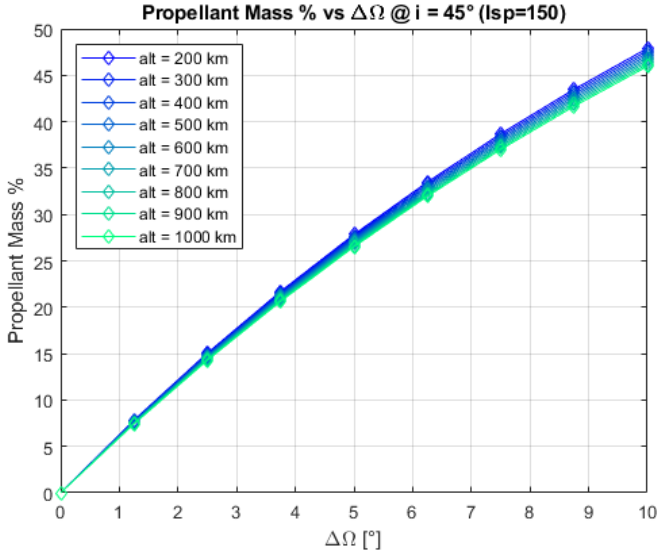

Figure 4.52: Required propellant mass % for a RAAN change maneuver in range $0 - 10^o$ with $I_{sp} = 150\ s$

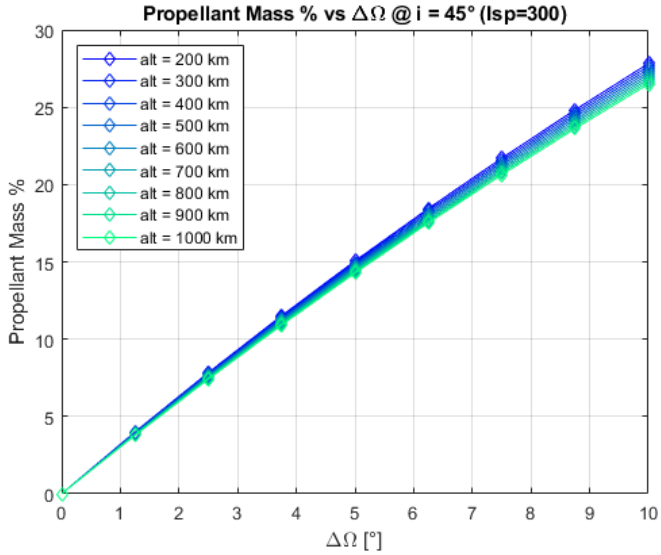

Figure 4.53: Required propellant mass % for a RAAN change maneuver in range $0 - 10^o$ with $I_{sp} = 300\ s$

Electric thruster

The RAAN change maneuver can also be performed with an electric thruster, considering the following formula for the required ΔV as described in [33].
However, since the impulse is not instant, the maneuver cannot be performed at the node. Hence, the calculated ΔV, is the total one dispensed during the whole maneuver.

$$\Delta V = \frac{\pi}{2}\sqrt{\frac{\mu}{a}}\, sin(i)\, |\Delta\Omega| \tag{4.24}$$

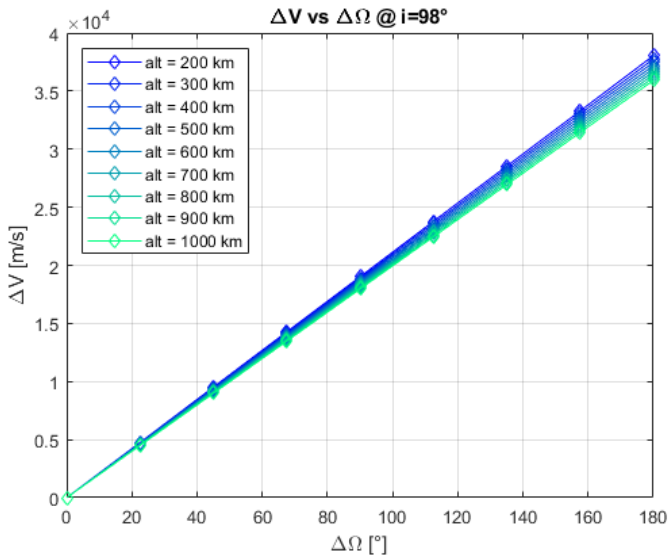

Figure 4.54: Required ΔV for a RAAN change maneuver at different altitudes and $i = 98^o$

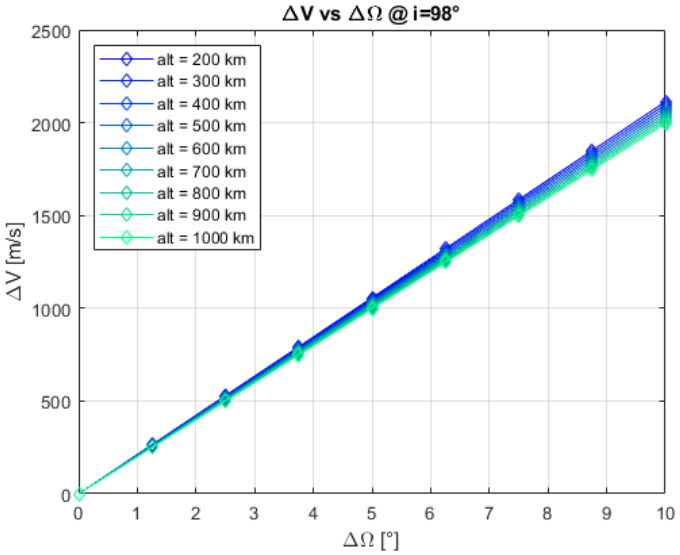

Figure 4.55: Required ΔV for a RAAN change maneuver at different altitudes and $i = 98^o$

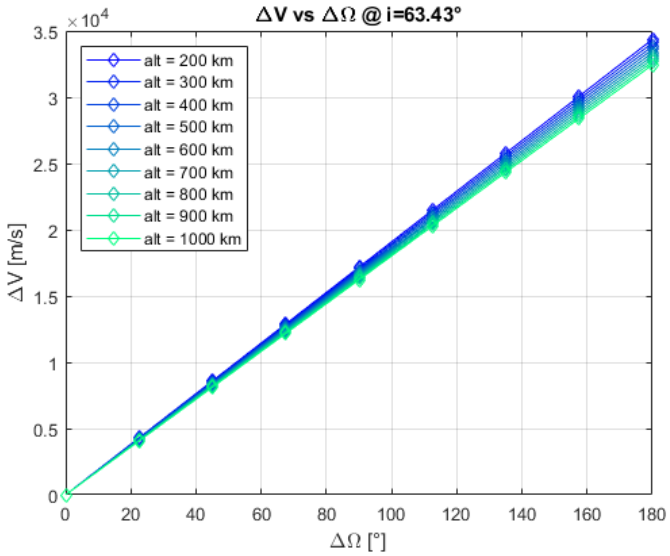

Figure 4.56: Required ΔV for a RAAN change maneuver at different altitudes and $i = 63.43^o$

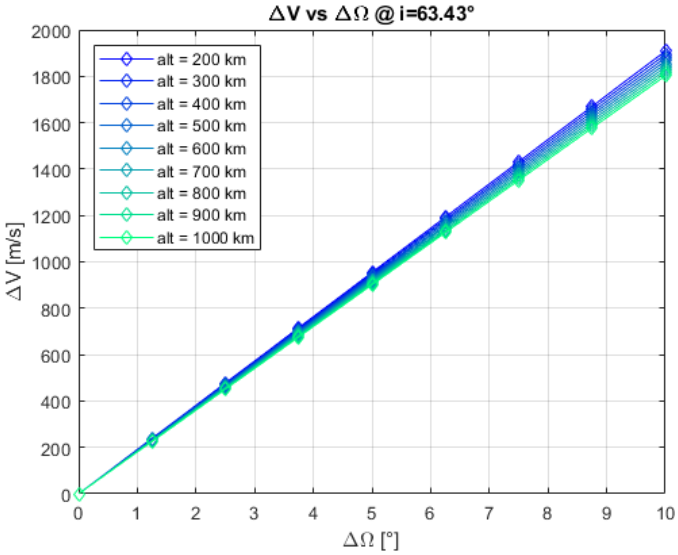

Figure 4.57: Required ΔV for a RAAN change maneuver at different altitudes and $i = 63.43^o$

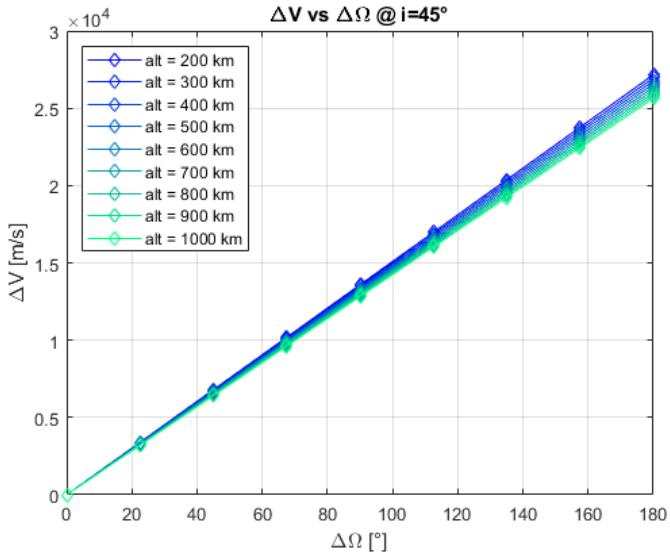

Figure 4.58: Required ΔV for a RAAN change maneuver at different altitudes and $i = 45^o$

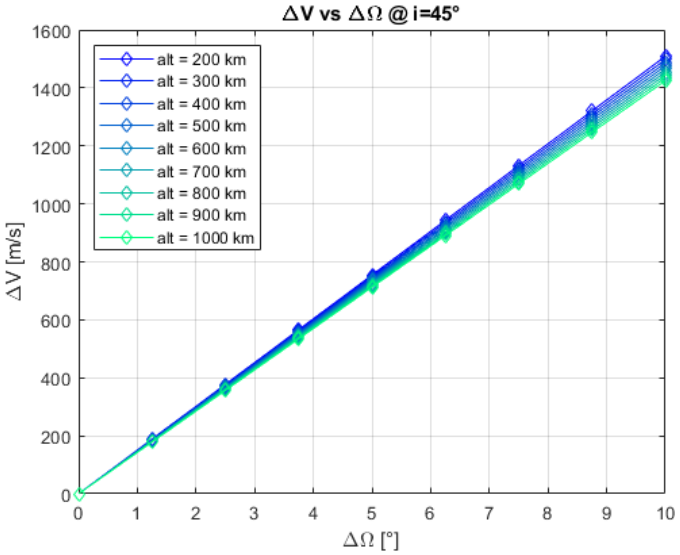

Figure 4.59: Required ΔV for a RAAN change maneuver at different altitudes and $i = 45^o$

Electric thruster - required propellant mass

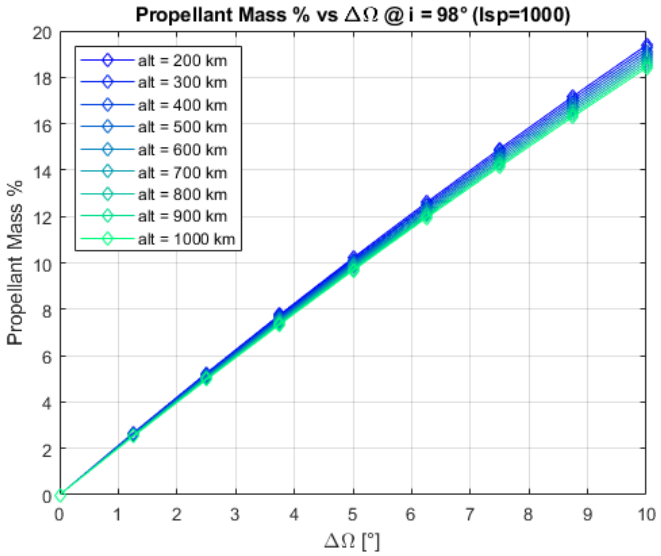

Figure 4.60: Required propellant mass % for a RAAN change maneuver in range $0 - 10^o$ with $I_{sp} = 1000\ s$

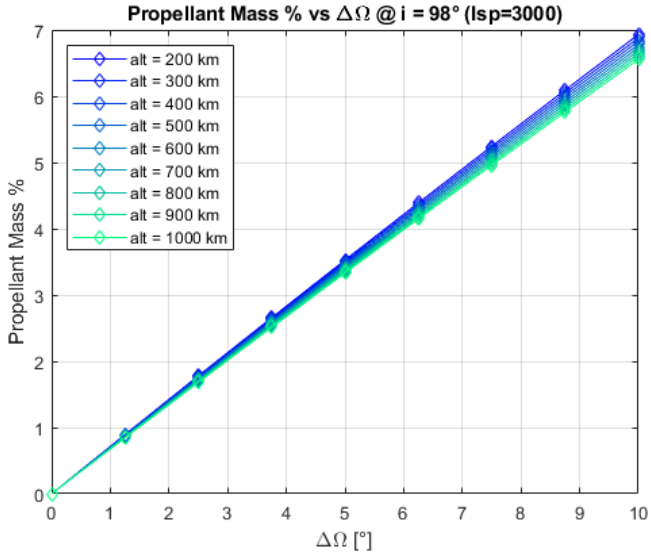

Figure 4.61: Required propellant mass % for a RAAN change maneuver in range $0 - 10^o$ with $I_{sp} = 3000\ s$

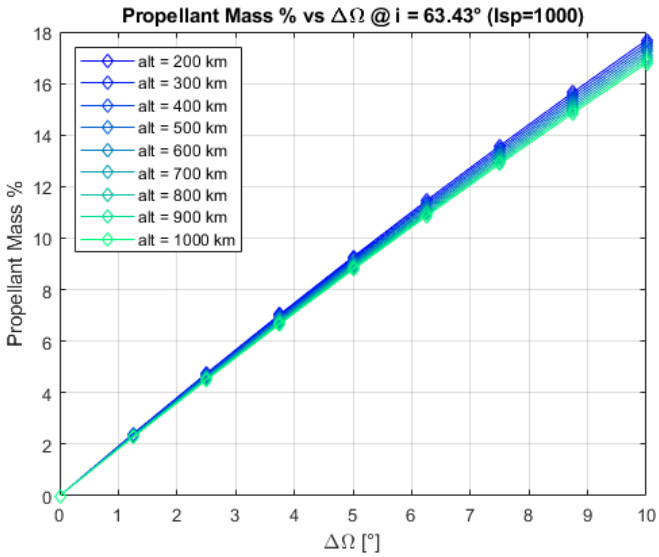

Figure 4.62: Required propellant mass % for a RAAN change maneuver in range $0 - 10^o$ with $I_{sp} = 1000\ s$

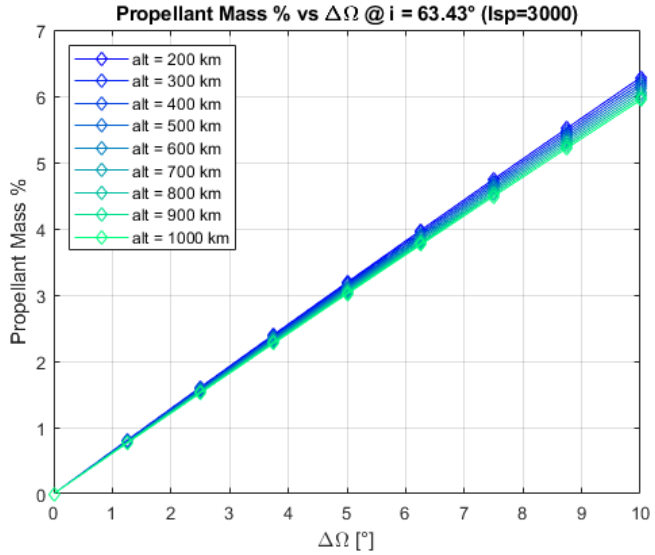

Figure 4.63: Required propellant mass % for a RAAN change maneuver in range $0 - 10^o$ with $I_{sp} = 3000\ s$

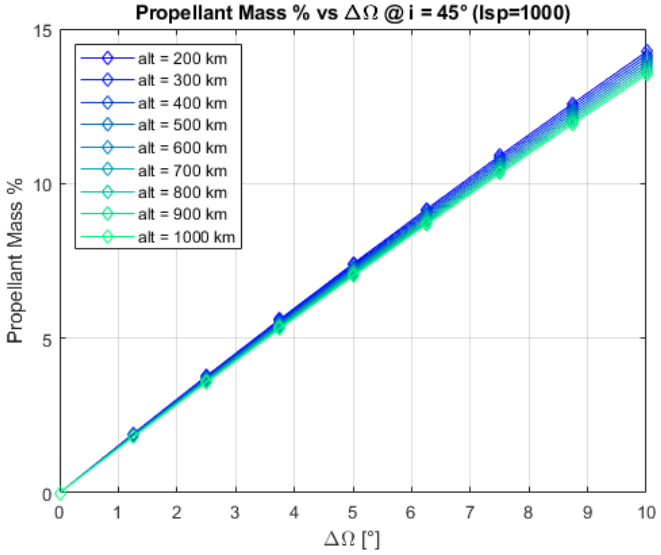

Figure 4.64: Required propellant mass % for a RAAN change maneuver in range $0 - 10^o$ with $I_{sp} = 1000\ s$

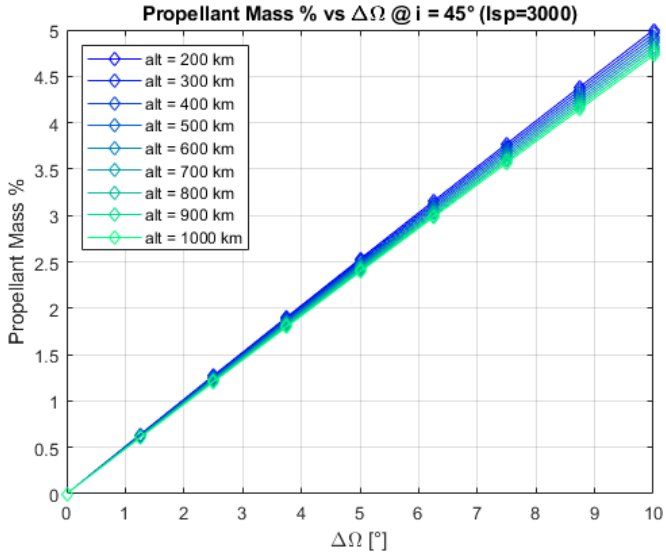

Figure 4.65: Required propellant mass % for a RAAN change maneuver in range $0 - 10^o$ with $I_{sp} = 3000\ s$

J_2 perturbation exploitation

This maneuver results to be very expansive in terms of ΔV and this is the reason why J_2 perturbation is exploited, avoiding the waste of a large amount of propellant.
In the following plots the J_2 perturbation effects are illustrated.

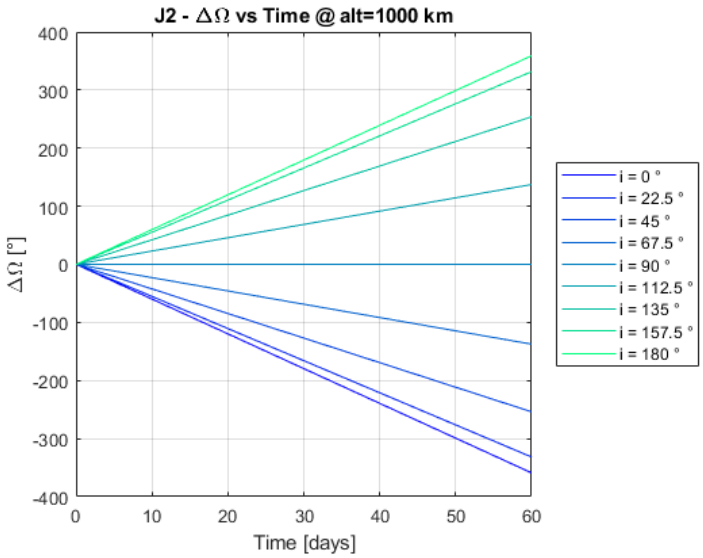

Figure 4.66: RAAN variation due to J_2 perturbation at different inclinations and fixed altitude

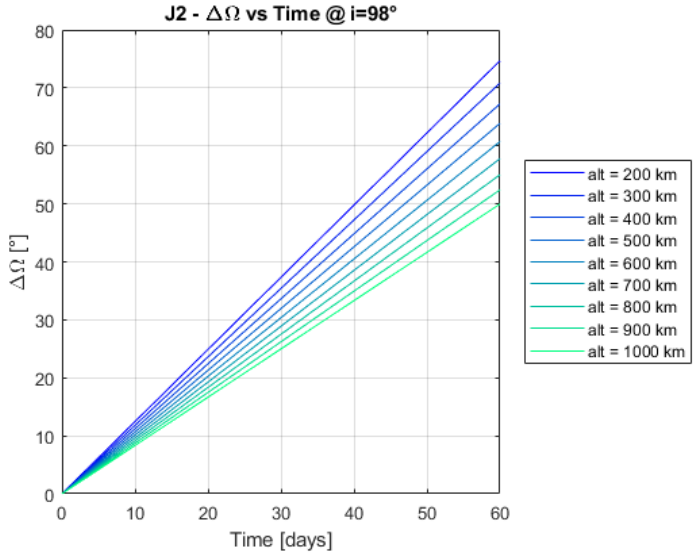

Figure 4.67: RAAN variation due to J_2 perturbation at different altitudes and $i = 98^o$

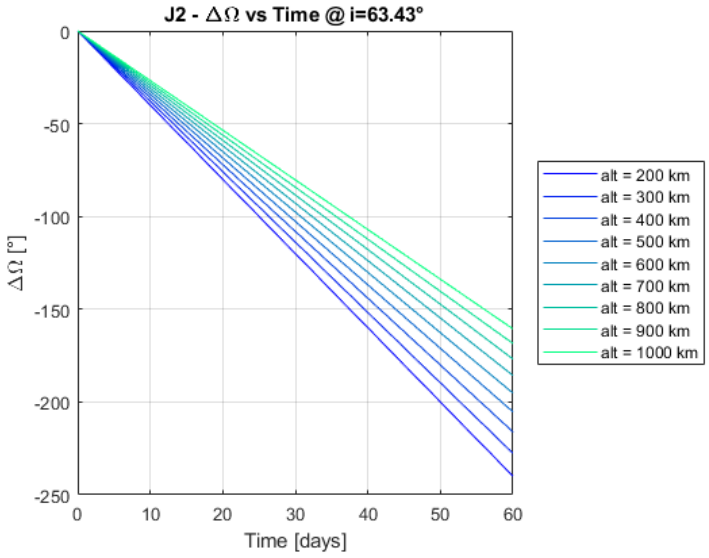

Figure 4.68: RAAN variation due to J_2 perturbation at different altitudes and $i = 63.43^o$

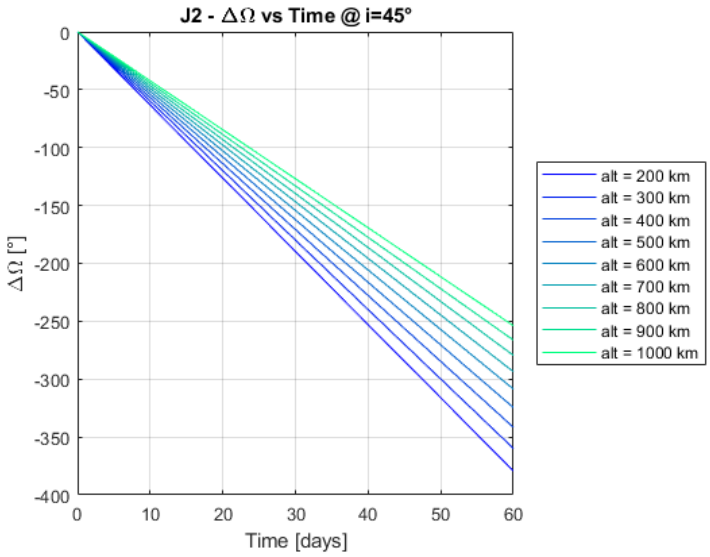

Figure 4.69: RAAN variation due to J_2 perturbation at different altitudes and $i = 45^o$

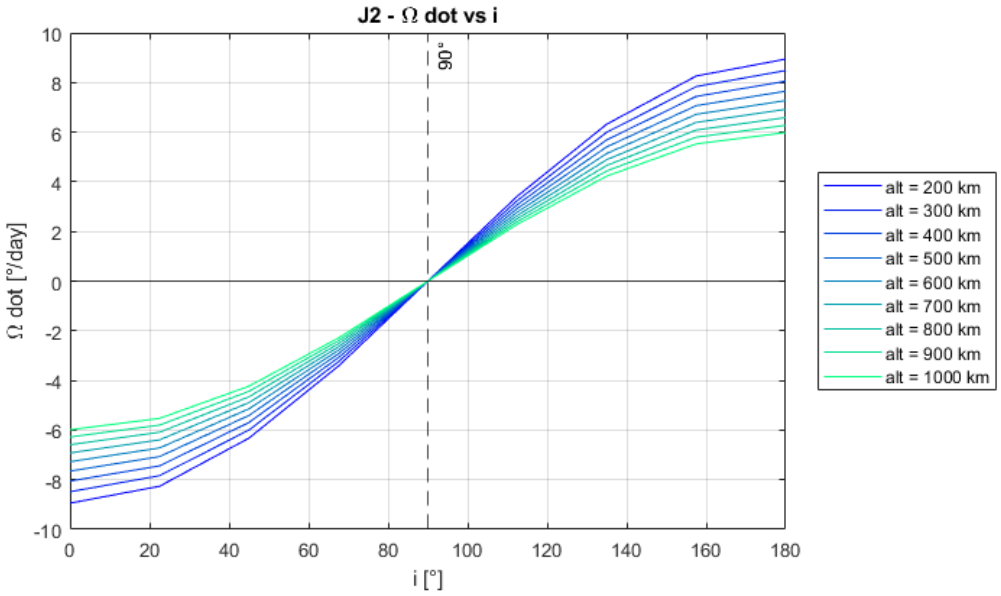

Figure 4.70: RAAN regression velocity due to J_2 perturbation at different inclinations

The following graphs represent the situation where 6 satellites are released at the same time in the same orbital position. Subsequently, the aim is to place them in various orbits separated by a phase equal to 60° in order to achieve a complete orbital coverage. To obtain the required phase shift, the fact that the orbits have different orbital speeds is exploited and it is sufficient to consider a certain wait time.
In considering this waiting time, the variation of $\Delta\Omega$ between the various satellites was also analysed. The situation just described has been studied considering different orbital inclinations.

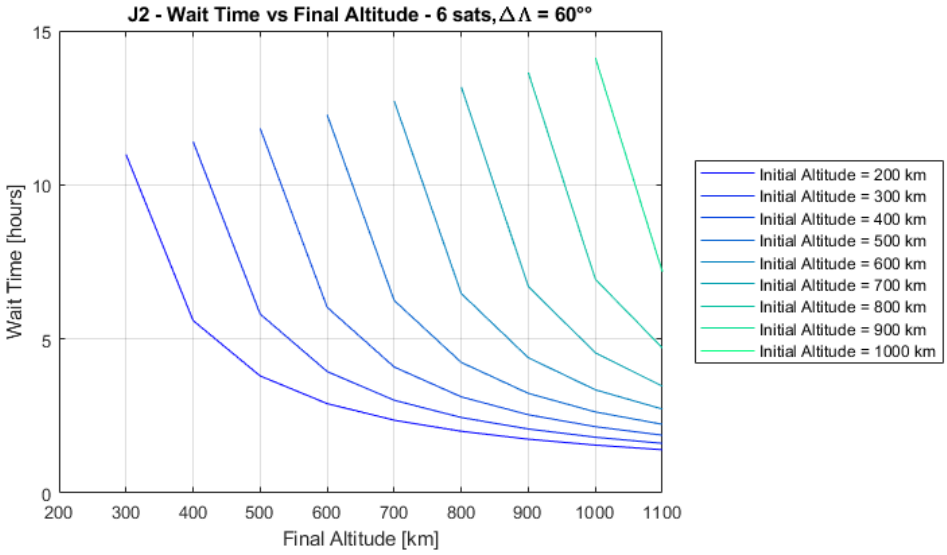

Figure 4.71: Required waiting time in order to have $\Delta\Lambda = 60^o$ for satellites positioning

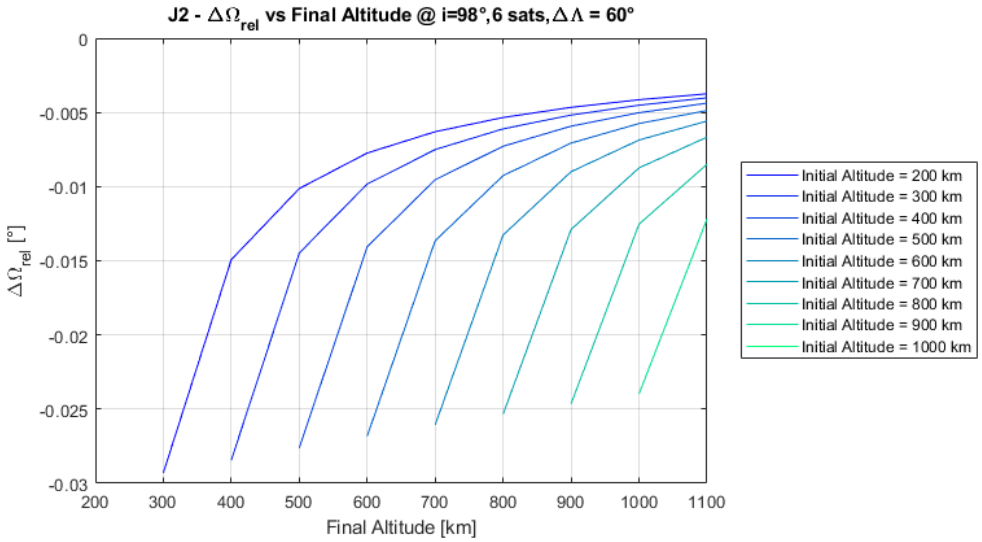

Figure 4.72: $\Delta\Omega_{rel}$ variation during the waiting time at $i = 98^o$

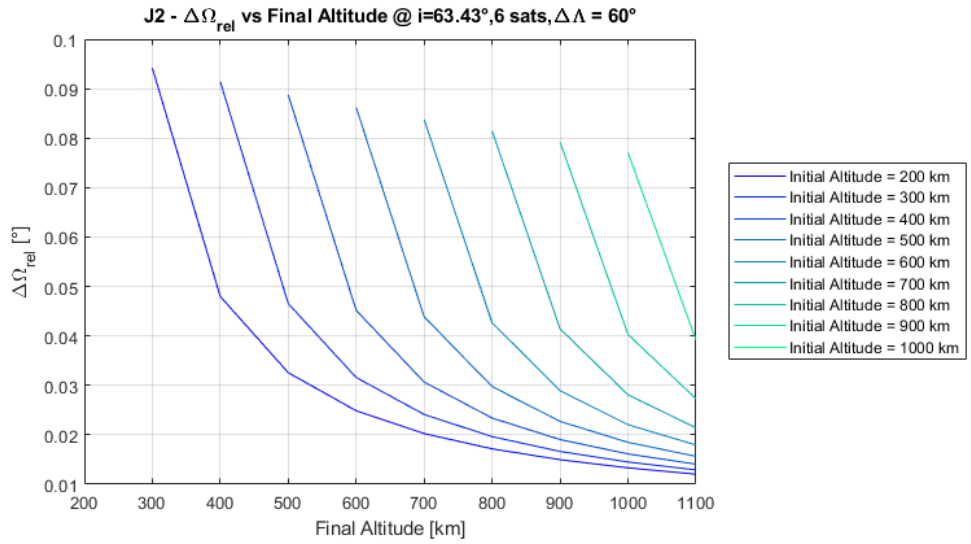

Figure 4.73: $\Delta\Omega_{rel}$ variation during the waiting time at $i = 63.43^o$

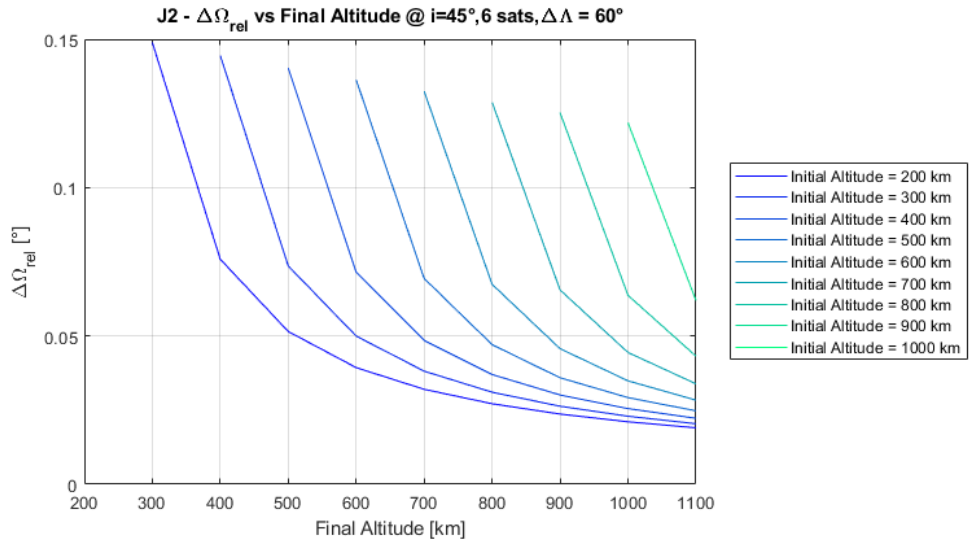

Figure 4.74: $\Delta\Omega_{rel}$ variation during the waiting time at $i = 45^o$

Differential $\Delta\Omega$ considering initial altitude of 600 km

In this section, it has been studied, considering different maneuvers and inclinations, how the $\Delta\Omega$ between two satellites vary starting from 600 km to different altitudes, due to the J_2 perturbation.

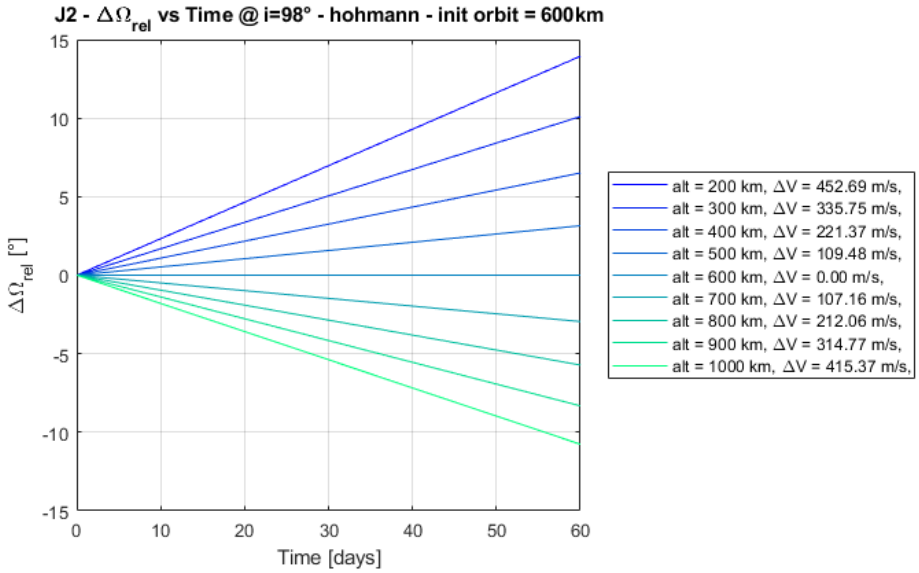

Figure 4.75: $\Delta\Omega_{rel}$ variation due to J_2 perturbation at $i = 98^o$ considering Hohmann transfer

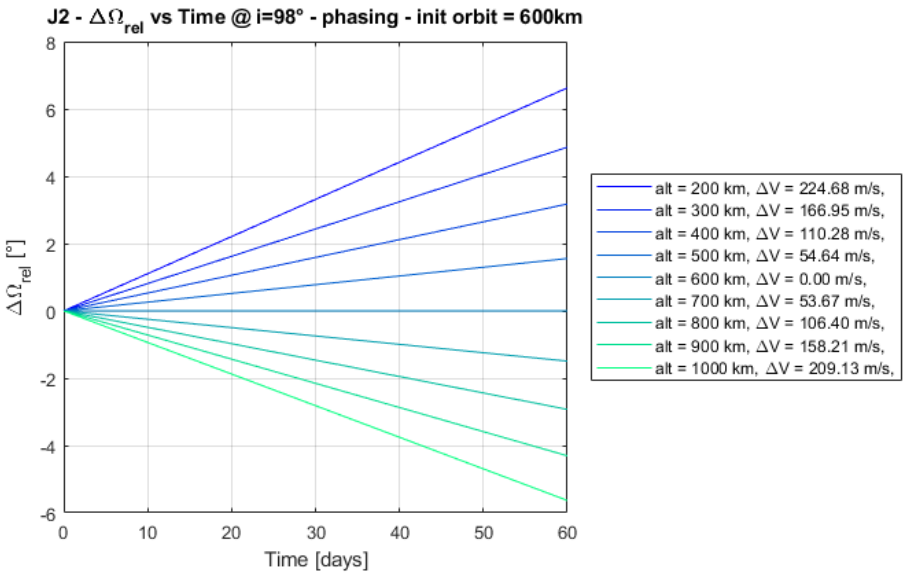

Figure 4.76: $\Delta\Omega_{rel}$ variation due to J_2 perturbation at $i = 98^o$ considering phasing transfer

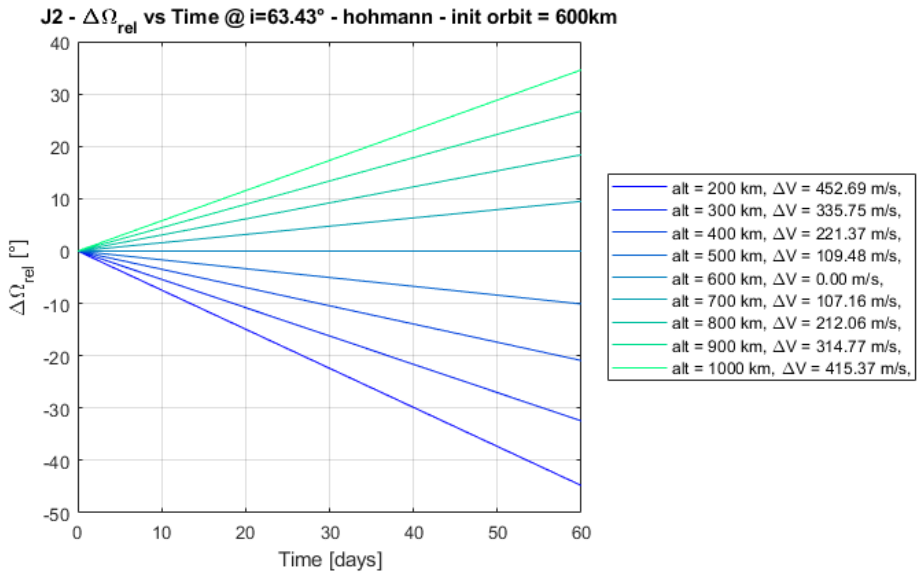

Figure 4.77: $\Delta\Omega_{rel}$ variation due to J_2 perturbation at $i = 63.43^o$ considering Hohmann transfer

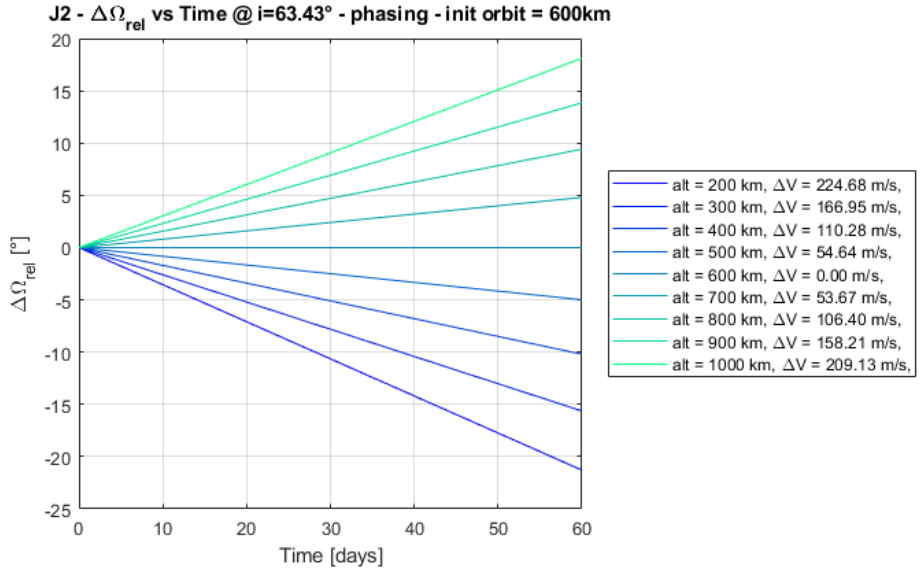

Figure 4.78: $\Delta\Omega_{rel}$ variation due to J_2 perturbation at $i = 63.43^o$ considering phasing transfer

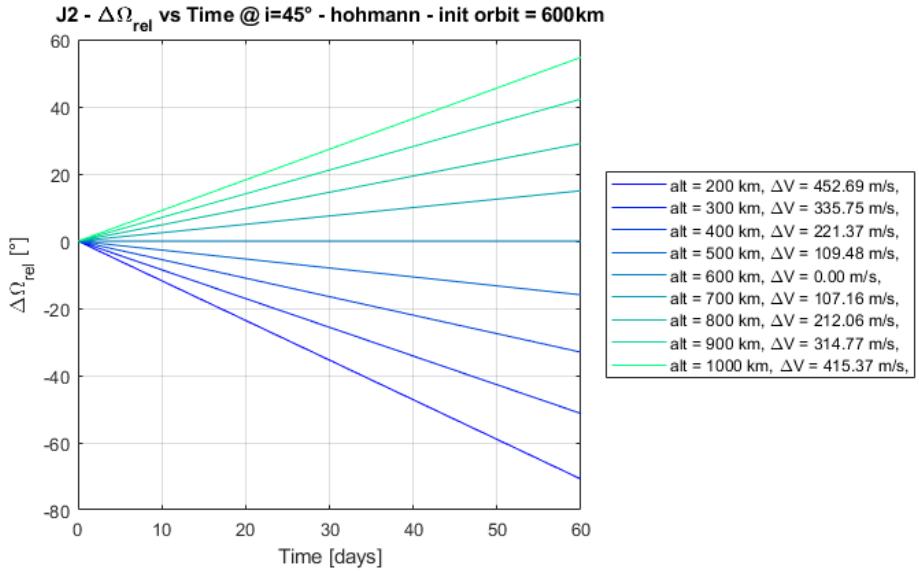

Figure 4.79: $\Delta\Omega_{rel}$ variation due to J_2 perturbation at $i = 45^o$ considering Hohmann transfer

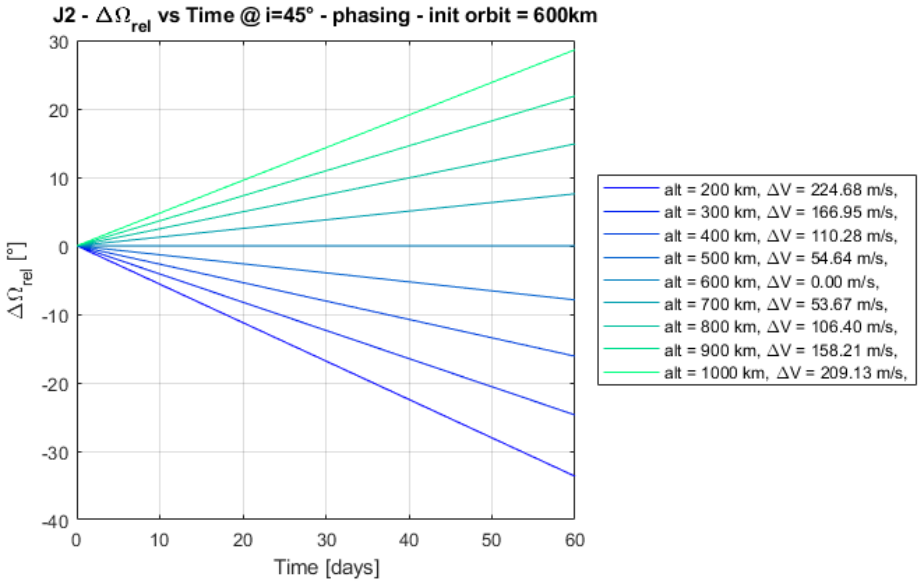

Figure 4.80: $\Delta\Omega_{rel}$ variation due to J_2 perturbation at $i = 45^o$ considering phasing transfer

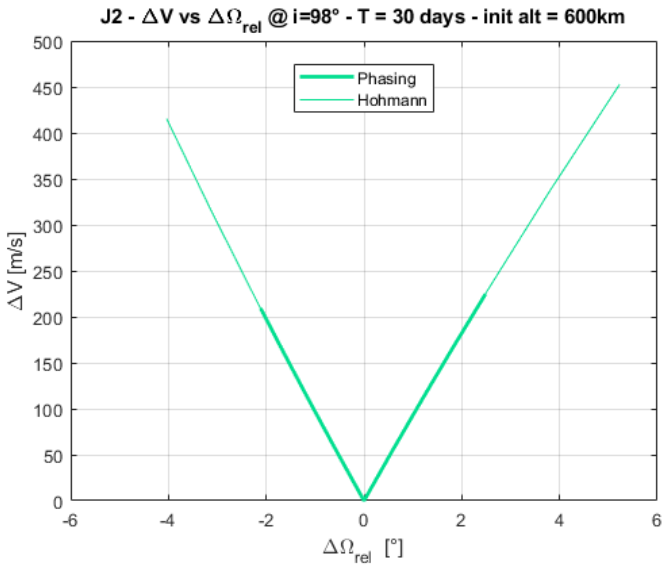

Figure 4.81: Hohmann and phasing transfer comparison for a period of 30 days

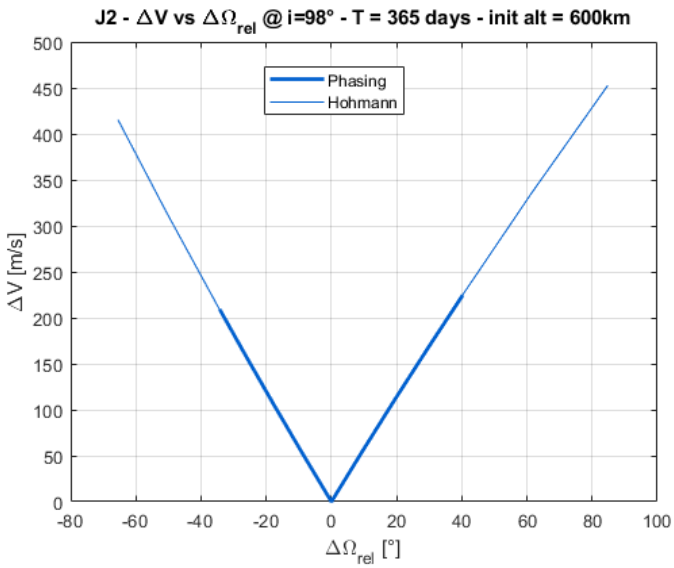

Figure 4.82: Hohmann and phasing transfer comparison for a period of 365 days

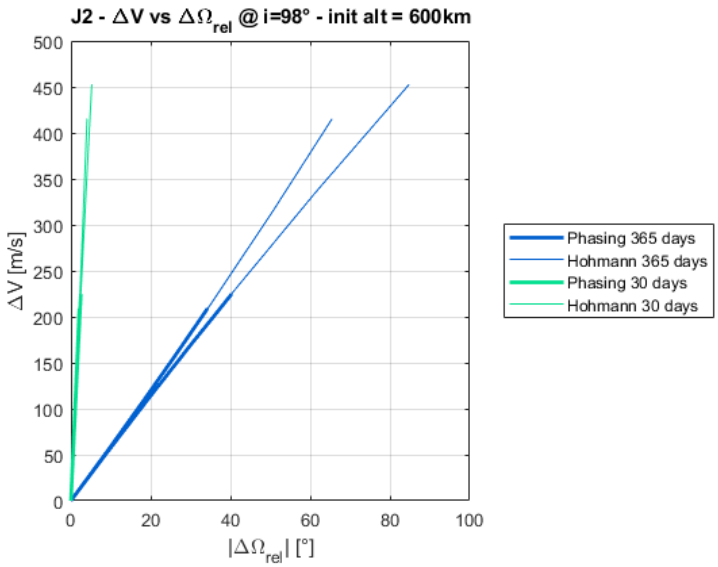

Figure 4.83: Hohmann and phasing transfer comparison

In the last graph, it is possible to see a comparison between the Hohmann and Phasing transfer for two different periods, in order to see the differences in time and costs.

Differential $\Delta\Omega$ considering initial altitude of 400 km

As in the previous section, it has been studied, considering Hohmann and Phasing maneuvers and different inclinations, how the $\Delta\Omega$ between two satellites vary starting from 400 km to different altitudes, due to the J_2 perturbation.

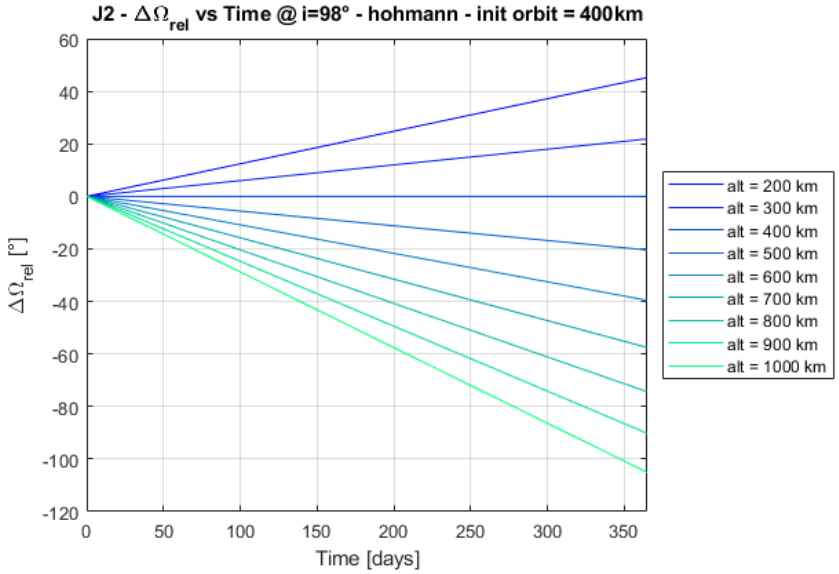

Figure 4.84: $\Delta\Omega_{rel}$ variation due to J_2 perturbation at $i = 98^o$ considering Hohmann transfer

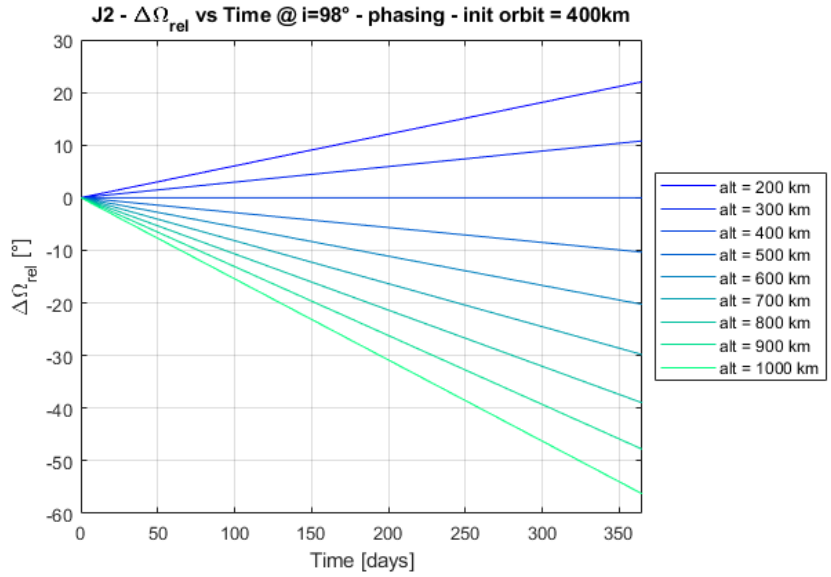

Figure 4.85: $\Delta\Omega_{rel}$ variation due to J_2 perturbation at $i = 98^o$ considering phasing transfer

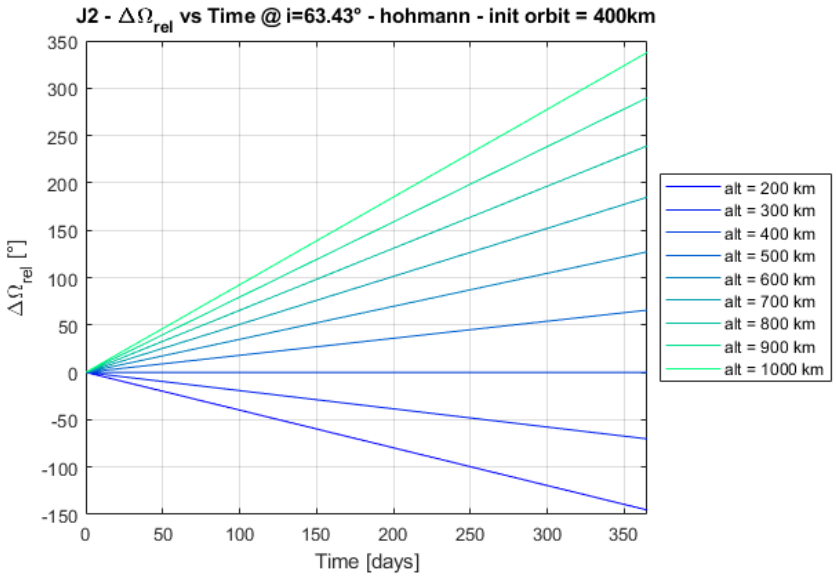

Figure 4.86: $\Delta\Omega_{rel}$ variation due to J_2 perturbation at $i = 63.43^o$ considering Hohmann transfer

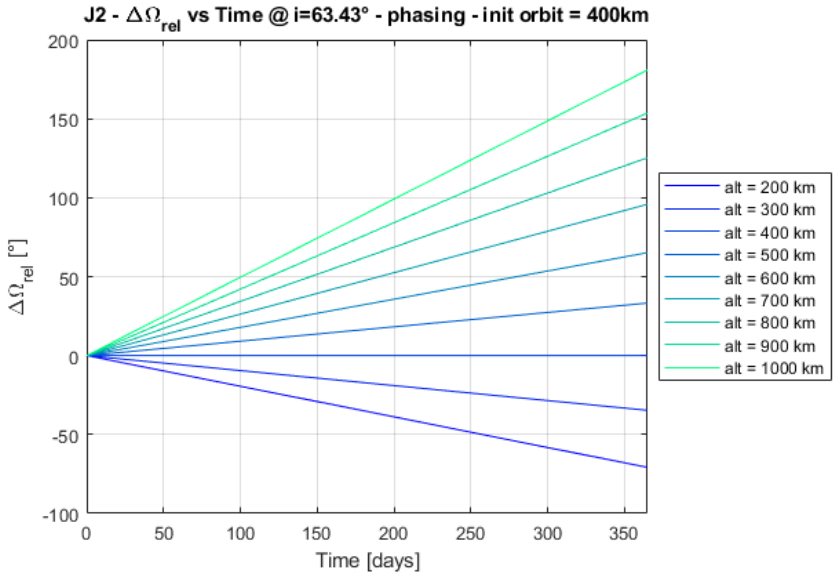

Figure 4.87: $\Delta\Omega_{rel}$ variation due to J_2 perturbation at $i = 63.43^o$ considering phasing transfer

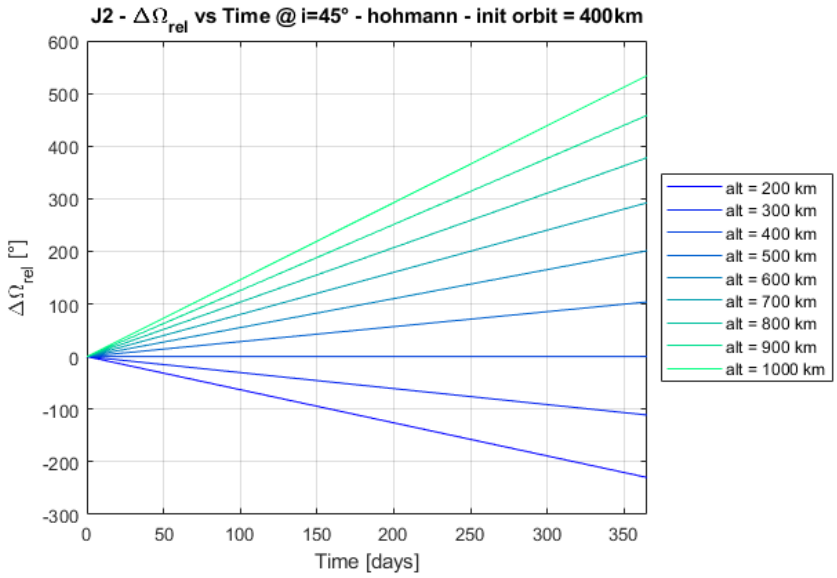

Figure 4.88: $\Delta\Omega_{rel}$ variation due to J_2 perturbation at $i = 45^o$ considering Hohmann transfer

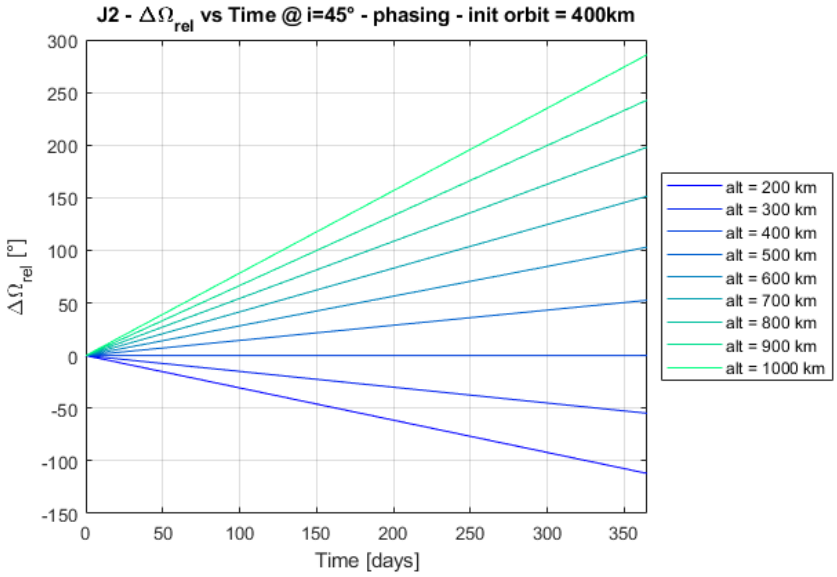

Figure 4.89: $\Delta\Omega_{rel}$ variation due to J_2 perturbation at $i = 45^o$ considering phasing transfer

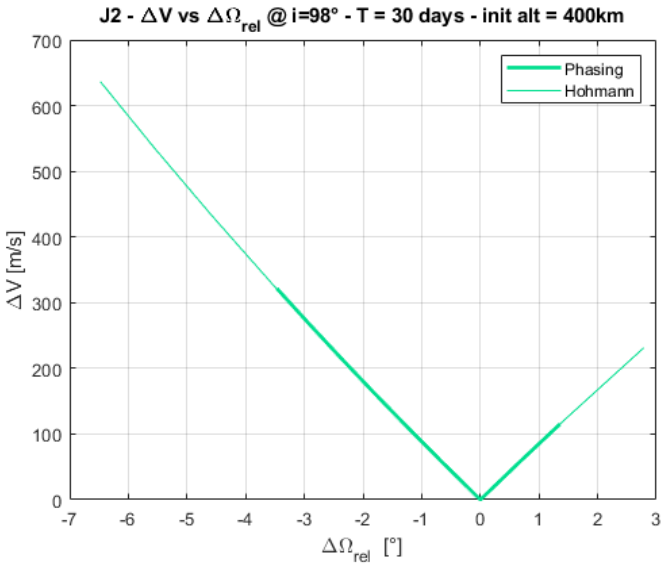

Figure 4.90: Hohmann and phasing transfer comparison for a period of 30 days

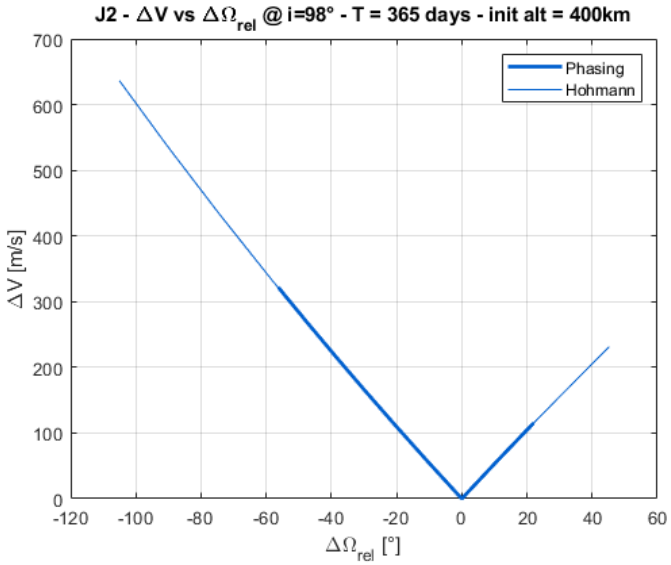

Figure 4.91: Hohmann and phasing transfer comparison for a period of 365 days

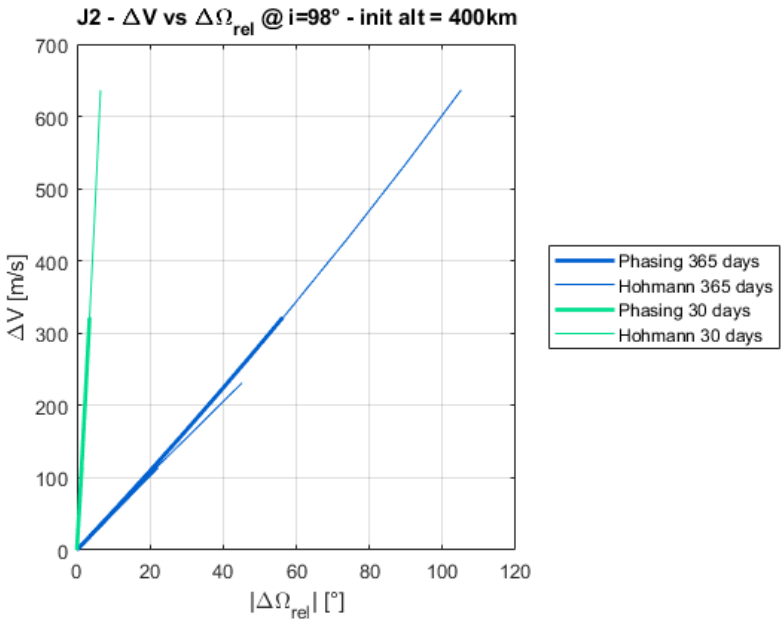

Figure 4.92: Hohmann and phasing transfer comparison

In the last graph, like in the previous section, it is possible to see a comparison between the Hohmann and Phasing transfer for two different periods in order to see the differences in time and costs.

Differential $\Delta\Omega$ considering initial altitude of 200 km

Considering different maneuvers and inclinations, it has been studied also how the $\Delta\Omega$ between two satellites vary starting from 200 km to different altitudes, due to the J_2 perturbation.

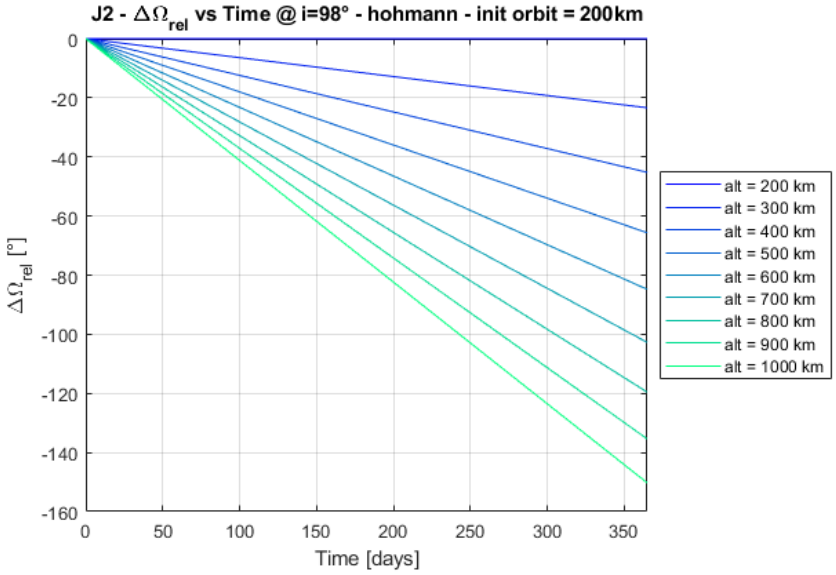

Figure 4.93: $\Delta\Omega_{rel}$ variation due to J_2 perturbation at $i = 98^o$ considering Hohmann transfer

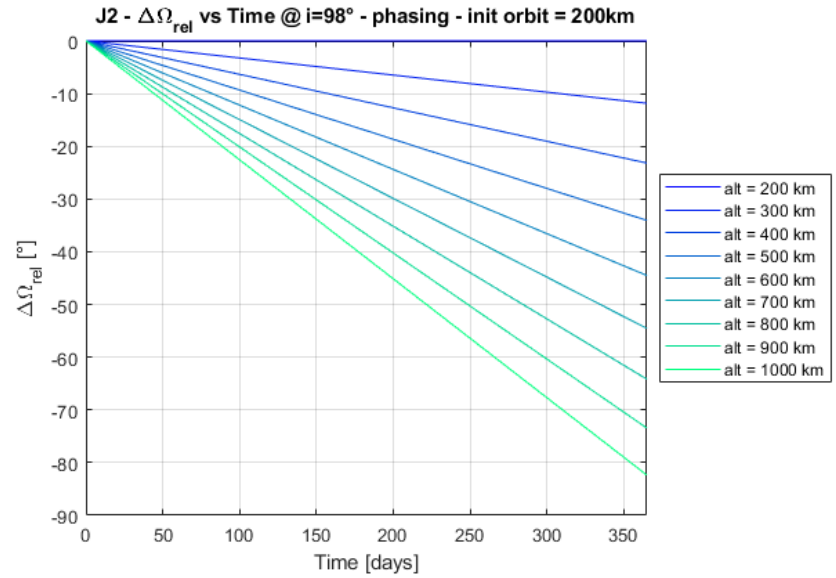

Figure 4.94: $\Delta\Omega_{rel}$ variation due to J_2 perturbation at $i = 98^o$ considering phasing transfer

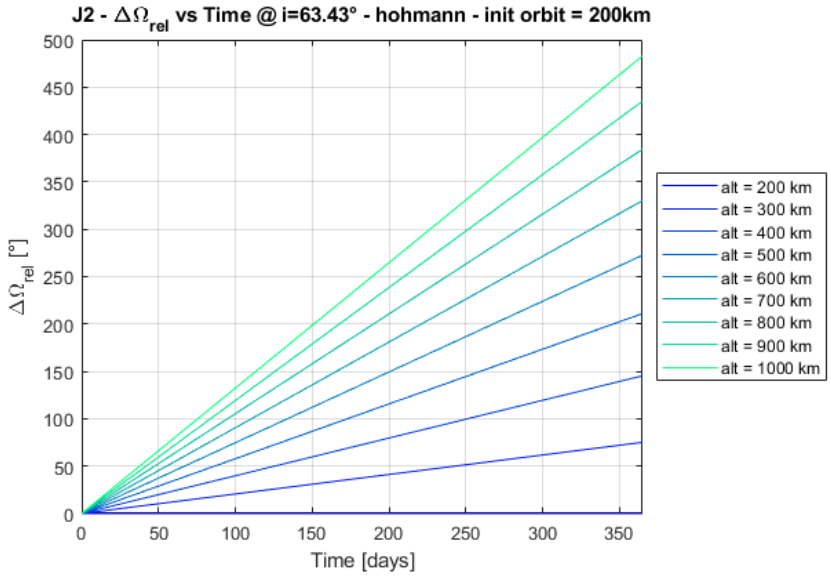

Figure 4.95: $\Delta\Omega_{rel}$ variation due to J_2 perturbation at $i = 63.43^o$ considering Hohmann transfer

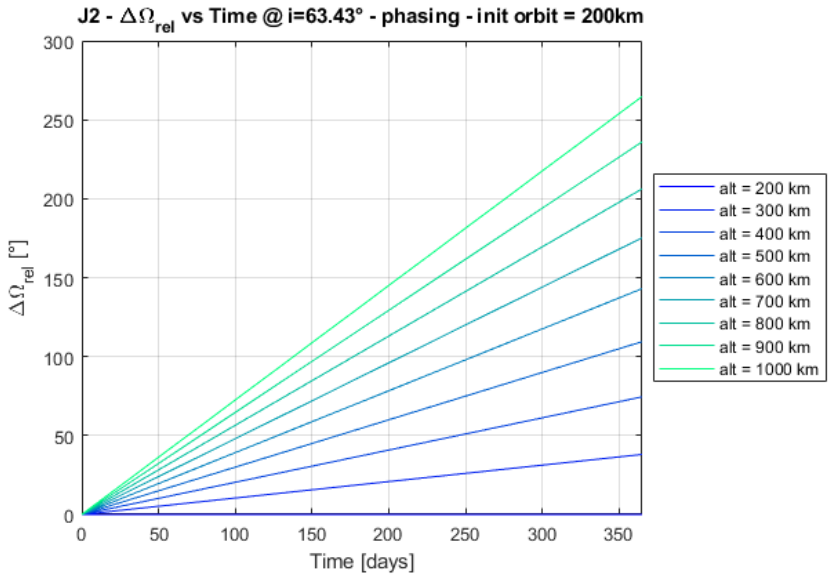

Figure 4.96: $\Delta\Omega_{rel}$ variation due to J_2 perturbation at $i = 63.43^o$ considering phasing transfer

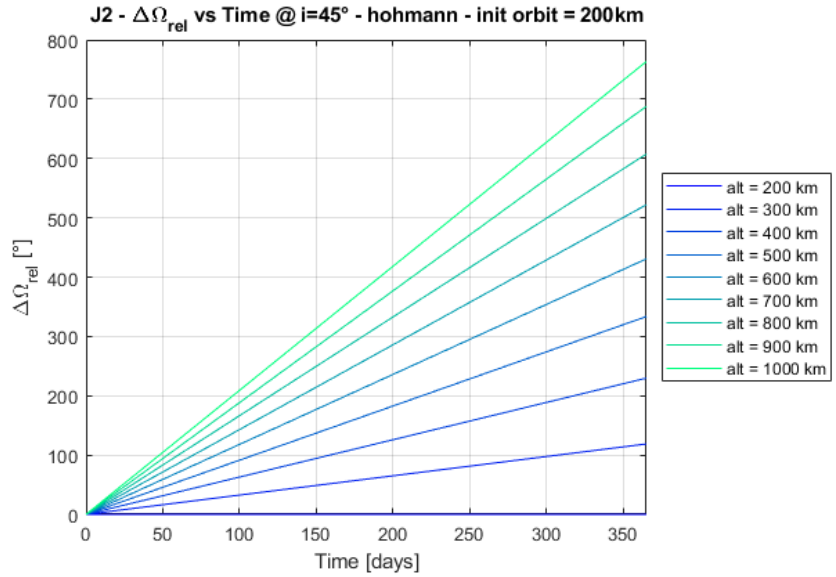

Figure 4.97: $\Delta\Omega_{rel}$ variation due to J_2 perturbation at $i = 45^o$ considering Hohmann transfer

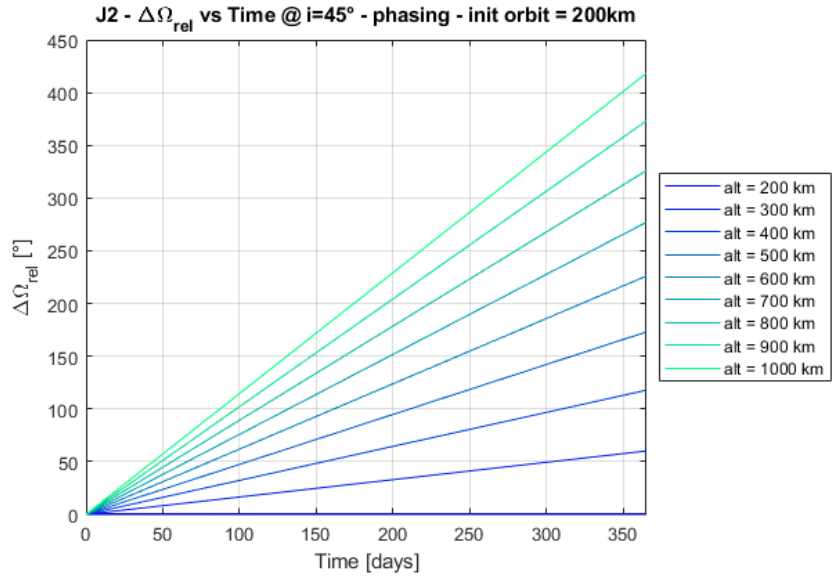

Figure 4.98: $\Delta\Omega_{rel}$ variation due to J_2 perturbation at $i = 45^o$ considering phasing transfer

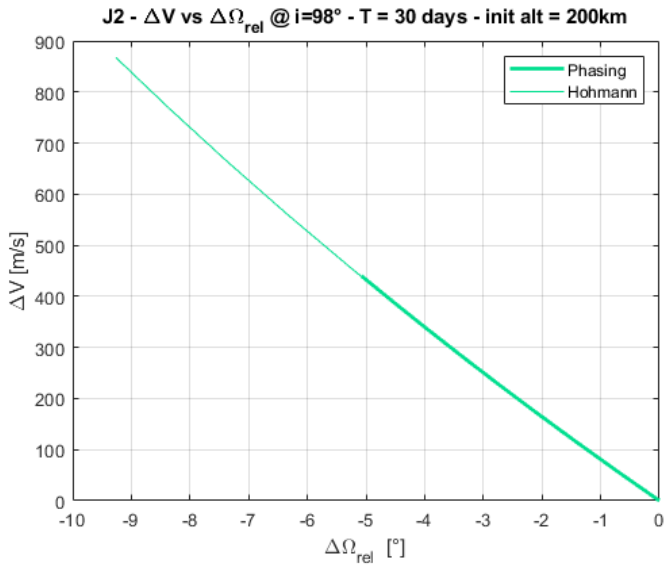

Figure 4.99: Hohmann and phasing transfer comparison for a period of 30 days

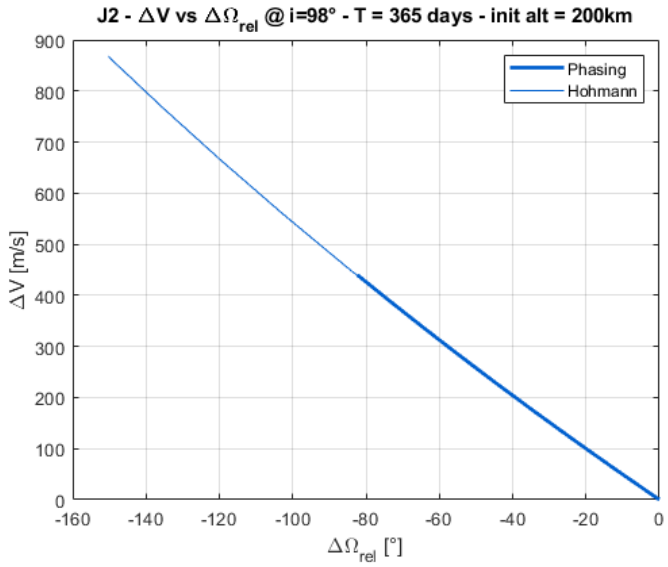

Figure 4.100: Hohmann and phasing transfer comparison for a period of 365 days

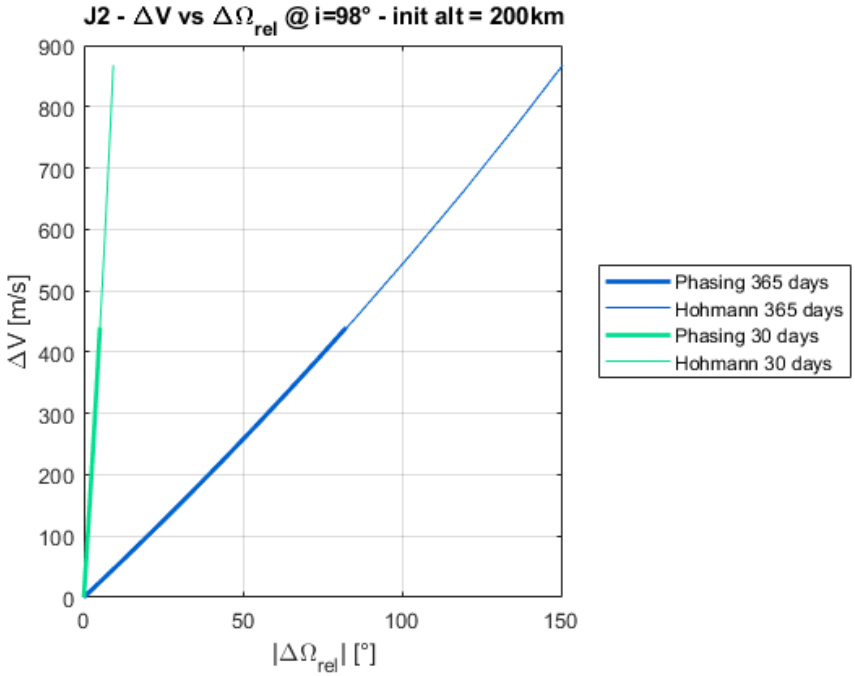

Figure 4.101: Hohmann and phasing transfer comparison

Considering an initial altitude equal to 200 km, it is possible to see the differences in time and costs between the Hohmann and Phasing transfer for two different periods as seen for the other previous cases.

4.3.7 Argument of Perigee change maneuver

The last maneuver that has been studied regards the change of the argument of perigee (Δw).

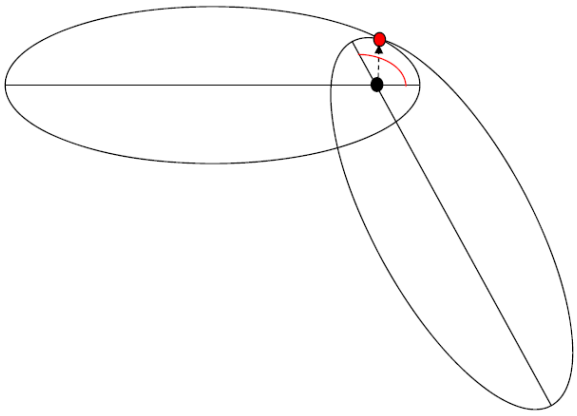

Figure 4.102: Representation of the argument of perigee change maneuver (angle of line rotation $\Delta\omega$ in red) [15]

The required ΔV to perform this maneuver can be expressed by the formula:

$$\Delta V = 2\sqrt{\frac{\mu}{a(1-e^2)}}\, e\, sin\left(\frac{\Delta\omega}{2}\right) \tag{4.25}$$

Considering the previous equation, the required ΔV in order to realize the maneuver is shown in the following graphs.

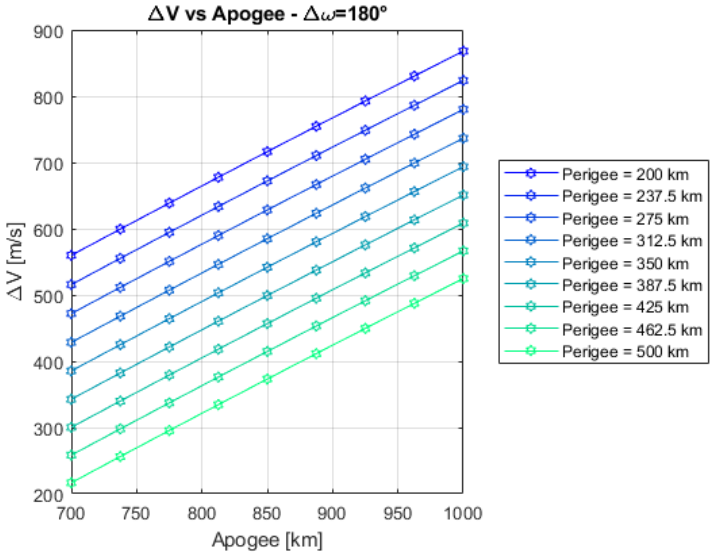

Figure 4.103: Required ΔV for a 180° argument of perigee change maneuver considering different altitudes of perigee and apogee

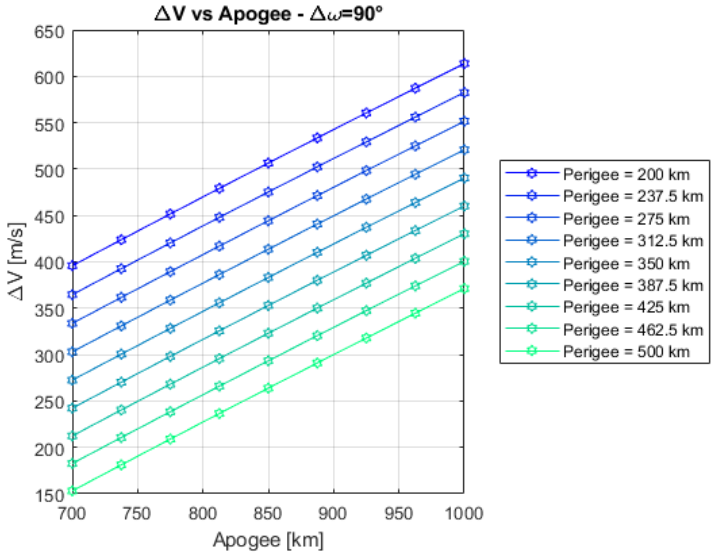

Figure 4.104: Required ΔV for a 90° argument of perigee change maneuver considering different altitudes of perigee and apogee

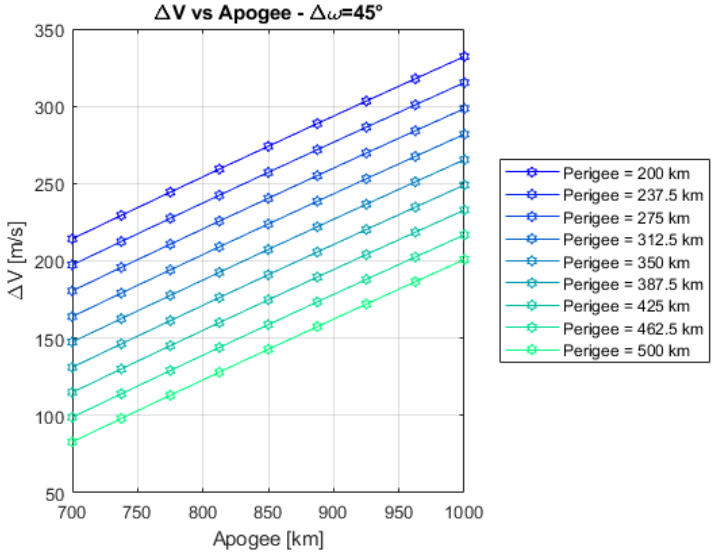

Figure 4.105: Required ΔV for a 45° argument of perigee change maneuver considering different altitudes of perigee and apogee

Chemical thruster - required propellant mass

First, it has been considered a constant $\Delta\omega$ and a variation of the apogee and perigee as it can be seen from the graphs below.

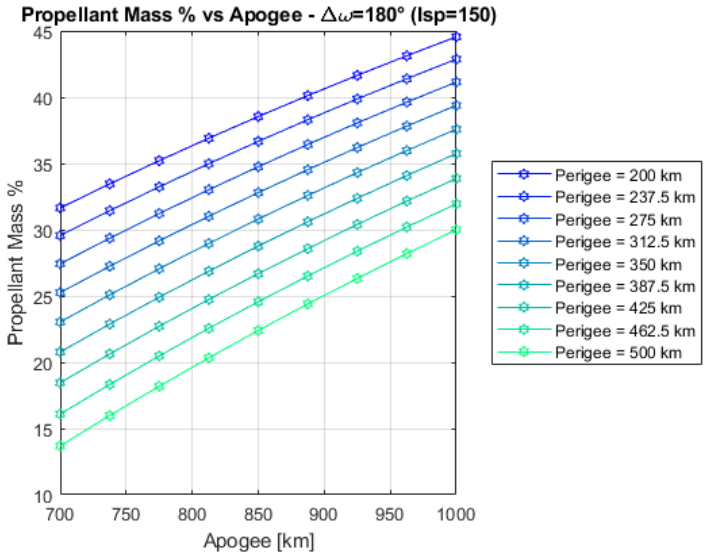

Figure 4.106: Required propellant mass % for a 180° argument of perigee change maneuver at different altitudes of apogee and perigee with Isp = 150 s

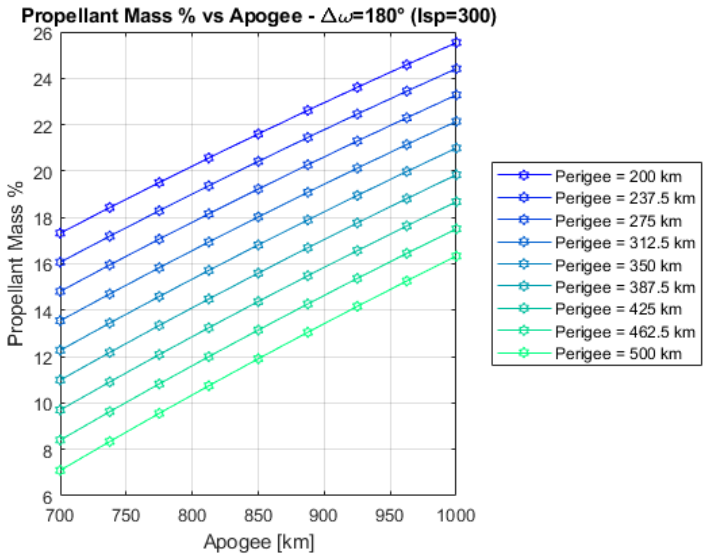

Figure 4.107: Required propellant mass % for a 180° argument of perigee change maneuver at different altitudes of apogee and perigee with Isp = 300 s

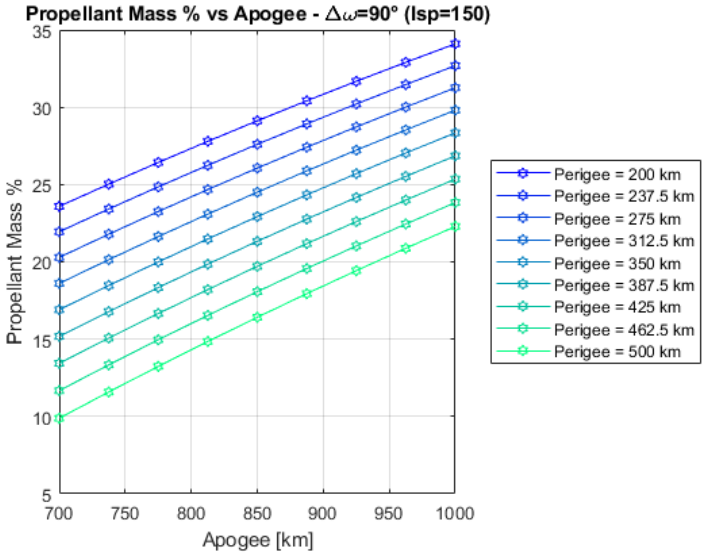

Figure 4.108: Required propellant mass % for a 90° argument of perigee change maneuver at different altitudes of apogee and perigee with Isp = 150 s

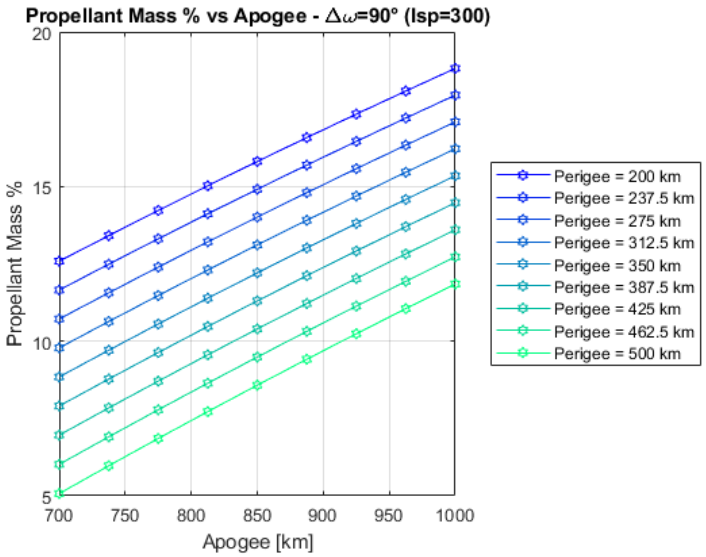

Figure 4.109: Required propellant mass % for a 90° argument of perigee change maneuver at different altitudes of apogee and perigee with Isp = 300 s

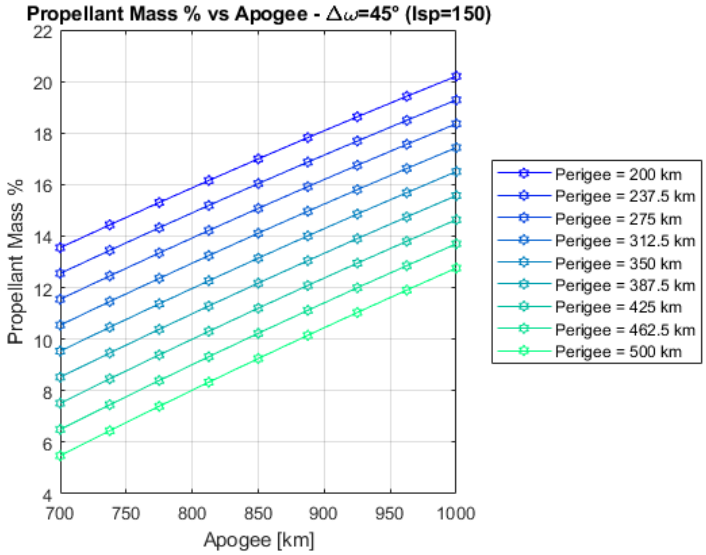

Figure 4.110: Required propellant mass % for a 45° argument of perigee change maneuver at different altitudes of apogee and perigee with Isp = 150 s

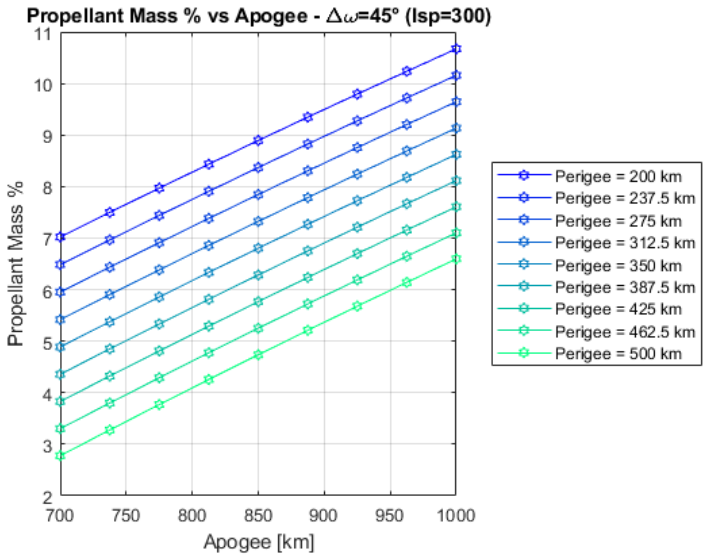

Figure 4.111: Required propellant mass % for a 45° argument of perigee change maneuver at different altitudes of apogee and perigee with Isp = 300 s

Then, a similar procedure has been implemented, considering initially a fixed perigee and after that the apogee is assumed constant, varyng the argument of perigee.

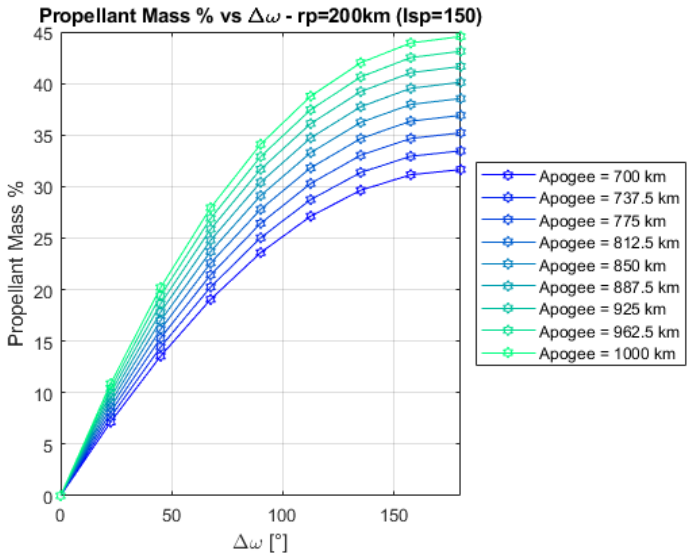

Figure 4.112: Required propellant mass % in function of the $\Delta\omega$, considering a fixed perigee and Isp = 150 s

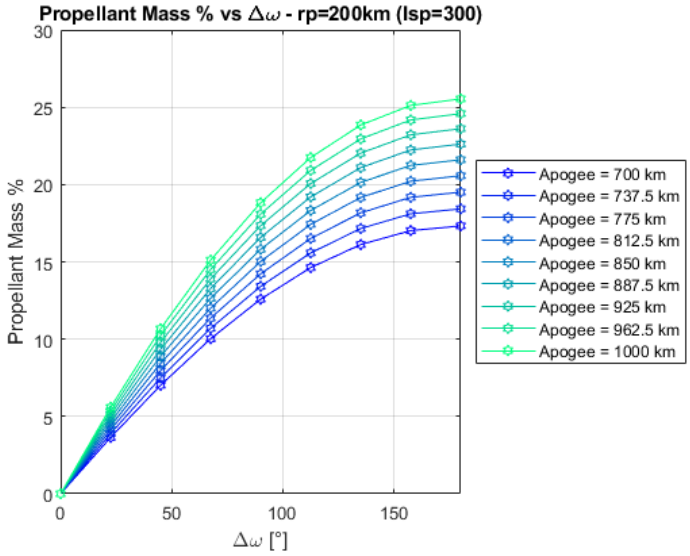

Figure 4.113: Required propellant mass % in function of the $\Delta\omega$, considering a fixed perigee and Isp = 300 s

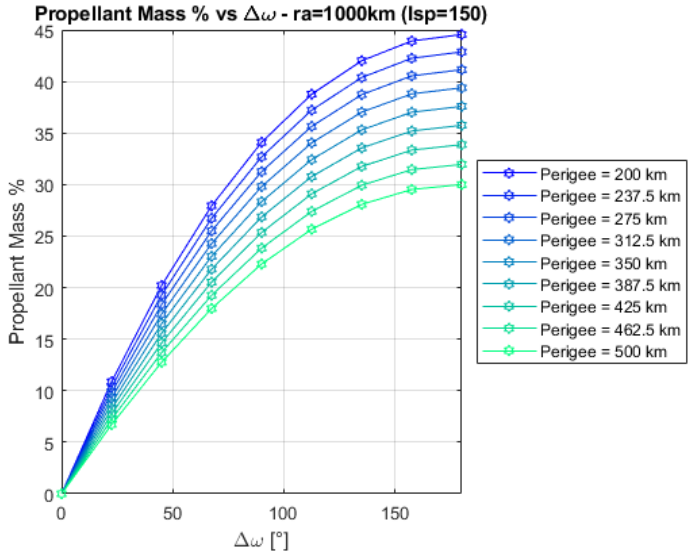

Figure 4.114: Required propellant mass % in function of the $\Delta\omega$, considering a fixed apogee and Isp = 150 s

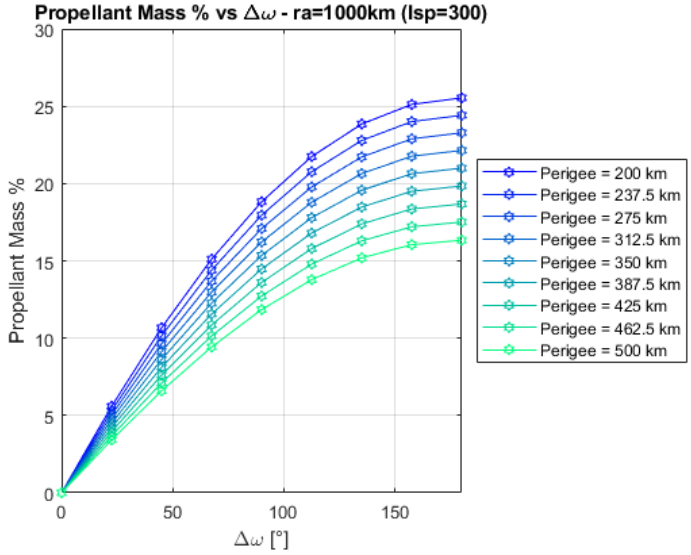

Figure 4.115: Required propellant mass % in function of the $\Delta\omega$, considering a fixed apogee and Isp = 300 s

Electric thruster - required propellant mass

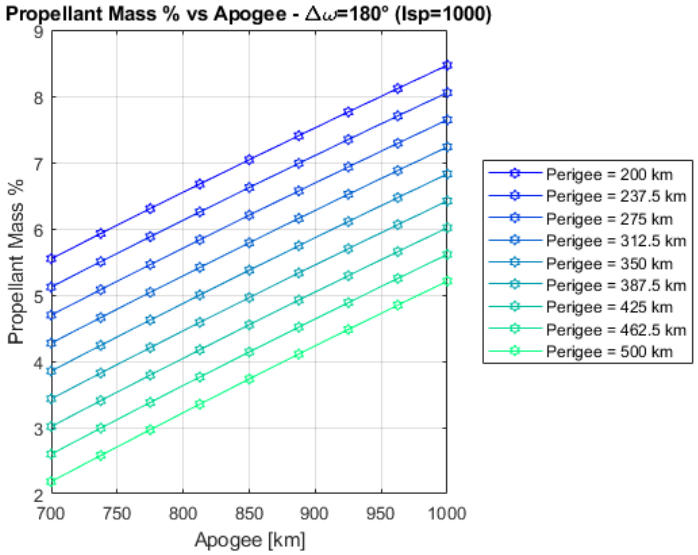

Figure 4.116: Required propellant mass % for a 180° argument of perigee change maneuver at different altitudes of apogee and perigee with Isp = 1000 s

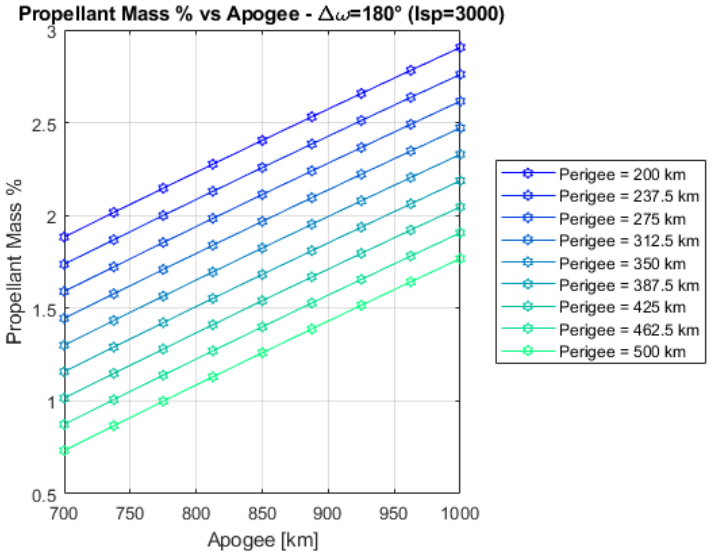

Figure 4.117: Required propellant mass % for a 180° argument of perigee change maneuver at different altitudes of apogee and perigee with Isp = 3000 s

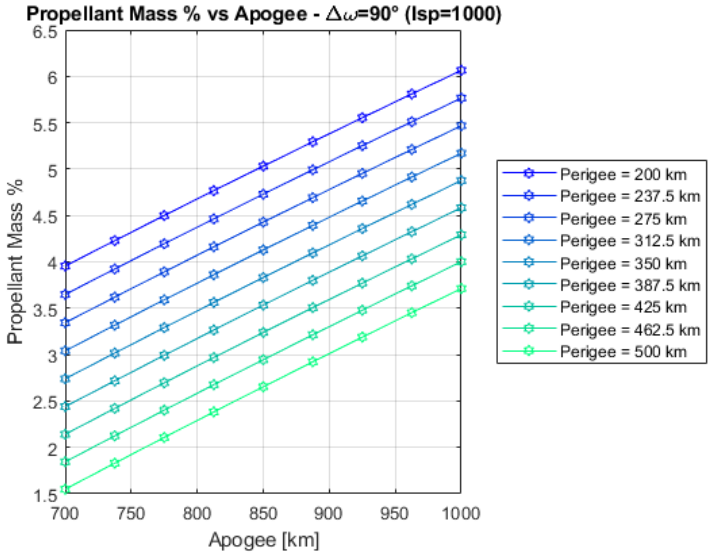

Figure 4.118: Required propellant mass % for a 90° argument of perigee change maneuver at different altitudes of apogee and perigee with Isp = 1000 s

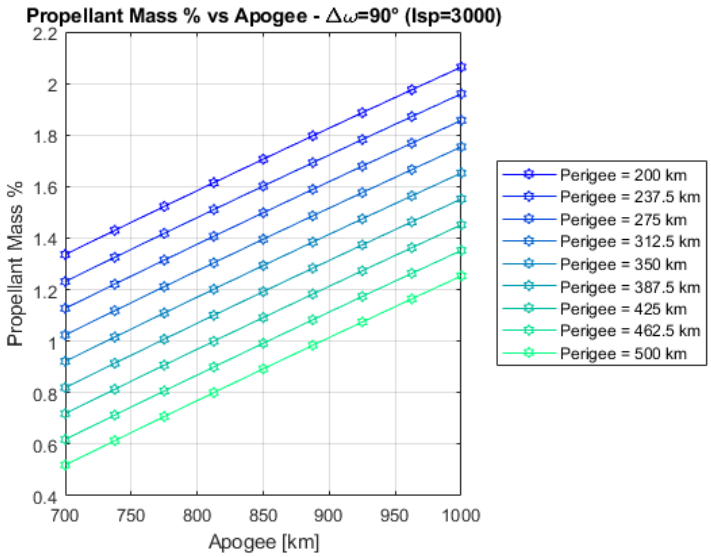

Figure 4.119: Required propellant mass % for a 90° argument of perigee change maneuver at different altitudes of apogee and perigee with Isp = 3000 s

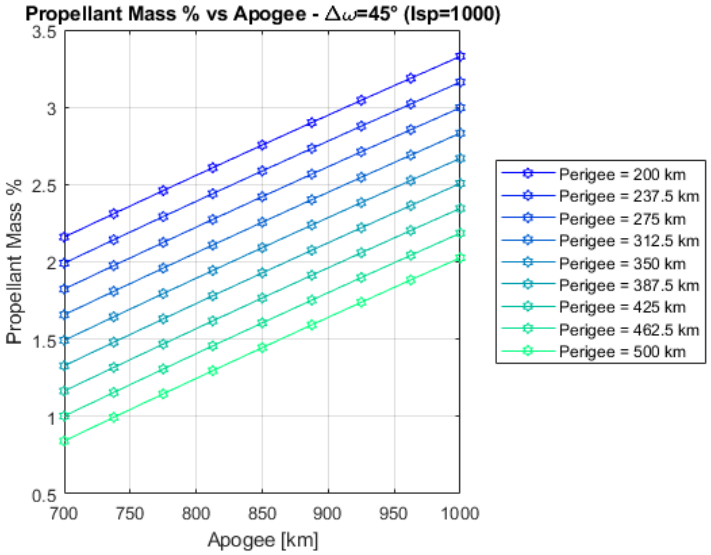

Figure 4.120: Required propellant mass % for a 45° argument of perigee change maneuver at different altitudes of apogee and perigee with Isp = 1000 s

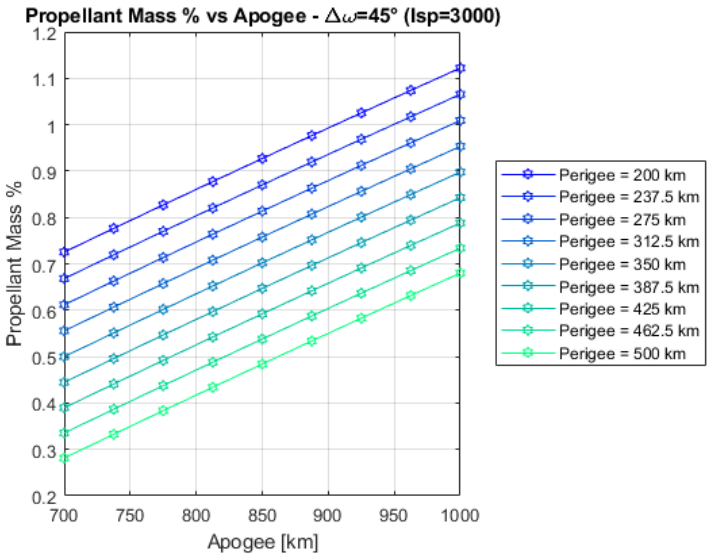

Figure 4.121: Required propellant mass % for a 45° argument of perigee change maneuver at different altitudes of apogee and perigee with Isp = 3000 s

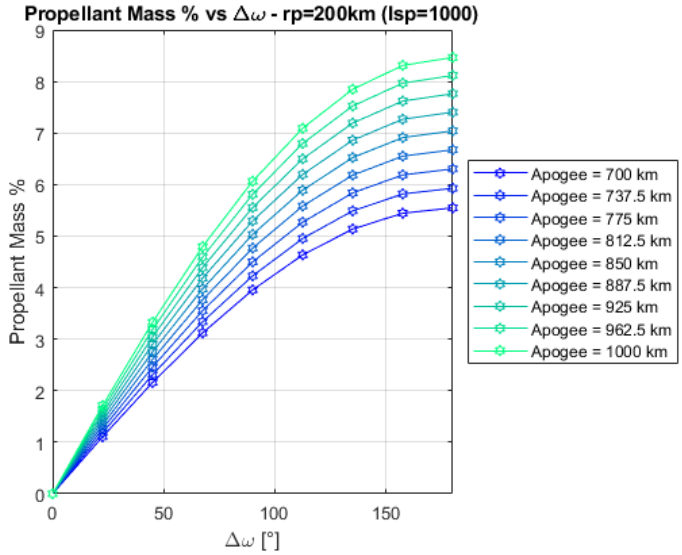

Figure 4.122: Required propellant mass % in function of the $\Delta\omega$, considering a fixed perigee and Isp = 1000 s

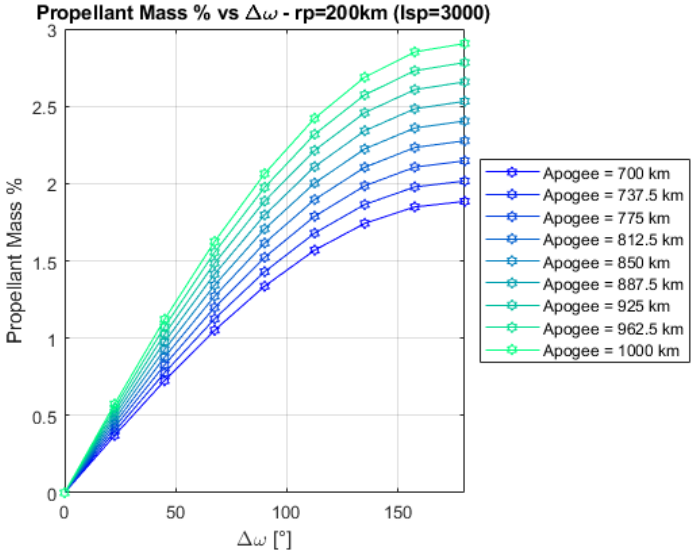

Figure 4.123: Required propellant mass % in function of the $\Delta\omega$, considering a fixed perigee and Isp = 3000 s

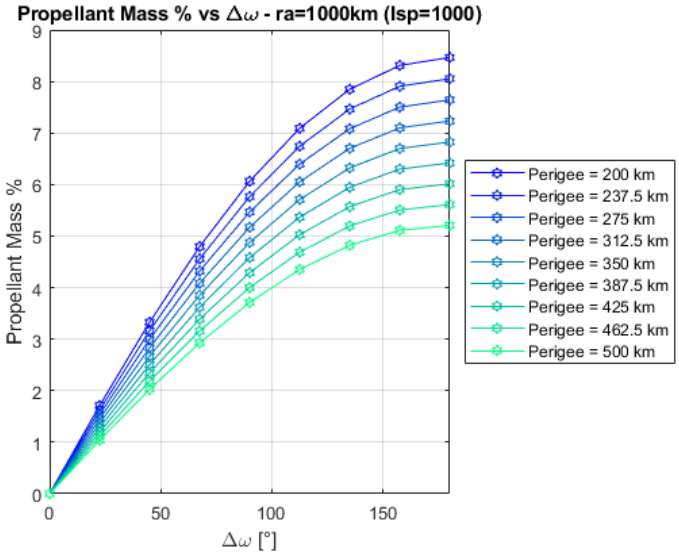

Figure 4.124: Required propellant mass % in function of the $\Delta\omega$, considering a fixed apogee and Isp = 1000 s

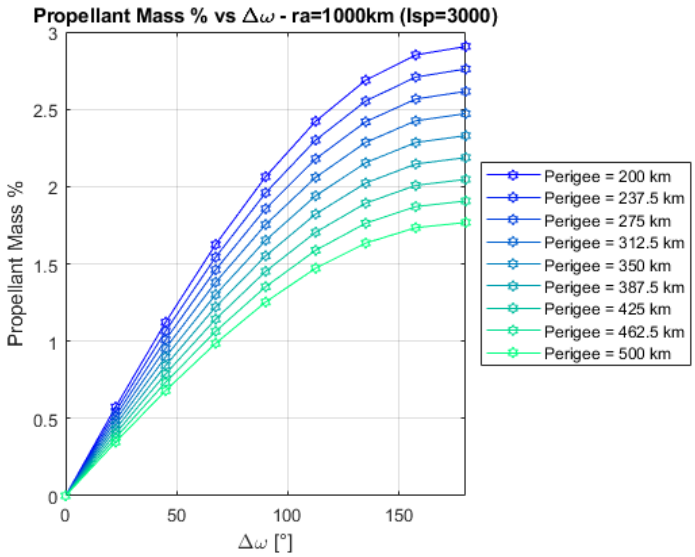

Figure 4.125: Required propellant mass % in function of the $\Delta\omega$, considering a fixed apogee and Isp = 3000 s

J_2 perturbation

An orbiting satellite is affected by the J_2 perturbation which also causes the apsidal line precession. The study of how the variation takes place and how great it is, is reported as follow by the graphs.

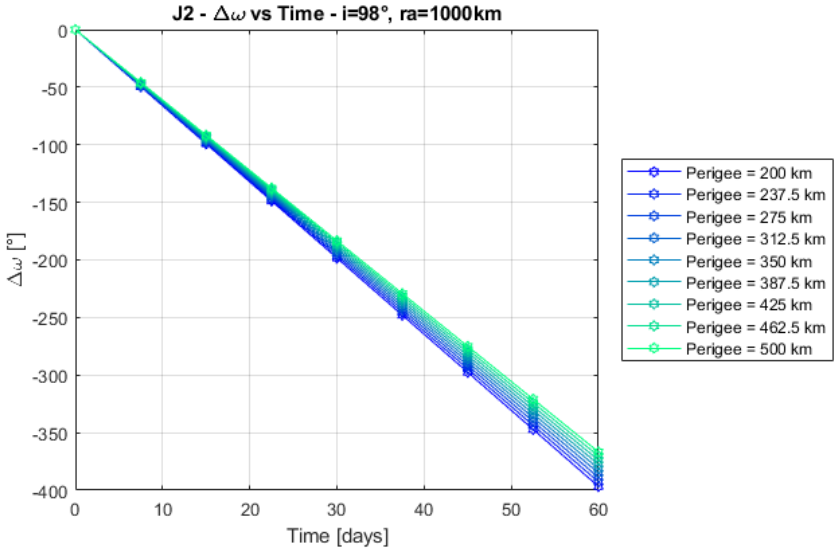

Figure 4.126: Argument of perigee variation in function of the time considering $i = 98^o$ and the apogee fixed at 1000 km

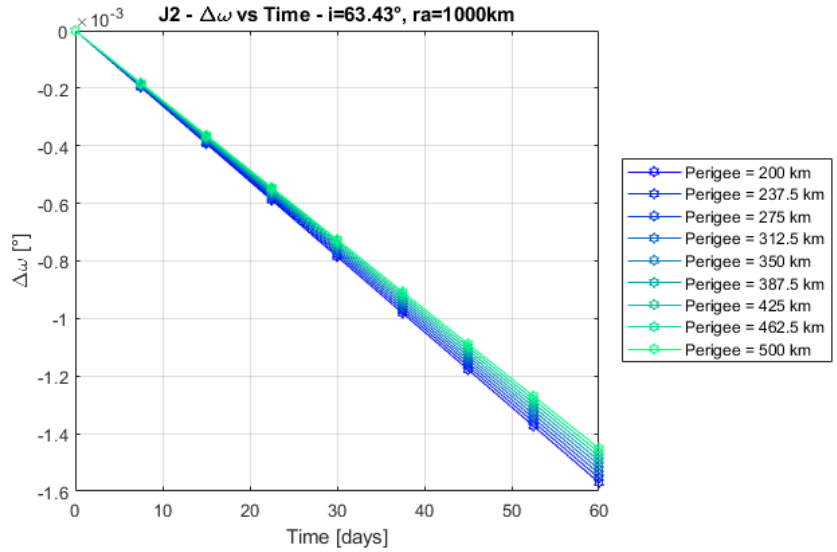

Figure 4.127: Argument of perigee variation in function of the time considering $i = 63.435^o$ and the apogee fixed at 1000 km

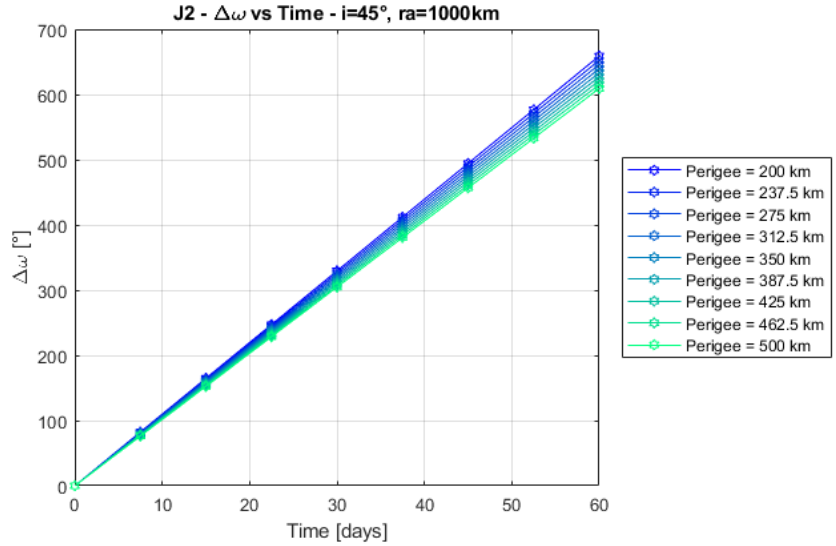

Figure 4.128: Argument of perigee variation in function of the time considering $i = 45^o$ and the apogee fixed at 1000 km

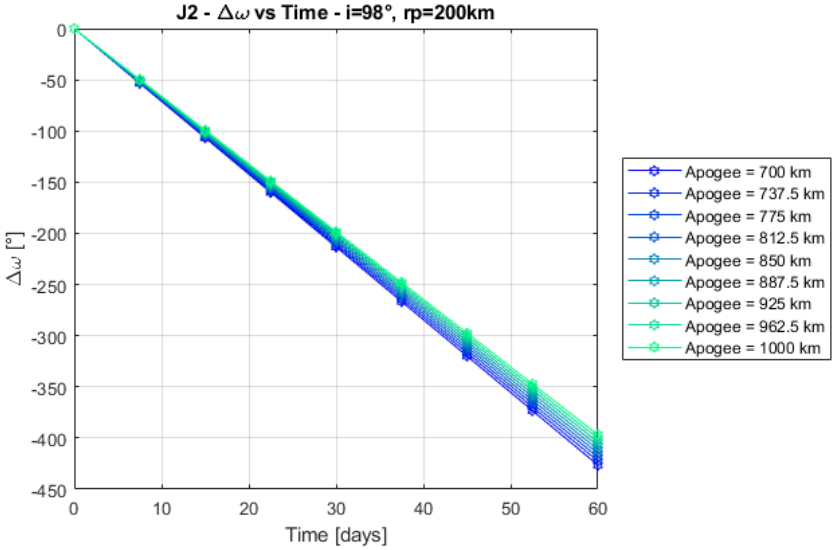

Figure 4.129: Argument of perigee variation in function of the time considering $i = 98^o$ and the perigee fixed at 200 km

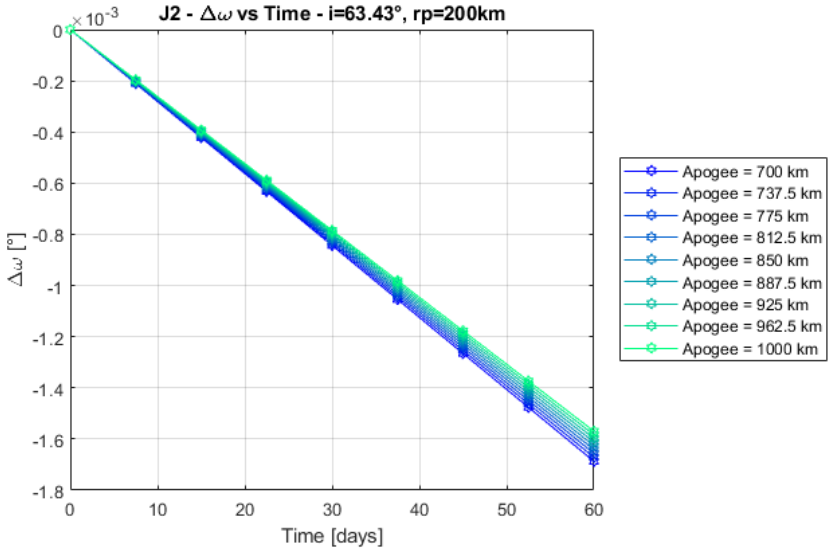

Figure 4.130: Argument of perigee variation in function of the time considering $i = 63.435^o$ and the perigee fixed at 200 km

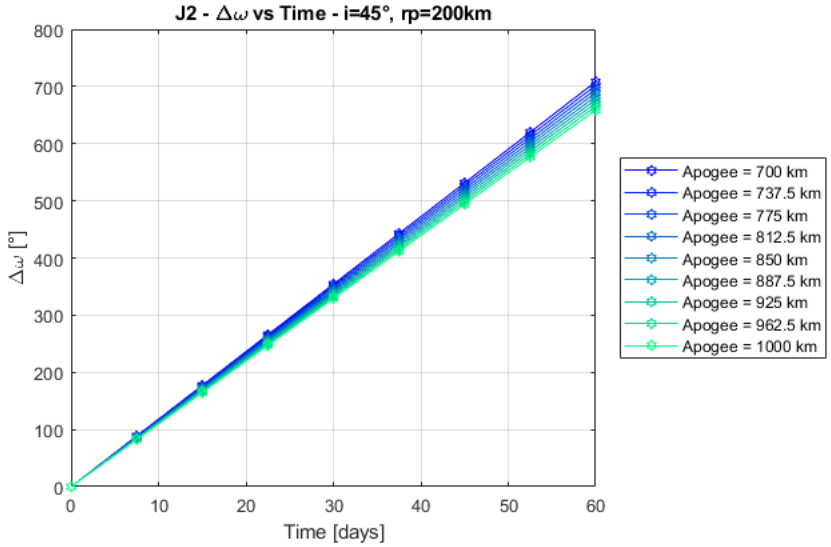

Figure 4.131: Argument of perigee variation in function of the time considering $i = 45^o$ and the perigee fixed at 200 km

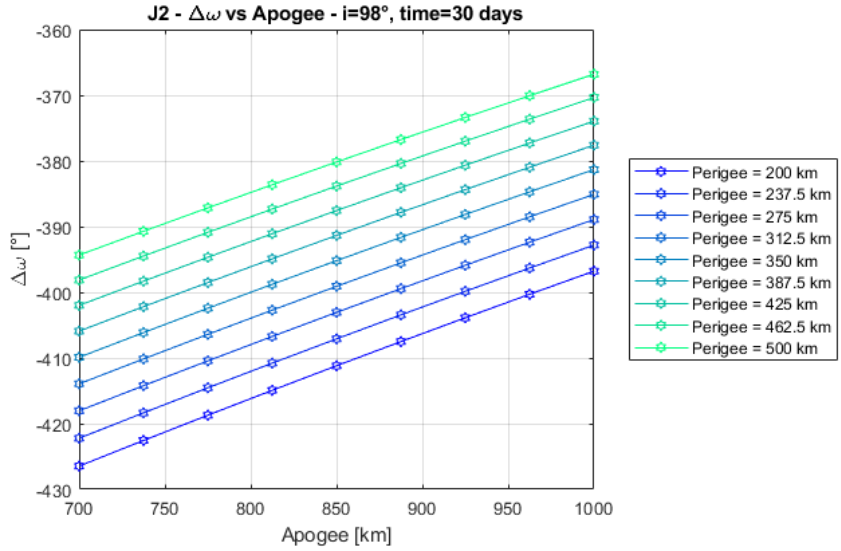

Figure 4.132: Argument of perigee variation in function of the apogee considering $i = 98^o$ and a period of 30 days

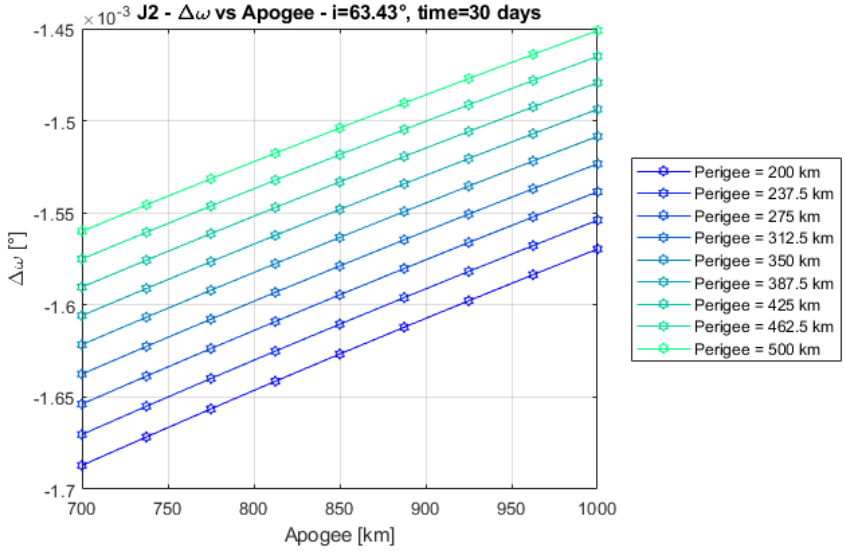

Figure 4.133: Argument of perigee variation in function of the apogee considering $i = 63.435^o$ and a period of 30 days

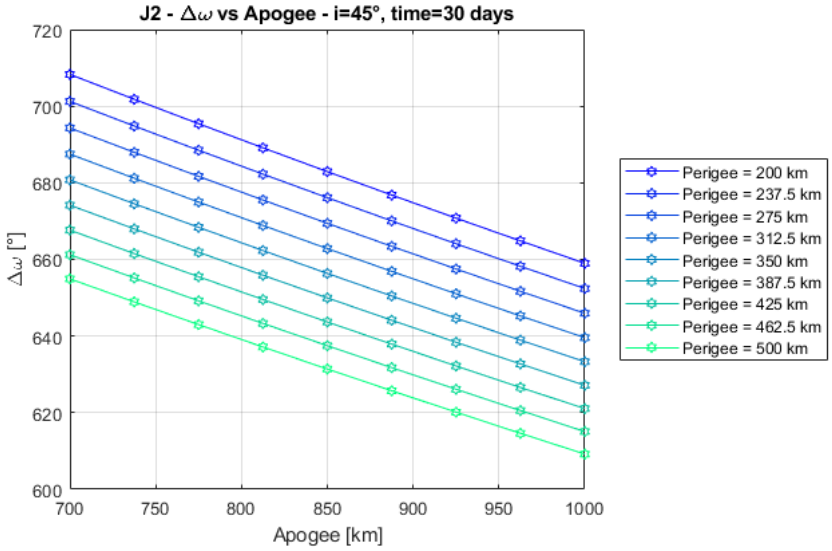

Figure 4.134: Argument of perigee variation in function of the apogee considering $i = 45^o$ and a period of 30 days

As can be seen from the graphs, the maneuver is too expensive and should be carried out too often due to the J_2 perturbation, so it cannot be taken into consideration.

Conclusions

The present document aims to indicate the preferable way to reach a certain orbit to place a small satellite, depending on the mission requirements.
In order to achieve this goal, a general overview about available launchers and microlaunchers has been initially given.

Initially, results regarding the maneuvers are shown in the table 4.1.

Maneuver	Specifics	ΔV $[\frac{m}{s}]$
Phasing	$\Delta\Lambda = 90^o$, $period = 30$ $days$	~ 4
Phasing	$\Delta\Lambda = 90^o$, $period = 365$ $days$	~ 2
Orbit raising	from 500 km to 800 km	~ 150
RAAN change	$\Delta\Omega_{rel} = -5.8^o$, $period = 30$ $days, i = 98^o$	~ 500
RAAN change	$\Delta\Omega_{rel} = -90^o$, $period = 365$ $days, i = 98^o$	~ 500
i change	$\Delta i = 1^o$	~ 160

Table 4.1: Maneuvers summary

From this table, it is initially clear that phasing maneuver allows positioning in a short time and with truly reduced costs.
Likewise, the orbit raising is a short term and quite low cost maneuver with a linear behaviour which allows to simply estimate the mission costs.
Conversely, the RAAN change and inclination change maneuvers require large quantities of propellant and this fact mainly bias the choice in favor of microlaunchers or transporter missions.
To avoid the propellant waste, the RAAN change is performed exploiting the J_2 perturbation, lengthening the mission time before final placement of the satellite.
Despite the high cost, the inclination change maneuver has to be considered because, since the value of inclination of the Sun-synchronous orbit (SSO) lies around 98^o of inclination depending on the altitude, it could be necessary to slightly change the inclination in case the satellite deployment takes place at altitudes very different from the final desired one.

The last maneuver computed, not shown in the table, was the argument of perigee change maneuver. From the calculation, it is demonstrated that the costs to perform this maneuver are too high and, since the parameter has a fast variability due to J_2 perturbation, it has no reason to be considered. One way around this is to place the satellite in a orbit with an inclination equal to 63.435^o which allows to freeze the perigee at the desired height so as to be able to carry out terrestrial observations at the perigee, at the latitude of interest in range from $-i$ to $+i$, and decrease the drag at the apogee.

As regards the choice between launcher and micro launcher, the costs of the satellite, propellant, launcher and micro launcher have been taken into consideration. Values about costs, in k€/kg unit, are:

- Satellite cost, $c_S = 12.5,\ 25,\ 50$
- Propellant cost, $c_P = 0.1$
- Launcher cost, $c_L = 5$
- Micro launcher cost, $c_{ML} = 12.5,\ 25,\ 50$

The total cost deriving from the choice of the launcher can be approximated by the formula:

$$COST_L = m_P\, c_P + m_f\, c_S + m_i\, c_L \tag{4.26}$$

Where m_i is the initial mass and m_f is the final mass.
Likewise, the total cost due to the micro launcher choice comes from:

$$COST_{ML} = m_{P/L}\,(c_s + c_{ML}) \tag{4.27}$$

Where $m_{P/L}$ is the payload mass.
The ratio between the micro launcher cost and the launcher one is the useful parameter considered to choose the preferable way to accomplish a certain mission.
Considering a required ΔV equal to 500, 1000, 1500 $\frac{m}{s}$, the following ratio are obtained.

$c_S \setminus c_{ML}$	12.5	25	50
12.5	1.2718	1.9076	3.1794
25	1.1370	1.5161	2.2741
50	1.0482	1.2579	1.6772

Table 4.2: Ratios considering $\Delta V = 500\ \frac{m}{s}$

$c_S \setminus c_{ML}$	12.5	25	50
12.5	1.1055	1.6583	2.7638
25	1.0118	1.3491	2.0236
50	0.9475	1.1370	1.5161

Table 4.3: Ratios considering $\Delta V = 1000\ \frac{m}{s}$

$c_S \setminus c_{ML}$	12.5	25	50
12.5	0.9315	1.3973	2.3289
25	0.8742	1.1656	1.7484
50	0.8332	0.9998	1.3331

Table 4.4: Ratios considering $\Delta V = 1500\ \frac{m}{s}$

From these tables it is possible to understand how the choice depends on the ratio: a value close to or lower than 1 indicates a greater convenience of the micro launcher, on the contrary, a value far from 1 makes the choice converge towards the launcher.

The last question dealt with, concerns the choice between dispenser, which deploys satellites, and satellites with their own propulsion.
It is known that deployers efficiency is always lower than or equal to the satellites with own propulsion.
Qualitatively, a first distinction comes from the fact deployers take advantage of the scale effect on size, this translates into better performance parameters. On the other hand, satellites exploit the same effect on number and not on size.
Consequently, the choice depends on the path the deployer or satellite has to travel.
Considering the deployment in high LEO and all final satellite orbits sequentially lower than the deployment altitude, the difference between deployers and satellites is minimal. The same consideration can be made if the satellites are released in low LEO and all the final orbits are sequentially higher.
The worst case can be represented in the following graph.

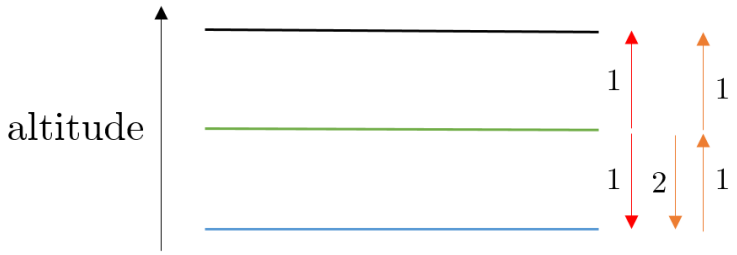

Figure 4.135: Orbit raising: deployer worst case representation

From the above image, satellite path is represented in red and the deployer one in orange. As it can be seen, considering a constant ΔV in both cases, the required total impulse is greater considering the deployer solution.
The same final consideration is obtained considering to change inclination instead of orbit raising.
Regarding the RAAN change or the phasing maneuver, it can be shown that the size of the maneuver representing the expenditure in terms of impulse is described by the following formulas:

$$(m\Delta V)_{free\ sat} = N_s - 1 \qquad (m\Delta V)_{deployer} = (N_s - 1)\ \frac{N_s}{2} \tag{4.28}$$

The factor $\frac{N_s}{2}$ is the discriminant between the two solutions, which leads to the choice of deployers for a small number of satellites while satellites with own propulsion are a more reasonable solution in the other case.

Bibliography

[1] DP Mishra. *Fundamentals of rocket propulsion*. CRC Press, 2017. ix, 2

[2] SpaceX. Falcon 9 payload user's manual. ix, 10, 11

[3] European Space Agency (ESA). Vega payload user's manual. ix, 11

[4] Relativity Space. Terran payload user's manual. ix, 12

[5] Japan Aerospace Exploration Agency (JAXA). Epsilon payload user's manual. ix, 13, 14

[6] China Academy of Launch Vehicle Technology (CALT). Long march 3a payload user's manual. ix, 14

[7] ABL Space Systems. Rs1 payload user's manual. ix, 15

[8] Virgin Orbits. Launcher one payload user's manual. ix, 16

[9] HyImpulse. Sl1 payload user's manual. ix, 16

[10] Rocket Lab. Electron payload user's manual. ix, 17

[11] Firefly. Alpha payload user's manual. ix, 18

[12] Skyrora. Skyrora xl payload user's manual. ix, 19

[13] Inigo Del Portillo, Bruce G Cameron, and Edward F Crawley. A technical comparison of three low earth orbit satellite constellation systems to provide global broadband. *Acta astronautica*, 159:123–135, 2019. ix, 23, 24, 25

[14] Howard D. Curtis. *Orbital Mechanics for Engineering Students*. B|H, Oxford, 2014. ix, x, xi, 27, 28, 30, 32, 39, 51

[15] Automation and Robotics Laboratory. Orbit transfer - orbit maneuvers. xii, 82

[16] Spacefund. `https://spacefund.com/in-space-transportation/`. xv, 22

[17] George P Sutton and Oscar Biblarz. *Rocket propulsion elements*. John Wiley & Sons, 2016. 1

[18] Exolaunch. Exopod user's manual. 20

[19] Gauss. Gpod user's manual. 20

[20] ISISpace. Isispace deployers user's manual. 20

[21] OHB. Satellite platforms. 21

[22] Avio. Ssms user's manual. 21

[23] D-Orbit. Ion user's manual. 21

[24] Firefly. Alpha suv user's manual. 21

[25] Moog. Comet user's manual. 21

[26] Moog. Sl-omv user's manual. 21

[27] Orbital ATK. Espastar user's manual. 21

[28] SAB Aerospace. Ssms user's manual. 21

[29] Sidus Space. Lizziesat user's manual. 21

[30] SNC. Platforms user's manual. 21

[31] Spaceflight. Sherpa user's manual. 21

[32] David A Vallado. *Fundamentals of astrodynamics and applications*, volume 12. Springer Science & Business Media, 2001. 51

[33] James Pollard. Evaluation of low-thrust orbital maneuvers. In *34th AIAA/ASME/SAE/ASEE Joint Propulsion Conference and Exhibit*, page 3486, 1998. 57

[34] Mason J Kelchner and Craig A Kluever. Rapid evaluation of low-thrust transfers from elliptical orbits to geostationary orbit. *Journal of Spacecraft and Rockets*, 57(5):898–906, 2020.